Université Fédérale
Toulouse Midi-Pyrénées

THÈSE

En vue de l'obtention du

DOCTORAT DE L'UNIVERSITÉ DE TOULOUSE

Délivré par :
l'Institut National des Sciences Appliquées de Toulouse (INSA de Toulouse)
Cotutelle internationale *University of Trento, (IT)*

Présentée et soutenue le *21/05/2019* **par :**

MATTEO COCETTI

Nonlinear and Hybrid Feedbacks with Continuous-Time Linear Systems

---

JURY

VINCENT ANDRIEU	Chargé de Recherche	Examinateur
BAYU JAYAWARDHANA	Full Professor	Examinateur
ENRICO BERTOLAZZI	Associate Professor	Examinateur
SOPHIE TARBOURIECH	Directeur de Recherche	Examinateur
CHRISTOPHE PRIEUR	Directeur de Recherche	Examinateur
ANDREA DEL PRETE	Associate Professor	Examinateur

École doctorale et spécialité :
EDSYS : Automatique 4200046
Unité de Recherche :
Laboratoire d'analyse et d'architecture des systèmes (LAAS)
Directeur(s) de Thèse :
Sophie TARBOURIECH et *Enrico BERTOLAZZI*
Rapporteurs :
Vincent ANDRIEU et *Bayu JAYAWARDHANA*

Acknowledgements

I would like to thank my advisors Luca Zaccarian, Sophie Tarbouriech and Enrico Bertolazzi for supporting my activities during the three years, while giving me the intellectual freedom to pursue the research directions that I liked the most. From Luca I learned many things, but the most important is certainly the ability to handle professionally more task in parallel. His dedication and constant support have been a valuable example during these years. Thanks to Sophie for welcoming me at LAAS, and for her friendly ans wise attitude that creates a nice working environment. Thanks also for her numerous advices and feedback on my research work. Thanks to Enrico, who gave me the freedom to follow a different path from the one originally planned, supporting me every time I needed. My sincere thank goes also to all members of the MAC group, who welcomed me in Toulouse and financially supported my participation to various conferences.

I would also like to express my sincere gratitude to Vincent Andrieu and Bayu Jayawardhana for accepting to review my thesis, and to Andrea del Prete and Christophe Prieur for agreeing to be part of my doctoral committee. It is really an honor for me.

Thanks to Dana-Rexroth Transmission Systems for challenging me with the nonovershooting problem contained in this thesis, and for making the experimental tests possible. In particular thanks to Pier Paolo Rinaldi and Alex Sassaro for their technical support and their friendly attitude. I learned a lot both from a technical and human point of view.

Thank to all the members of the gang "Il pranzo è servito", a group that collects Italians that perform research at LAAS and who like to share dinners and fun together. Thanks to Antonino Sferlazza, Luca Bettamin, Matteo Della Rossa, Nicola Accettura, Valeria De Paolis and Bruno Rossi for making me feel like I never left Italy.

Thanks to Luciano Moreira for sharing the office with me and for the numerous conversation about research and life. I really enjoyed the time that we spent together, and I hope I will the chance to visit Brasil in the future. Thanks to David Tocaven, for sharing the office with me during the last six months and for repeatedly invite me out. In the end I had to accept and I had a lot of fun. His positive attitude and a little bit of craziness made my last weeks at LAAS more memorable.

Thanks to Luca De Pascali, Mirko Brentari and Matteo Ragni for being the best buddies that one can hope for. They are the most generous and selfless persons I know and I have been so lucky to have all them at my side during this journey. During these six (almost seven) years they influenced and helped me in so many ways that listing them all would require another thesis. A heartfelt thank you to all of you.

A special thank goes also to Veronica Neri and Giuseppe Bellavita, strong and generous friends that always supported me. Every time I came home, our reunions always made me feel like I'd never left.

I am incredibly grateful to my family, especially to my parents Liliana, Piero and to my brother Francesco for supporting my decisions, (even if that meant for me moving away and not calling home as often as I should), and for have been always available for me. Without their support and love this achievement would not have been possible. I also want to thank Clara and Andrea that over the years have become a second family for me. Their hospitality and undivided generosity have always made me feel like at home.

Finally, I want to thank my love Ottavia, who followed me during this journey astride Italy and France. Ottavia has lovingly endured all my quirks and odd working hours, showing me all her love and support. I am very lucky to have her at my side.

Contents

List of symbols

$\mathbb{N}$	the set of natural numbers
$\mathbb{R}$	the set of real numbers
$\mathbb{R}_{>0},\ (\mathbb{R}_{\geq 0})$	the set of strictly positive (nonnegative) real numbers
$\mathbb{R}^n$	the set of n-dimensional real vectors
$\mathbb{R}^n_{>0},\ (\mathbb{R}^n_{\geq 0})$	the strictly positive (positive) orthant of the n-dimensional real vector space
$\mathrm{Diag}^n_{>0},\ (\mathrm{Diag}^n_{\geq 0})$	the set of diagonal and positive definite (semidefinite) $n \times n$ matrices
$\mathrm{Sym}^n_{>0},\ (\mathrm{Sym}^n_{\geq 0})$	the set of symmetric and positive definite (semidefinite) $n \times n$ matrices
$A \in \mathbb{R}^{n \times m}$	$n \times m$ matrix with real entries
$A^\top$	the transpose of matrix A
A^{-1}	the inverse of matrix A (if it exists)
$A^{-\top}$	$:= (A^{-1})^\top$ with A an invertible matrix
$\mathrm{He}(A)$	$:= (A + A^\top)$ the Hermitian component of the square matrix A
$\mathrm{diag}(A_1, A_2)$	the $n \times n$ matrix resulting from the diagonal block-wise concatenation of $A_1 \in \mathbb{R}^{n_1 \times n_1}$ and $A_2 \in \mathbb{R}^{n_2 \times n_2}$, where $n := n_1 + n_2$
$\sqrt{A}$	the square root of the positive definite matrix A, i.e. $\sqrt{A}\sqrt{A} = A$
$\mathrm{eig}(A)$	the set of eigenvalues of the matrix A
$\mathrm{rank}(A)$	the rank of the matrix A
$\lambda_{\min}(A)$	the minimum eigenvalue of the symmetric matrix A
$\lambda_{\max}(A)$	the maximum eigenvalue of the symmetric matrix A
$\sigma(A)$	the set of singular values of the matrix A
$\sigma_{\min}(A)$	the minimum singular value of the matrix A
$\sigma_{\max}(A)$	the maximum singular value of the matrix A

$A > 0$ $(A \geq 0)$	matrix A is positive definite (semidefinite)
$A < 0$ $(A \leq 0)$	matrix A is negative definite (semidefinite)
$\lvert x\rvert_p$	the p norm of the vector x
(x, y)	equivalent to $[x^\top, y^\top]^\top \in \mathbb{R}^{n+m}$ for every $x \in \mathbb{R}^n$ and $y \in \mathbb{R}^m$
$\langle x, y\rangle$	equivalent to $x^\top y$ for vectors x, $y \in \mathbb{R}^n$
$x \geq y$	component-wise vector inequality; equivalent to $x_i \geq y_i$ for $i = 1, \ldots$
$F : \mathbb{R}^m \rightrightarrows \mathbb{R}^n$	a set-valued map from $\mathbb{R}^m$ to $\mathbb{R}^n$
$\mathrm{dom}(F)$	$:= \{x \in \mathbb{R}^n \ : \ F(x) \neq \emptyset\}$ the domain of the map F
$\mathrm{rge}(F)$	$:= \{y \in \mathbb{R}^n \ : \ \exists x \in \mathbb{R}^m$ such that $y \in F(x)\}$ the range of the map F
$\mathrm{gph}(F)$	$:= \{(x, y) \in \mathbb{R}^m \times \mathbb{R}^n \ : \ y \in F(x)\}$ the graph of the map F
$\mathcal{A}$	a set, often an attractor whose stability we are interested in studying
$\lvert x\rvert_{\mathcal{A}}$	$:= \inf_{a \in \mathcal{A}}(\lvert x - a\rvert)$ is the distance of the vector x to the set $\mathcal{A}$
$\mathbb{B}$	the n-dimensional closed unit ball centered at zero
$\overline{\mathrm{co}}(\mathcal{A})$	the closed convex hull of the set $\mathcal{A}$
$\mathbf{1}$	$:= (1, 1, \ldots, 1) \in \mathbb{R}^n$
$\mathrm{sat}_a(x)$	$:= \min\{a, \max\{x, -a\}\}$ the symmetric saturation function of magnitude a
$\mathrm{dz}_a(x)$	$:= x - \mathrm{sat}_a(x)$ the symmetric dead-zone function of dead-band $2a$
$\nabla f(x)$	the gradient of the function $f : \mathbb{R}^n \to \mathbb{R}$

Introduction

Linear Time-Invariant (LTI) systems are probably one of the most well-established areas in control, and more than eighty years of extensive studies produced a wide range of techniques for stabilization, regulation, inversion, identification, and model reduction. Thanks to all these powerful tools, LTI models are popular and frequently used in practice, even when they provide just a rough approximation of the physical system under consideration. For many applications, linear models are accurate enough, and nonlinearities are treated as disturbances or model imperfections, and compensated with robust or adaptive control techniques. However, this is not always possible, and some nonlinearities that are frequent in technologically relevant applications cannot be approximated as linear ones; a few examples are relays, saturation, dead-zones, and quantization. All these phenomena can create several undesired behaviors that largely deviate from a linear behavior.

The possible behaviors of LTI systems are fairly well understood. Uniform asymptotic stability is exponential, equilibrium sets are linear subspaces, and solutions are sums and products of sinusoidal, exponential and polynomial functions. Nevertheless, the presence of even a single nonlinear element destroys all the nice properties cited above, and can drastically alter the response of the system.

In order to study what happens when nonlinearity is inserted within a linear loop, one of the simplest setups that we can consider is a Single-Input Single-Output (SISO) linear system, feedback interconnected with a static nonlinearity. This problem is known in the literature as Lure problem, and it has been studied in the absolute stability framework starting from the 1940s. Typically the nonlinearity satisfies a sector condition and is in negative feedback with the linear part of the loop. Using the special structure of Lure systems and the sector condition, it is possible to obtain sharper stability results compared to fully nonlinear approaches.

In this thesis we follow this spirit, and we study three problems arising from considering the feedback interconnection of a linear block with an isolated nonlinearity. The nonlinearity can be part of the plant, or part of the controller. When the nonlinearity belongs to the plant, it is used to capture a nonlinear behavior of the physical system, while when it is part of the controller, it is usually introduced to improve a specific performance. In contrast to the classical Lure problem, the nonlinearities considered in this thesis can have a memory, they can be discontinuous, or even hybrid (they introduce a state reset into the loop).

The first nonlinearity that we consider is the play operator (also known as backlash). The play operator is a simple example of hysteresis that frequently appears in mechanical

systems. Numerous mechanical actuators and sensors possess this hysteretic characteristic, and consequently many real control loops contain a backlash-like nonlinearity. Failure to compensate for the backlash may lead to limit cycles, poor tracking performance or even instability. From a dynamical point of view, the play operator is a nonlinearity with memory, and requires an internal state to be properly described. The extra state associated to the play operator creates a compact set of equilibria, and in Chapter 2 we characterize the stability properties of this set. In the main result we prove that global exponential stability, uniform global asymptotic stability, and global pointwise asymptotic stability are all equivalent for this class of systems. We also provide a necessary and sufficient eigenvalue test to check whenever the above-mentioned stability properties hold. Finally, we show that stability is robust with respect to properly defined perturbations of the system dynamics.

The second loop that we consider contains a hybrid mechanism that is a combination of a switch and of a reset (i.e., a discontinuous change of the system state). This switching-reset mechanism is triggered by an external signal, which is mainly unknown, and which satisfies only mild regularity properties (a direct and a reverse dwell-time condition). Because the reset action introduces a discontinuity in the system state, a proper formalism and notion of solution must be used. In contrast to classical smooth ordinary differential equations with absolutely continuous solutions, here we need a notion that allows for discontinuities that we informally call "jumps". The simultaneous action of switches and resets greatly enriches the range of behaviors of this dynamical system, opening the possibility of using resets and switches to shape the response of the closed-loop system. These additional degrees of freedom are used to overcome the classical trade-off between rising time and overshoot, typical of linear control systems. The loop switches between two different linear controllers, and the resets are designed to keep the solutions well behaved during transients. The final result is a cooperation between switches and reset that achieves global exponential stability to the origin under a large class of switching signals.

The third loop involves an adaptive dead-zone, which is placed at the output injection of a Luenberger observer. This dead-zone filters out the high-frequency noise that affects the measurements and improves the observer noise sensitivity. The adaptation mechanism is designed to ensure uniform global asymptotic stability of the estimation error in the absence of noise, and input-to-state stability from the noise input. As compared to a classical Luenberger observer, we show through simulations that these "dead-zone observers" have better noise rejection properties. Moreover,we show that these observers are not restrictive for LTI systems, and that they can be designed solving a Linear Matrix Inequality (LMI). Finally, we provide a nonlinear extension for nonlinear systems in strict feedback form.

The study of the stability properties of these three loops is the main theoretical contribution of the thesis, which, however, is not limited to this. In a separate second part the switching-hybrid mechanism and the dead-zone observer are applied to automotive applications, showing the relevance of the theoretical results previously obtained.

The switching-reset mechanism is used to design a non-overshooting set-point pressure regulator for a wet clutch. For this specific application, the overshoot and the rise time are critical parameters, and the simultaneous optimization of both is a challenging problem. For this reason, we use the switching-reset mechanism to overcome the limitation between rising time and overshoot typical of linear control systems.

The adaptive dead-zone mechanism is instead used to improve the performance of the Farrelly and Wellstead kinematic observer. This observer is widely used in the automotive industry to estimate the side-slip angle of cars. The idea that we propose is to add the adaptive dead-zone at the output injection term. This augmentation results in a better noise rejection capability, and preserves the desirable features of the classical kinematic observer. Moreover, the improved noise rejection performance allows for more aggressive observer gains, which robustify the observer against accelerator biases.

Since the range of possible behaviors of these nonlinear loops is broad (discontinuous changes of the state, compact sets of equilibria, state constraints), we cast the problems into the hybrid systems framework that has been recently proposed in the literature. The generality of this framework easily accommodates for all these possible behaviors, and provides a unified language to develop stability and robustness results. Fundamental results as direct, converse Lyapunov theorem, and the invariance principle are available, and allow for a rigorous stability analysis.

The thesis starts with Chapter 1, where the hybrid system formalism is briefly recalled. The fundamental notions of hybrid inclusions, hybrid time domains, and the most common stability definitions are detailed in this chapter. All the material contained in this overview will be used throughout the rest of the thesis.

After the preliminary chapter the thesis is organized in three main blocks; 1) theoretical results, 2) applications, and 3) conclusions. The first block, named “theoretical results”, contains the main theoretical stability results. The second block, named “applications”, contains the non-overshooting pressure control for the wet clutch, and the kinematic Farrelly and Wellstead observer. Finally, the third block, named “conclusions” summarizes the results and outlines possible future developments and future research directions.

Résumé

Les systèmes linéaires à temps invariant (LTI) sont probablement l'un des domaines de contrôle les mieux établis, et plus de quatre-vingts années d'études approfondies ont produit un large éventail de techniques pour la stabilisation, la régulation, l'inversion, l'identification et la réduction de modèle. Grâce à tous ces outils puissants, les modèles LTI sont très populaires et fréquemment utilisés dans la pratique, même lorsqu'ils ne fournissent qu'une approximation du système physique considéré. Pour de nombreuses applications, les modèles linéaires sont suffisamment précis et les non-linéarités sont traitées comme des perturbations ou des imperfections du modèle et compensées par des techniques de contrôle robustes ou adaptatives. Cependant, ce n'est pas toujours possible et certaines non-linéarités qui sont fréquentes dans des applications technologiquement pertinentes ne peuvent être approximées an des fonctions linéaires : quelques exemples sont les relais, la saturation, les zones mortes et la quantification. Tout cela peut créer plusieurs comportements indésirables qui s'écartent largement d'un comportement linéaire.

Les comportements possibles des systèmes de LTI sont assez bien compris. La stabilité asymptotique uniforme est exponentielle, les ensembles d'équilibre sont des sous-espaces linéaires et les solutions sont des sommes et des produits de fonctions sinusoïdales, exponentielles et polynomiales. Néanmoins, la présence d'un seul élément non linéaire détruit toutes les belles propriétés citées ci-dessus, et peut modifier radicalement la réponse du système.

Afin d'étudier ce qui se passe lorsque la non-linéarité est insérée à l'intérieur d'une boucle linéaire, l'une des configurations les plus simples que l'on puisse envisager est un système linéaire SISO (Single-Input Single-Output), avec un retour interconnecté avec une non-linéarité statique. Ce problème est connu dans la littérature sous le nom de problème de Lure, et il a été étudié dans le cadre de la stabilité absolue à partir des années 1940. Normalement, la non-linéarité satisfait une condition de secteur et est en rétroaction négative avec la partie linéaire de la boucle. En utilisant la structure spéciale des systèmes Lure et la condition de secteur, il est possible d'obtenir des résultats de stabilité plus nets par rapport aux systèmes entièrement non linéaires.

Dans cette thèse, nous suivons cet esprit, et nous étudions trois problèmes qui se posent an système en considérant l'interconnexion par rétroaction d'un bloc linéaire avec une non-linéarité isolée. La non-linéarité peut faire partie de l'installation ou du régulateur. Lorsque la non-linéarité appartient elle est utilisé pour capturer un comportement non-linéaire du système physique, alors que lorsqu'elle fait partie du contrôleur est généralement introduite pour améliorer une performance spécifique. Contrairement au problème classique de Lure, les non-linéarités considérées dans cette thèse peuvent avoir une mémoire, elles peuvent

être discontinues, voire hybrides (elles introduisent une réinitialisation d'état dans la boucle de commande).

La première non-linéarité que nous considérons est l'opérateur de jeu (aussi connu sous le nom de jeu). L'opérateur de jeu est un exemple simple d'hystérésis qui apparaît fréquemment dans les systèmes mécaniques. De nombreux actionneurs et capteurs mécaniques possèdent cette caractéristique hystérétique et, par conséquent, de nombreuses boucles de régulation réelles contiennent une non-linéarité de type backlash. L'absence de compensation du jeu peut entraîner une limitation des cycles, des performances de suivi médiocres ou même de l'instabilité. D'un point de vue dynamique, l'opérateur de jeu est une non-linéarité avec mémoire, et nécessite un état interne pour être correctement décrit. L'état supplémentaire associé à l'opérateur de jeu crée un ensemble compact d'équilibres, et dans le Chapitre 2 nous caractérisons les propriétés de stabilité de cet ensemble. Dans le résultat principal, nous prouvons que la stabilité exponentielle globale, la stabilité asymptotique globale uniforme et la stabilité asymptotique globale par points sont toutes équivalentes pour cette classe de systèmes. Nous fournissons également un test de valeur propre nécessaire et suffisant pour vérifier chaque fois que les propriétés de stabilité mentionnées ci-dessus se maintiennent. Enfin, nous montrons que la stabilité est robuste par rapport à une perturbation bien définie de la dynamique du système.

La deuxième boucle que nous considérons contient un mécanisme hybride qui est une combinaison d'un commutateur et d'un reset (c'est-à-dire un changement discontinu de l'état du système). Ce mécanisme de remise à zéro est déclenché par un signal externe, principalement inconnu, qui ne satisfait que de faibles propriétés de régularité (une condition de temporisation directe et une condition de temporisation inverse). Parce que l'action de réinitialisation introduit une discontinuité dans l'état du système, un formalisme et une notion de solution appropriés doivent être utilisés. Contrairement aux équations différentielles ordinaires lisses classiques avec des solutions absolument continues, nous avons besoin ici d'une notion qui autorise les discontinuités que nous appelons de façon informelle des "sauts". L'action simultanée des interrupteurs et des réenclenchements enrichit considérablement l'éventail des comportements de ce système dynamique, ouvrant la possibilité d'utiliser des réenclenchements et de commuter pour façonner la réponse du système en boucle fermée. Ces degrés de liberté supplémentaires sont utilisés pour surmonter le compromis classique entre le temps ascendant et le dépassement typique des systèmes de contrôle linéaire. La boucle commute entre deux régulateurs linéaires différents, et les réinitialisations sont conçues pour conserver les solutions que nous proposons. Le résultat final est une coopération entre les commutateurs et la réinitialisation qui permet d'atteindre une stabilité exponentielle globale à l'origine sous une grande classe de signaux de commutation.

La troisième boucle implique une zone morte adaptative, qui est placée à la sortie de l'injection d'un observateur de Luenberger. Cette zone morte filtre le bruit à haute

fréquence qui affecte les mesures et améliore la sensibilité au bruit de l'observateur. Le mécanisme d'adaptation est conçu pour assurer une stabilité asymptotique globale uniforme de l'erreur d'estimation en l'absence de bruit, et pour contribuer à la stabilité de l'état en présence de celui-ci. Comparé à l'observateur classique de Luenberger, nous montrons par des simulations que ces "observateurs avec zones mortes" ont de meilleures propriétés de rejet du bruit. De plus, nous montrons que ces observateurs ne sont pas restrictifs pour les systèmes LTI, et qu'ils peuvent être conçus à partir de la résolution d' une inégalité matricielle linéaire (LMI). Enfin, nous fournissons une extension pour une classe particuliere de systèmes non-linéaires.

L'étude des propriétés de stabilité de ces trois boucles est la principale contribution théorique de la thèse, qui n'est cependant pas limitée à cela. Dans une deuxième partie séparée, le mécanisme hybride de commutation et l'observateur de zone morte sont évalués dans le contexte des applications automobiles, montrant la pertinence des résultats théoriques précédemment obtenus aussi, le mécanisme de remise à zéro est utilisé pour la conception d'un régulateur de pression de point de consigne sans dépassement pour un embrayage à bain d'huile. Pour cette application spécifique, le dépassement et le temps de montée étaient des paramètres très critiques, et l'optimisation simultanée des deux était un problème difficile. L'utilisation du mécanisme de remise à zéro a permis de surmonter la limitation entre le temps de montée et le dépassement typique des systèmes de contrôle linéaire. Le mécanisme adaptatif des zones mortes est quant-à lui plutôt utilisé pour améliorer la performance de l'observateur cinématique de Farrelly et Wellstead. Cet observateur est largement utilisé dans l'industrie automobile pour estimer l'angle de dérapage latéral dans les voitures. L'idée que nous proposons est d'ajouter la zone morte adaptative au terme d'injection de sortie. Ce changement permet d'obtenir une meilleure capacité de rejet du bruit et préserve toutes les bonnes caractéristiques de l'observateur cinématique classique. De plus, l'amélioration des performances de rejet du bruit permet des gains plus agressifs pour l'observateur, ce qui le protège contre les distorsions de l'accélérateur.

Il est egalement important de saliguer que ètant donnè que l'éventail des comportements possibles de ces boucles non linéaires est très large (changements discontinus d'état, ensembles compacts d'équilibres, contraintes d'état), nous avons abordè les problèmes dans le cadre des systèmes hybrides qui a été récemment proposé dans la littérature. La grande généralité de ce framework s'adapte facilement à tous ces comportements possibles, et fournit un langage unifié pour développer la stabilité et la robustesse du résultat. Des résultats fondamentaux comme le théorème de Lyapunov direct et inverse, et le principe d'invariance, sont disponibles, et permettent une analyse rigoureuse de la stabilité.

L'organisation du manuscrit de thése est la suivante. La thèse commence par Chapter 1, où le formalisme des systèmes dynamiques hybrides est brièvement rappelé. Les notions fondamentales d'inclusion différentielle hybride, de domaine temporel hybride et les définitions de stabilité les plus utilisées sont détaillées dans ce chapitre. Tout le matériel contenu

dans ce chapitre sera utilisé tout au long de la thèse. Après le chapitre préliminaire, la thèse est organisée en trois blocs principaux : 1) résultats théoriques, 2) applications et 3) conclusions. Le premier bloc, appelé "Résultats théoriques", contient les principaux résultats théoriques de stabilité. Le deuxième bloc, appelé "Applications", contient le contrôle de la pression sans dépassement pour l'embrayage humide et l'observateur cinématique de Farrelly et Wellstead. Enfin, le troisième bloc, intitulé "Conclusions", résume les résultats et décrit les développements futurs possibles et les orientations futures de recherche.

Chapter 1

Preliminaries on Hybrid Systems

Hybrid systems are mathematical models describing a large variety of physical and engineering systems, such as mechanical systems with impacts, analog and digital circuits, biological systems, and finite-state machines. In hybrid systems, the state evolves continuously in time or experiences instantaneous changes. Mathematically, these two possibilities are obtained through a combination of a differential equation, which is active on a special set called flow set, and of a difference equation, which is active on another set called jump set (differential and difference inclusions are also possible). This combination provides a new mathematical object (a hybrid system) with a powerful descriptive capability. State constraints have been used intensively in the context of viability theory, but it has been only recently that the viability constraints have been recognized as a useful tool to model hybrid dynamical systems. This intuition opened a completely new direction of research in the hybrid systems community, allowing for the extension of classical stability results (such as Lyapunov theorems and the invariance principle) to hybrid dynamical systems.

In this thesis, we exploit many results from this new hybrid systems framework to obtain new results for a few special nonlinear loops. In this chapter we present the hybrid systems formalism, we fix some terminology, and we recall the most relevant stability notions.

1.1 The Hybrid Systems Framework

Hybrid systems can be represented using a variety of different formalisms. In this chapter we use constrained differential and difference inclusions as a modeling tool [58]. The inclusions are constrained in the sense that they are active only on some special sets of the overall state space as will be clear soon. Formally a hybrid system is a 4-tuple (C, D, F, G), where C and D are closed subsets of $\mathbb{R}^n$ and $F : \text{dom } F \rightrightarrows \mathbb{R}^n$ and $G : \text{dom } G \rightrightarrows \mathbb{R}^n$ are set-valued maps. The hybrid system $\mathcal{H}$ is represented in the following form

$$\mathcal{H} := \begin{cases} x \in C & \dot{x} \in F(x) \\ x \in D & x^+ \in G(x), \end{cases} \tag{1.1}$$

where $x \in C \cup D$ is the state. The ordering suggests that when $x \in C$, the state obeys the differential inclusion $\dot{x} \in F(x)$, while when $x \in D$, the state obeys the difference inclusion $x^+ \in G(x)$. The symbol x^+ is used to denote the value of x after an instantaneous change. It may happen that $x \in C \cap D$; in this case, the state can evolve both according to F or G. To highlight that the differential inclusion is responsible for the continuous change of the state we name F *flow map*, and the set C where it is active *flow set*. Similarly, the difference inclusion is responsible for instantaneous (discontinuous) changes in the state; for this reason we name G *jump map*, and the set D where it is active *jump set*. It must hold that $C \subset \text{dom } F$ and $D \subset \text{dom } G$, otherwise one can restrict C and D in such a way that those conditions are met. Solutions to hybrid systems of the form (1.1) experience both flows and jumps. A convenient time parametrization that keeps track of both is provided by a generalized notion of time. We denote by $t \in \mathbb{R}_{\geq 0}$ the ordinary continuous time and by $j \in \mathbb{N}_{\geq 0}$ the number of jumps or discrete steps. The discrete time j can be interpreted as a counter that keeps track of the number of jumps that occurred. Because continuous-time solutions are defined over real intervals, and discrete recurrence are defined over integer sequences, it is quite natural to consider *hybrid time* domains as a subset of $\mathbb{R}_{\geq 0} \times \mathbb{N}_{\geq 0}$. In general, not all subsets of $\mathbb{R}_{\geq 0} \times \mathbb{N}_{\geq 0}$ are compatible with the evolution of (1.1). For this reason, we say that the solutions itself build its own hybrid time domain.

Definition 1.1 (Hybrid time domain)
A subset $E \subset \mathbb{R}_{\geq 0} \times \mathbb{N}_{\geq 0}$ is a compact hybrid time domain if

$$E = \bigcup_{j=0}^{J-1} (I^j, j), \tag{1.2}$$

where $I^j = [t_j, t_{j+1}]$, for some finite sequence of times $0 = t_0 \leq t_1 \leq t_2 \leq \cdots \leq t_J$. It is a hybrid time domain if for all $(T, J) \in E$, $E \cap ([0, T] \times \{0, 1, \ldots, J\})$ is a compact hybrid time domain.

Informally, E is a compact hybrid time domain if E is the union of a finite sequence of intervals $[t_j, t_{j+1}] \times \{j\}$, while E is a hybrid time domain if it is a union of a finite or infinite sequence of intervals $[t_j, t_{j+1}] \times \{j\}$, with the last interval (if existent) possibly being of the form $[t_j, T)$ with T finite or $T = \infty$. For each hybrid time domain, there is a lexicographical order; given (t_1, j_1), $(t_2, j_2) \in E$, $(t_1, j_1) \leq (t_2, j_2)$ if $t_1 < t_2$, or $t_1 = t_2$ and $j_1 \leq j_2$. Equivalently, as long as the points are taken from the same hybrid time domain E, $(t_1, j_1) \leq (t_2, j_2)$ if and only if $t_1 + j_1 \leq t_2 + j_2$. Points belonging to different hybrid time domains do not need to be comparable. Given a hybrid time domain E, we define

the following operators,

$$\sup_t E := \sup\{t \in \mathbb{R}_{\geq 0} : \exists j \in \mathbb{N}_{\geq 0} \text{ such that } (t,j) \in E\}, \tag{1.3a}$$

$$\sup_j E := \sup\{j \in \mathbb{N}_{\geq 0} : \exists t \in \mathbb{R}_{\geq 0} \text{ such that } (t,j) \in E\}. \tag{1.3b}$$

The operators $\sup_t$ and $\sup_j$ on a hybrid time domain E return the supremum of the t and j coordinates respectively. Furthermore, $\sup E := (\sup_t E, \sup_j E)$ and length $E := \sup_t E + \sup_j E$.

Hybrid time domains allow for a precise definition of solution of (1.1). In the literature, there are many different solution notions for hybrid systems and sometimes they are called with different names such as *execution* and *trajectory*. The notion that we use in this manuscript is taken from [59].

Definition 1.2 (Hybrid arc)
A function $\phi : E \to \mathbb{R}^n$ is a hybrid arc if E is a hybrid time domain and if for each $j \in \mathbb{N}_{\geq 0}$, the function $t \mapsto \phi(t,j)$ is locally absolutely continuous on the interval $I^j := \{t : (t,j) \in E\}$.

It is worth to notice that a hybrid arc ϕ is differentiable almost everywhere on I^j. To compact the notation we denote by $\dot{\phi} := \dot{\phi}(t,j) := \mathrm{d}\phi(t,j)/\,\mathrm{d}t$, the standard derivative of ϕ with respect to t (whenever it exists), and by $\phi^+ := \phi^+(t,j) := \phi(t,j+1)$ the value of ϕ at $(t,j+1)$, i.e. after a jump. Given a hybrid arc ϕ, the notation dom ϕ represents its domain, which is a hybrid time domain. It is interesting to notice that the hybrid arc itself can be thought of as a *multivalued map*, $\phi : \mathbb{R}^2 \rightrightarrows \mathbb{R}^n$ that is single-valued on its domain dom ϕ. The domain of a hybrid arc ϕ is a hybrid time domain, and is then the subset of $\mathbb{R}_{\geq 0} \times \mathbb{N}_{\geq 0}$ where $\phi(t,j) \neq \emptyset$. This highlights the fact that solutions define their own hybrid time domains, and not vice-versa. This fact is especially true for hybrid systems where the relationship between solutions and time domains is more complicated than for ordinary differential equations or difference equations. According to the type of hybrid time-domains possessed by a solution, we can distinguish the following cases.

Definition 1.3 (Types of hybrid arcs)
A hybrid arc ϕ is called: (1) nontrivial *if* dom ϕ *contains at least two points, (2)* complete *if* dom ϕ *is unbounded i.e., if* length $E = \infty$*, (3)* Zeno *if it is complete and* $\sup_t$ dom $\phi < \infty$*, (4)* eventually discrete *if* $T = \sup_t$ dom $\phi < \infty$ *and* dom $\phi \cap (\{T\} \times \mathbb{N}_{\geq 0})$ *contains at least two points, (5)* discrete *if it is nontrivial and* dom $\phi \subset \{0\} \times \mathbb{N}$*, (6)* eventually continuous *if* $J = \sup_j$ dom $\phi < \infty$ *and* dom $\phi \cap (\mathbb{R}_{\geq 0} \times \{J\})$ *contains at least two points, (7)* continuous *if it is nontrivial and* dom $\phi \subset \mathbb{R}_{\geq 0} \times \{0\}$*, (8)* compact *if* dom ϕ *is compact.*

1.2 Hybrid Solutions and Their Properties

Informally given a hybrid system $\mathcal{H}$, its solutions are hybrid arcs ϕ that satisfy the flow map when $x \in C$, and the jump map when $x \in D$.

Definition 1.4 (Solution to a hybrid system)
A hybrid arc ϕ is a solution to the hybrid system $\mathcal{H}$ if $\phi(0,0) \in \overline{C} \cup D$, and

- *for all $j \in \mathbb{N}_{\geq 0}$ such that $I^j := \{t : (t,j) \in \text{dom } \phi\}$ has nonempty interior $\phi(t,j) \in C$ for all $t \in \text{int } I^j$, and $\dot{\phi}(t,j) \in F(\phi(t,j))$ for almost all $t \in I^j$,*

- *for all $(t,j) \in \text{dom } \phi$ such that $(t, j+1) \in \text{dom } \phi$, $\phi(t,j) \in D$, and $\phi(t,j+1) \in G(\phi(t,j))$.*

The definition is quite broad. It does not require that $\phi(t,j) \in C$ at the endpoints of I^j, nor does it insist that $\phi(t,j) \notin D$ when $t \in \text{int } I^j$. Moreover, we do not require completeness or uniqueness of the solutions. This should not be surprising, because nonuniqueness and non completeness are already possible behaviours of ordinary differential equations. For example, continuity of the vector field ensures existence of the solutions, but uniqueness requires additional properties, such as Lipschitz right hand sides. The multitude of solutions is even more accentuated in hybrid systems of the form (1.1), where it may be due to the multivalued nature of the vector fields, or to an overlap of the flow and jump sets.

Definition 1.5 (Complete solution)
A solution ϕ to $\mathcal{H}$ is (forward) complete if dom ϕ *is unbounded.*

Definition 1.6 (Maximal solution)
A solution ϕ_1 to $\mathcal{H}$ is maximal if there does not exist another solution ϕ_2 to $\mathcal{H}$ such that dom ϕ_1 *is a proper subset of* dom ϕ_2 *and $\phi_1(t,j) = \phi_2(t,j)$ for all $(t,j) \in$ dom ϕ_1.*

Clearly, complete solutions are maximal, but the converse statement is not true. We denote by $\mathcal{S}_{\mathcal{H}}(S)$ the set of all maximal solutions ϕ to $\mathcal{H}$ with $\phi(0,0) \in S$. If the set S is not mentioned, $\phi \in \mathcal{S}_{\mathcal{H}}$ means that ϕ is a maximal solution to $\mathcal{H}$, or in other words, $\mathcal{S}_{\mathcal{H}} := \mathcal{S}_{\mathcal{H}}(\overline{C} \cup D)$.

1.3 Stability for Hybrid Systems

The classical Lyapunov theory deals with stability of a single equilibrium for continuous-time or discrete-time systems. In hybrid systems of the form (1.1) stability concepts need to be generalized or interpreted from a different perspective. The state of hybrid systems often contains logic variables or timers that keep changing and do not converge to any special value. Those variables are used for modeling purposes, but they are unimportant for the goal of stability analysis. Then, it is necessary to study the stability of only a part of the state, or in other words we do not care about the value assumed by certain variables in the overall state of the hybrid system. An elegant approach is then to generalize stability from points to sets considering a distance function of the form

$$|x|_{\mathcal{A}} := \text{dist}(x, \mathcal{A}) := \inf_{y \in \mathcal{A}} |x - y|. \tag{1.4}$$

Here we assume that $\mathcal{A}$ is a closed subset of $\mathbb{R}^n$. Another conceptual difficulty comes from considering solutions that are constrained in the sets C and D. Because of these constraints, solutions to (1.1) do not need to be complete and the notion of Lyapunov stability needs to be correctly interpreted. We believe that completeness and stability are rather different properties and they should not depend on each other. According with this interpretation the definition of Lyapunov stability that we employ here does not require completeness of solutions. This definition includes trajectories that may look unstable, but that are instead Lyapunov stable because their domain is bounded (they are not complete).

Definition 1.7 (Lyapunov stability)
Let $\mathcal{A} \subset \mathbb{R}^n$ be closed. We say that $\mathcal{A}$ is Lyapunov stable if for each $\epsilon > 0$, there exists $\delta > 0$ such that $|x(0,0)|_{\mathcal{A}} \leq \delta$ implies $|x(t,j)|_{\mathcal{A}} \leq \epsilon$ for all $(t,j) \in \text{dom } \phi$.

Remark 1.1
Notice that Lyapunov stability of $\mathcal{A}$ is a local concept. Solutions stay close to $\mathcal{A}$ only if they start in a proper neighborhood of $\mathcal{A}$. Once again we stress that, in general, existence, uniqueness or completeness of the solutions are not required for Lyapunov stability. ⌟

Definition 1.8 (Basin of attraction)
The basin of attraction $\mathcal{B}_{\mathcal{A}} \subset \mathbb{R}^n$ for the set $\mathcal{A} \subset \mathbb{R}^n$ is the set of initial conditions from which there are no finite escape times, and all complete solutions $\phi \in \mathcal{S}_{\mathcal{H}}(\mathcal{B}_{\mathcal{A}})$ satisfy $\lim_{t+j\to\infty} |\phi(t,j)|_{\mathcal{A}} = 0$ for $(t,j) \in \text{dom } \phi$.

Remark 1.2
Points outside $\overline{C} \cup D$ are in the basin of attraction of $\mathcal{A}$ because the arising solutions do not exhibit finite escape time and are not complete. Moreover, under the hybrid basic conditions discussed in Definition 1.19, the basin of attraction $\mathcal{B}_{\mathcal{A}}$ of a compact attractor $\mathcal{A}$ that is locally asymptotically stable is an open set. ⌟

Definition 1.9 (Local attractivity)

Let $\mathcal{A} \subset \mathbb{R}^n$ be closed. The set $\mathcal{A}$ is said to be attractive if there exists $\epsilon > 0$ such that $\mathcal{A} + \epsilon\mathbb{B} \subset \mathcal{B}_\mathcal{A}$.

In other words a set $\mathcal{A}$ is locally attractive if the basin of attraction contains an inflation of $\mathcal{A}$; if the basin of attraction of $\mathcal{A}$ coincides with $\mathbb{R}^n$, we say that $\mathcal{A}$ is globally attractive.

Definition 1.10 (Global attractivity)
Let $\mathcal{A}$ be closed. The set $\mathcal{A}$ is globally attractive if $\mathcal{B}_A = \mathbb{R}^n$.

Global attractivity is a desirable and strong property, but alone does not guarantee robustness with respect to perturbations and unmodeled dynamics. What is missing is a uniform speed of convergence with respect to compact sets of initial conditions. The addition of this uniformity property makes the attractivity robust and thus provides a more desirable property that we define as uniform attractivity.

Definition 1.11 (Uniform Global Attractivity)
Let $\mathcal{A} \subset \mathbb{R}^n$ be closed. The set $\mathcal{A}$ is Uniformly Globally Attractive for $\mathcal{H}$ if for each $\epsilon > 0$ and $r > 0$, there exists $T > 0$ such that, for any solution ϕ to $\mathcal{H}$ with $|\phi(0,0)|_\mathcal{A} \leq r$, $(t,j) \in \text{dom } \phi$ and $t + j \geq T$ imply $|\phi(t,j)| \leq \epsilon$. The property is local if it holds for small enough values of r.

Definition 1.12 (Uniform Local Asymptotic Stability)
Let $\mathcal{A} \subset \mathbb{R}^n$ be closed. We way that $\mathcal{A}$ is Uniformly Locally Asymptotically Stable (ULAS) if it is Lyapunov stable and uniformly locally attractive.

Definition 1.13 (Uniform Global Asymptotic Stability)
Let $\mathcal{A} \subset \mathbb{R}^n$ be closed. We way that $\mathcal{A}$ is Uniformly Globally Asymptotically Stable (UGAS) if it is Lyapunov stable and uniformly globally attractive.

The definitions above involve $\delta - \epsilon$ arguments, but from an operative point of view, it is often convenient to work with comparison functions.

Definition 1.14 (Class-$\mathcal{K}_\infty$ function)
A function $\alpha : \mathbb{R}_{\geq 0} \to \mathbb{R}_{\geq 0}$ is class $\mathcal{K}_\infty$ function, also written $\alpha \in \mathcal{K}_\infty$, if α is zero at zero, continuous, strictly increasing, and unbounded.

It is worth to notice that a class $\mathcal{K}_\infty$ function does not need to be differentiable.

Definition 1.15 (Uniform Global Stability)
A closed set $\mathcal{A}$ is Uniformly Globally Stable (UGS) for $\mathcal{H}$, if there exists a class $\mathcal{K}_\infty$ function α such that any solution ϕ to $\mathcal{H}$ satisfies $|\phi(t,j)|_\mathcal{A} \leq \alpha(|\phi(0,0)|_\mathcal{A})$ for all $(t,j) \in \text{dom } \phi$.

It is worth to notice that Definition 1.15 ensures that all solutions remain contained in a ball of radius $\alpha(|\phi(0,0)|_{\mathcal{A}})$, and that the radius of the ball increases continuously with $|\phi(0,0)|_{\mathcal{A}}$. The notion of Uniform Global Asymptotic Stability can be captured also using a class-$\mathcal{KL}$ function as follows.

Definition 1.16 (Class-$\mathcal{KL}$ functions)
A function $\beta : \mathbb{R}_{\geq 0} \times \mathbb{R}_{\geq 0} \to \mathbb{R}_{\geq 0}$ is a class-$\mathcal{KL}$ function, also written $\beta \in \mathcal{KL}$, if it is non-decreasing in its first argument, non-increasing in its second argument, $\lim_{r \to 0^+} \beta(r,s) = 0$ for each $s \in \mathbb{R}_{\geq 0}$, and $\lim_{s \to \infty} \beta(r,s) = 0$ for each $r \in \mathbb{R}_{\geq 0}$.

The notion of class-$\mathcal{KL}$ function can be used to conveniently combine global stability and uniform global attractivity into a convenient single bound.

Theorem 1.1 (Equivalence of UGAS and class-$\mathcal{KL}$ bound)
Let $\mathcal{H}$ be a hybrid system and $\mathcal{A} \subset \mathbb{R}^n$ be closed. The following statements are equivalent:

- *The set $\mathcal{A}$ is UGAS for $\mathcal{H}$.*
- *There exists a class-$\mathcal{KL}$ function β such that any solution ϕ to $\mathcal{H}$ satisfies*

$$|\phi(t,j)|_{\mathcal{A}} \leq \beta(|\phi(0,0)|_{\mathcal{A}}, t+j), \quad \forall (t,j) \in \text{dom } \phi.$$

We can also think of the $class-\mathcal{KL}$ function β as the product between a suitable $\mathcal{K}_\infty$ function and an exponentially decaying function measuring $t+j$. This implies that when the distance to the set $\mathcal{A}$ is viewed through an appropriate function, the convergence rate toward the attractor appears to be exponential. This idea is due to Massera and Sontag (see [110, Proposition 7], and Section 12 of [83]) and it is formalized in the following lemma.

Lemma 1.1 (Massera-Sontag Lemma on class-$\mathcal{KL}$ functions.)
For each class-$\mathcal{KL}$ function β and each $\lambda \in \mathbb{R}_{>0}$ there exists a class-$\mathcal{K}_\infty$ functions α_1, α_2 such that, for all $r, s \in \mathbb{R}_{\geq 0}$, $\alpha_1(\beta(r,s)) \leq \alpha_2(r)\mathrm{e}^{-\lambda s}$.

Using the Massera-Sontag Lemma 1.1 we can easily provide an alternative representation for UGAS stability in terms only of $\mathcal{K}_\infty$ functions.

Theorem 1.2 (UGAS stability with $\mathcal{K}_\infty$ functions)
Let $\mathcal{H}$ be a hybrid system and $\mathcal{A} \subset \mathbb{R}^n$ be closed. The following statements are equivalent:

- *The set $\mathcal{A}$ is UGAS for $\mathcal{H}$.*
- *For each $\lambda \in \mathbb{R}_{>0}$ there exist $\mathcal{K}_\infty$ functions α_1 and α_2 such that any solution ϕ to $\mathcal{H}$*

satisfies

$$\alpha_1(|\phi(t,j)|_{\mathcal{A}}) \leq \alpha_2(|\phi(0,0)|_{\mathcal{A}})\mathrm{e}^{-\lambda(t+j)} \quad \forall (t,j) \in \mathrm{dom}\ \phi.$$

Further details about equivalent characterizations of uniform global asymptotic stability for hybrid systems can be found in [58, pag. 68].

A special case of uniform global stability for hybrid systems is when the convergence happens to be exponential, and the "overshoot" grows linearly with the distance of the initial condition with respect to the attractor $\mathcal{A}$, we call this property Global Exponential Stability (GES). For hybrid systems the notion of GES has been introduced in [117].

Definition 1.17 (Global Exponential Stability)
Let $\mathcal{A}$ be compact. The set $\mathcal{A}$ is globally exponentially stable (GES) for $\mathcal{H}$, if there exist $m > 0$, $\lambda > 0$ such that all solutions satisfy $|\phi(t,j)|_{\mathcal{A}} \leq m \exp(-\lambda(t+j))|x(0,0)|_{\mathcal{A}}$, for all $(t,j) \in \mathrm{dom}(\phi)$.

Neither Uniform Global Asymptotic Stability nor Global Exponential Stability imply that the solutions converge to a specific point in $\mathcal{A}$. Both only establish convergence in terms of distance; hence oscillations and curling phenomena are possible while approaching $\mathcal{A}$. These possibilities are ruled out by a related, but stronger property called Global Pointwise Asymptotic Stability (GPAS) that has been introduced in the present form in [94].

Definition 1.18 (Global Pointwise Asymptotic Stability)
A compact attractor $\mathcal{A}$ is Globally Pointwise Asymptotically Stable (GPAS) for $\mathcal{H}$ if:

- *every $a \in \mathcal{A}$ is Lyapunov stable, that is, for every $\epsilon > 0$ there exists $\delta > 0$ such that every solution ϕ to $\mathcal{H}$ with $|\phi(0,0) - a| \leq \delta$ satisfies $|\phi(t,j) - a| \leq \epsilon$, for all $(t,j) \in \mathrm{dom}\ \phi$,*
- *for every solution ϕ to $\mathcal{H}$, there exists $a \in \mathcal{A}$ such that $\lim_{t+j\to+\infty} \phi(t,j) = a$.*

It is important to mention that in general asymptotic stability in the usual set sense, and Lyapunov stability of every point of the attractor are not sufficient to conclude global pointwise asymptotic stability [16].

In this thesis, we always assume that the hybrid systems under consideration satisfy some regularity properties called *hybrid basic conditions*. The hybrid basic conditions guarantee the existence of solutions, but more importantly, they enable proving the converse Lyapunov theorems, which imply robustness of uniform global/local stability. Because hybrid systems are more complicated than ordinary continuous or discrete time systems, also

the robustness concept requires some attention. Robustness for a compact set of equilibria is considered with respect to properly defined perturbations of the flow/jump maps and flow/jump sets. For more details we refer the reader to [58, Ch. 6].

Definition 1.19 (Hybrid basic conditions (HBCs))
We say that $\mathcal{H}$ satisfies the hybrid basic conditions if:

- *C and D are closed subsets of $\mathbb{R}^n$,*
- *$F : \text{dom } F \rightrightarrows \mathbb{R}^n$ is outer semicontinuous and locally bounded relative to C, $C \subset \text{dom } F$, and $F(x)$ is convex for every $x \in C$,*
- *$G : \text{dom } G \rightrightarrows \mathbb{R}^n$ is outer semicontinuous and locally bounded relative to D, and $D \subset \text{dom } G$.*

One way to obtain the above properties is to use the Krasovskii regularization, for more details see [58].

In order to investigate the robustness properties of compact sets, we consider a perturbed version of the hybrid system presented in (1.1). The perturbation is set-valued, and produces a ρ-inflated version of (1.1) defined as follows [58, Chapter 7].

Definition 1.20
Given a hybrid system $\mathcal{H}$ and a continuous function $\rho : \mathbb{R}^n \to \mathbb{R}_{\geq 0}$, the ρ-perturbation of $\mathcal{H}$, denoted by $\mathcal{H}_\rho$ is the hybrid system

$$\mathcal{H}_\rho := \begin{cases} x \in C_\rho & \dot{x} \in F_\rho(x) \\ x \in D_\rho & x^+ \in G_\rho(x), \end{cases} \tag{1.5}$$

where

$$\begin{aligned} C_\rho &:= \{x \in \mathbb{R}^n : (x + \rho(x)\mathbb{B}) \cap C \neq \emptyset\}, \\ F_\rho(x) &:= \overline{\text{co}}\ F((x + \rho(x)\mathbb{B}) \cap C) + \rho(x)\mathbb{B}, \quad \forall x \in C_\rho, \\ D_\rho &:= \{x \in \mathbb{R}^n : (x + \rho(x)\mathbb{B}) \cap D \neq \emptyset\}, \\ G_\rho(x) &:= \{v \in \mathbb{R}^n : v \in g + \rho(x)\mathbb{B},\ g \in G((x + \rho(x)\mathbb{B}) \cap D)\}, \quad \forall x \in D_\rho. \end{aligned}$$

The notion of inflated hybrid system can be conveniently used to study the robustness properties of compact sets. Below we report the definition of robust uniform global asymptotic stability, uniform global pointwise asymptotic stability and robust global exponential stability.

Definition 1.21 (Robustness)
A compact attractor $\mathcal{A}$ is robustly uniformly globally asymptotically stable, (resp. robustly globally pointwise asymptotically state, resp. robustly exponentially stable) for $\mathcal{H}$, if there exists a continuous function $\rho : \mathbb{R}^n \to \mathbb{R}_{\geq 0}$ that is positive on $\mathbb{R}^n \backslash \mathcal{A}$ and such that $\mathcal{A}$ is globally asymptotically stable (resp. robustly globally pointwise asymptotically state, resp. robustly exponentially stable) for $\mathcal{H}_\rho$.

In many applications, it is interesting to study how a dynamical system behaves when affected by external signals, for this reason, a relevant class of dynamical systems is the hybrid systems with inputs. Consider a hybrid system $\mathcal{H}_u$ with state x and input (or disturbance) u as follows

$$\mathcal{H}_u := \begin{cases} (x,u) \in C \times C_u & \dot{x} \in F(x,u) \\ (x,u) \in D \times D_u & x^+ \in G(x,u), \end{cases} \tag{1.6}$$

where C_u and D_u are proper subsets of the input space $\mathbb{R}^m$. Given any hybrid input $u : \text{dom } u \mapsto \mathbb{R}^m$, let $(t_1, j_1) \in \text{dom } u$ and $(t_2, j_2) \in \text{dom } u$ satisfy$(t_1, j_1) \preceq (t_2, j_2)$ and define

$$||u||_{[(t_1,j_1),(t_2,j_2)]} := \max \left\{ \text{ess} \sup_{(t,j) \in \text{dom } u \backslash \Theta(u),\ (t_1,j_1) \preceq (t,j) \preceq (t_2,j_2)} , \sup_{(t,j) \in \Theta(u),\ (t_1,j_1) \preceq (t,j) \preceq (t_2,j_2)} |u(t,j)| \right\},$$

where $\Theta(u)$ denotes the set of all $(t, j) \in \text{dom } u$ such that $(t, j + 1) \in \text{dom } (u)$. To shorten the notation we define $||u||_{[(0,0),(t_2,j_2)]}$ as $||u||_{(t_2,j_2)}$. We denote by $\mathcal{S}_u(x)$ the set of all maximal solution pairs (ϕ, u) to $\mathcal{H}_u$ with $\phi(0, 0) = x \in C \cup D$ and finite $||u||_{(\sup \text{ dom } u)}$.

Definition 1.22 (Input-to-State stability (ISS) [28])
System $\mathcal{H}_u$ is Input-to-state stable (ISS) with respect to a compact set $\mathcal{A}$ if there exist a class $\mathcal{KL}$ function β and a class $\mathcal{K}$ function γ such that, for each $x \in C \cup D$ each solution pair $(\phi, u) \in \mathcal{S}_u(x)$ satisfies

$$|\phi(t,j)|_{\mathcal{A}} \leq \beta(|\phi(0,0)|_{\mathcal{A}}, t + j) + \gamma(||u||_{(t,j)}), \quad \forall (t,j) \in \text{dom } \phi.$$

The definition above resembles the standard notion of ISS for continuous and discrete time systems, however, a distinguishing feature of ISS for hybrid systems is that solutions are not guaranteed to be complete.

Part I
Theoretical results

Chapter 2

Stability Results for SISO Linear Systems Feedback with Play and Stop Operators

---

In this chapter we study the feedback interconnection of a strictly proper linear system with two simple nonlinear elements with memory, play and stop. This setup frequently arises in mechanics, aerodynamics, and electromagnetic applications, where play and stop can be used as elementary blocks to build complex hysteresis models. The presence of play and stop may produce a richness of nonlinear behaviors, ranging from stable limit cycles to continuum sets of equilibria (multistability). We focus on the characterization of multiple attracting equilibria in single-input, single-output systems feedback with play/stop. We assume that disregarding the presence of play/stop, the feedback loop is globally exponentially stable, and we show that assuming the existence of a common quadratic Lyapunov function between a special matrix pair, the presence of these nonlinearities creates a compact set of equilibria. We propose a simple necessary and sufficient LMI condition testing the existence of a common Lyapunov function, and we show that, in case of an affirmative answer, the set of equilibria is globally exponentially stable. Additionaly we prove the equivalence between robust global exponential stability and robust global pointwise asymptotic stability for the class of systems under investigation. We formulate play and stop as constrained differential inclusions and we link our formulation with other models in the literature. Finally, we illustrate our findings through a few examples. The results presented in this chapter are adapted from [37] and [38].

2.1 Introduction

The study of the stability properties of linear systems in feedback loop with an isolated nonlinearity is a classical topic that dates back to the seminal work of Lure [81]. Common (static) nonlinearities are saturation, dead-zone, and quantization, which often occur in real applications, and for this reason Lure systems are still an active area of research [23, 24]. To study the stability of these loops many tools have been developed; a few examples

are sector conditions, circle criteria, passivity and integral quadratic constraints. All these tools can be effectively formulated as convex problems [22], making the stability analysis numerically tractable. Although Lure systems are a fairly general class of systems, many relevant physical phenomena show a path dependent behavior that is generically called hysteresis. Hysteresis cannot be described using a static nonlinearity but requires a memory effect that can be obtained by introducing additional memory. For example, hysteresis can be obtained through properly formulated operators [27], [39], discontinuous differential equations [13], variational inequalities [123] or differential inclusions.

One of the simplest example of hysteresis is the play, also known in mechanical engineering as backlash. Despite its simplicity, the play has an important role in the description of numerous physical phenomena, such as plasticity, friction, and magnetization [123]. Well studied examples are gear train systems, shape memory actuators, and electric transformers. Play is often associated to a degradation of performance and with a reduction of controllability, and this is the reason why much effort has been devoted to designing control laws that are able to compensate these undesired side effects [112, 127, 43, 92, 95, 69]. It is well known that the presence of play in the actuator and the lack of a proper compensation strategy can result in persistent oscillations and poor tracking performance [92]. For these reasons we believe that it is important to understand the behavior of dynamical systems in the presence of hysteretic elements.

In this chapter we focus on the analysis of a simple system with great practical relevance. We consider a Lure like setup, where a linear single-input single-output system is feedback interconnected with play/stop. For this interconnection we establish the equivalence between robust global exponential stability, and robust global pointwise asymptotic stability, providing a numerically tractable LMIs test. We hope that the precise characterization of this simple setup may lead to interesting extensions in the future.

2.1.1 Literature review

In this work the play is formulated using a constrained differential inclusion, that turns out to be equivalent to a discontinuous differential equation. Existence and regularity of solutions for these types of formulations can be deduced from general results for discontinuous differential equations [63] or differential inclusions [42]. A more specific result has been obtained in [77], where the authors consider the feedback interconnection of a nonlinear differential equation with a play operator. Stability results appeared for the first time in [124], where different types of hysteresis elements are considered. Building up from these results, further developments are scattered in different areas of systems and control such as absolute stability, passivity and operator theory [14], [78], [61]. More recently the problem of providing a numerically tractable outer approximations of the omega-limit set for linear

systems in feedback with hysteresis operators has been addressed in [113] and [114] using an LMI-based formulation.

2.1.2 Contributions

The contributions of the work presented in this chapter are threefold. First, we explicitly characterize the compact set of equilibria created by the play. Therefore, as compared to [113] and [114], we do not aim at establishing conservative bounds, but we provide an exact characterization.

Second, we re-interpret the results in [124] providing a simple algebraic condition that ensure robust global exponential stability of the equilibrium set. In contrast to [124, Theorems 3, 4], which establishes exponential convergence under a Hurwitz stability assumption plus an additional frequency-domain condition, we replace the frequency-condition with a state space formulation that can be easily tested numerically. We also refine upon [124, Theorem 5], which establishes convergence for the special case of a single integrator plant. In particular, we show that for the single integrator case the convergence is not exponential, see also Example 2.5.1.

Third, we show that the equilibrium set is made of robustly Lyapunov stable equilibria and that all trajectories converge exactly to one point inside the set. We call this property global pointwise asymptotic stability. Finally, for the class of systems under investigation, we show that robust global exponential stability and robust global pointwise asymptotic stability are equivalent.

2.1.3 Chapter organization

The chapter is organized as follows: Section 2.2 presents the problem formulation and the main result. Models for play and stop are formulated in Section 2.3. In Section 2.3 we discuss existence, uniqueness and continuous dependence on initial data of the solutions. We also relate our play and stop models with others in the literature and, under mild regularity assumptions, we show their equivalence. Section 2.4 contains the proof of the main result and two lemmas of independent interest. Finally Section 2.5 presents two examples to show the effectiveness of the theoretical findings. Conclusions and future research directions are offered in Section 2.6.

2.2 Problem formulation and main result

We consider the feedback interconnection of a single-input single-output (SISO) linear system with the play and stop operators. The two representations are complementary because of the following identity[1], see [123],

$$\mathscr{P} + \mathscr{S} = \mathscr{I}, \tag{2.1}$$

where $\mathscr{P}$ is the play, $\mathscr{S}$ is the stop and $\mathscr{I}$ is the identity operator. A pictorial representation of the two systems under investigation is shown in (2.2) and (2.3), and using (2.1) we deduce that $A_1 := A + BK$.

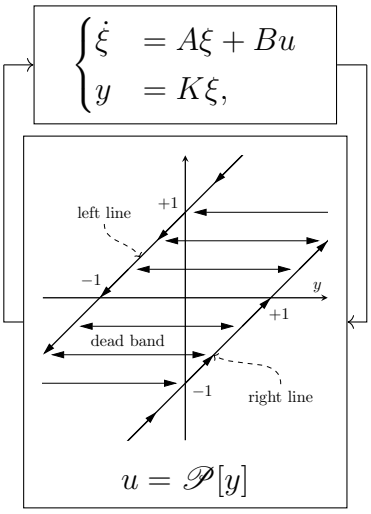

(2.2)

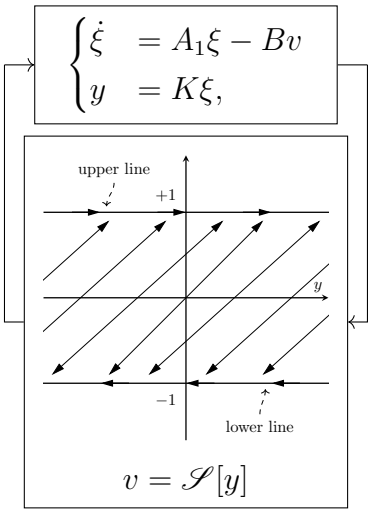

(2.3)

In (2.2) and (2.3), $\xi \in \mathbb{R}^m$ is the state associated to the linear part of the system, while $u \in \mathbb{R}$ and $v \in \mathbb{R}$ are additional states keeping memory of the play and the stop output. We use square brackets to stress that play and stop operators depend on the entire history of y and not only by its instantaneous value [2].

The qualitative behavior of play and stop is as follows. The output of the play remains constant whenever the pair (y, u) belongs to the region between the left and the right line, it positively increases as $\dot{u} = \dot{y} \geq 0$ when (y, u) belongs to the right line and negatively decreases as $\dot{u} = \dot{y} \leq 0$ when (y, u) belongs to the left line. Similarly the output of the stop changes as $\dot{v} = \dot{y}$ whenever (y, v) is between the upper/lower line, and remains constant when (y, v) belongs to the upper/lower line. From this description we can already

[1]Play and stop operators can be thought of as transformations with an internal memory. Their output not only depends on the instantaneous value of y, but on its whole history plus an initial condition. Notice also that identity (2.1) requires proper initial conditions to hold.

[2]Initial conditions for play and stop are not free, but must be consistent. In the case of play $(y(0), u(0))$ must belong to the strip between the right and the left line, while in the case of stop $(y(0), v(0))$ must belong to strip between the upper and the lower line.

understand that this response can be well described using a discontinuous differential equation, whose vector field changes across the lines pictured in (2.2) and (2.3). To simplify the presentation we will assume that play and stop have a specific shape, however the results presented in this chapter apply to more general play and stop operators [3].

Assumption 2.1
Play has unitary slope, the dead-band is centered in zero and has width equal to 2*.*

Assumption 2.1 ensures that the stop is centered around the zero of the vertical line and that $v \in [-1, 1]$. Using Assumption 2.1 and (2.1) we define an attractor $\mathcal{A}$ of candidate equilibrium points. With a slight abuse of notation we denote by $\mathcal{A}$ both the set of equilibria for (2.2) and for (2.3). Geometrically the set of points is the same, but is parametrized using two different sets of coordinates.

$$\begin{aligned} \mathcal{A} :&= \{(\xi, u) \in \mathbb{R}^m \times \mathbb{R} : K\xi - 1 \leq u \leq K\xi + 1 \text{ and } 0 = A\xi + Bu\} \\ &= \{(\xi, v) \in \mathbb{R}^m \times [-1, 1] : 0 = A_1\xi - Bv\}. \end{aligned} \tag{2.4}$$

Assumption 2.2
The matrix A_1 is Hurwitz, and shares with $A_2 := (I - A_1^{-1}BK)A_1$ a Common Quadratic Lyapunov Function (CQLF).

The matrix A_2 posses a particular structure, and it can be seen as the matrix A under the change of coordinates A_1, indeed the following Lemma holds.

Lemma 2.1
If A_1 is Hurwitz, then $\text{eig}(A_2) = \text{eig}(A)$*.*

Proof. Recalling that $A_1 := A + BK$, and using a few manipulations, we get $A_2 = (I - A_1^{-1}BK)A_1 = A_1^{-1}(A_1 - BK)A_1 = A_1^{-1}AA_1$, which shows that A_2 coincides with A under the change of coordinates A_1 (which is nonsingular by assumption). □

Moreover, if the pair (A, B) is controllable and A_1 is Hurwitz, then also (A_1, B) is controllable. To show this we can apply the Popov-Belevitch-Hautus test [64] to obtain

$$\text{rank } [A_1 - \lambda I, B] = \text{rank } \left([A + BK - \lambda I, B] \begin{bmatrix} I & 0 \\ -K & 1 \end{bmatrix} \right) = \text{rank } [A - \lambda I, B] = n,$$

[3] The only restriction required in (2.1) is that the slopes of the right (respectively upper) and left (respectively lower) lines coincide, otherwise the play (respectively the stop) degenerates into a different hysteresis operator.

for all $\lambda \in \mathbb{C}$, which shows that (A_1, B) is controllable as well. Another interesting observation is that A_1 and A_2 differ for a rank one perturbation, indeed rank $(A_1 - A_2) =$ rank $(A_1^{-1}BKA_1) \geq 1$, and rank $(A_1^{-1}BKA_1) \leq \min\{\text{rank } (A_1^{-1}BK), \text{rank } (A_1)\} = 1$. This observation can be used in combination with the following Lemma [108], [74], to reformulate Assumption 2.2 in a different manner.

Lemma 2.2
Let A_1, A_2 be two Hurwitz matrices in $\mathbb{R}^{m\times m}$ with rank $(A_1 - A_2) = 1$. *A necessary and sufficient condition for the existence of a common quadratic Lyapunov function (CQLF) for A_1, A_2 is that the matrix pencil $A_1^{-1} + \gamma A_2$ is non-singular for all $\gamma \in [0, +\infty)$.*

We are now ready to state the main result of this chapter, which provides a characterization of many equivalent stability properties for $\mathcal{A}$.

Theorem 2.1
If Assumptions 2.1 and 2.2 hold true, then the attractor $\mathcal{A}$ is Globally Expontially Stable and the following statements are equivalent:

(i) $\mathcal{A}$ is Globally Exponentially Stable (GES),

(ii) $\mathcal{A}$ is Robustly Exponentially Stable (RGES),

(iii) $\mathcal{A}$ is Global Pointwise Asymptotically Stable (GPAS),

(iv) $\mathcal{A}$ is Robustly Global Pointwise Asymptotically Stable (RGPAS).

Theorem 2.1 provides many desirable and equivalent stability properties for the attractor $\mathcal{A}$, which can arise frequently in many relevant applications. For example, the block diagram in (2.2) may represent a linear mechanical system to be controlled through an actuator subject to backlash. In this scenario, the play is interpreted as the mechanical backlash of the actuator and it is standard to assume that (A, B) is controllable (or stabilizable) so that it is possible to find a vector K such that $A + BK := A_1$ is Hurwitz.

2.3 Differential models for play and stop

In this section we propose models for play and stop operators. These models are formulated as constrained differential equations with discontinuous right-hand side, but to

ensure existence and regularity of solutions we consider a regularized version according to Krasovskii, yielding constrained differential inclusions.

According to the qualitative description in Section 2.2 the play dynamics can be formulated using the following constrained differential equation,

$$(y-u) \in [-1,1] \quad \dot{u} = P_d(y-u,\dot{y}) := \begin{cases} \dot{y} - \max\{\dot{y},0\} & \text{if } y-u=-1 \\ 0 & \text{if } y-u \in (-1,1)\,, \\ \dot{y} - \min\{\dot{y},0\} & \text{if } y-u=1 \end{cases} \tag{2.5}$$

where the vector field P_d is discontinuous. Similarly, the stop dynamics yields

$$v \in [-1,1] \quad \dot{v} = S_d(v,\dot{y}) := \begin{cases} \max\{\dot{y},0\} & \text{if } v=-1 \\ \dot{y} & \text{if } v \in (-1,1)\,, \\ \min\{\dot{y},0\} & \text{if } v=1 \end{cases} \tag{2.6}$$

where the vector field S_d is again discontinuous. Because of the discontinuity, standard existence results do not apply, one can consider the Krasovskii regularization of (2.5) providing

$$(y-u) \in [-1,1] \quad \dot{u} \in P(y-u,\dot{y}) := \begin{cases} \dot{y} - \overline{\text{co}}\ \{\dot{y},\max\{\dot{y},0\}\} & \text{if } y-u=-1 \\ 0 & \text{if } y-u \in (-1,1)\,, \\ \dot{y} - \overline{\text{co}}\ \{\dot{y},\min\{\dot{y},0\}\} & \text{if } y-u=+1 \end{cases} \tag{2.7}$$

and similarly for (2.6) yields

$$v \in [-1,1], \quad \dot{v} \in S(v,\dot{y}) := \begin{cases} \overline{\text{co}}\ \{\dot{y},\max\{\dot{y},0\}\} & \text{if } v=-1 \\ \dot{y} & \text{if } v \in (-1,1)\,. \\ \overline{\text{co}}\ \{\dot{y},\min\{\dot{y},0\}\} & \text{if } v=1 \end{cases} \tag{2.8}$$

The Krasovskii regularization does nothing but make the graph of S_d and P_d closed at the edges of $[-1,1]$. This operation does not introduce additional solutions because v and $(y-u)$ are constrained in the set $[-1,1]$. It is easy to check that $\dot{v} \in S(v,\dot{y}) \cap T_{[-1,1]}(v) = S_d(v,\dot{y})$, and $\dot{u} \in P(y-u,\dot{y}) \cap T_{[-1,1]}(y-u) = P_d(y-u,\dot{y})$, where $T_{[-1,1]}(v)$ denotes the tangent cone to the set $[-1,1]$ at point v.

From now on we will focus on the stop representation because it is more convenient for stability analysis, however all the following derivations can be obtained also using the play representation, but with more involved calculations. For shortness of presentation let us define an aggregate state $z := (z_1, z_2) = (\xi, v) \in \mathbb{R}^n$, $n := m+1$, and consider the interconnection of (2.3) with (2.8). The resulting loop can be represented as a constrained

differential inclusion as follows

$$z \in C := \mathbb{R}^m \times [-1, 1] \quad \dot{z} \in G(z) := \begin{bmatrix} A_1 z_1 - B z_2 \\ S(z_2, K A_1 z_1 - K B z_2) \end{bmatrix}. \tag{2.9}$$

Here C is nonempty and closed; and the set-valued mapping $G : \mathrm{dom}(G) \rightrightarrows \mathbb{R}^n$, with $\mathrm{dom}(G) := \{z \in \mathbb{R}^n \mid G(z) \neq \emptyset\} = C$, is outer semicontinuous and locally bounded [4], and such that for every $z \in C$, $G(z)$ is closed and convex. Additionally, one can verify that for every $z \in C$, $G(z) \cap T_C(z) \neq \emptyset$, where $T_C(z)$ is the tangent cone to C at z, given in this case by $T_C((z_1, z_2)) = \mathbb{R}^m \times [0, \infty)$ if $z_2 = -1$, $T_C((z_1, z_2)) = \mathbb{R}^n$ if $z_2 \in (-1, 1)$, and $T_C((z_1, z_2)) = \mathbb{R}^m \times (-\infty, 0]$ if $z_2 = 1$. Because $G(z) \cap T_C(z) \neq \emptyset$, local existence of solutions follows from a standard viability theory result [11]. Uniqueness of solutions, and completeness of maximal ones is formalized in the next proposition whose proof directly follows from a one-sided Lipschitz condition

$$\langle z^1 - z^2, g^1 - g^2 \rangle \leq L |z^1 - z^2|^2, \quad \forall g^i \in G(z^i) \cap T_C(z^i),\ i = 1, 2,$$

that is satisfied for $L = \max \left\{ \sigma_{\max} \left[\begin{smallmatrix} A_1 & -B \\ 0 & 0 \end{smallmatrix} \right], \sigma_{\max} \left[\begin{smallmatrix} A_1 & -B \\ KA_1 & -KB \end{smallmatrix} \right] \right\}$, where $\sigma_{\max}$ is the maximum singular value.

Proposition 2.1
For every initial condition in C a forward complete solution to (2.9) exists, is unique, and depends continuously on the initial condition.

Proof. Existence and continuous dependence on initial conditions follow combining the regularity properties of the set-valued map G (outer semi-continuity, local boundedness and convexity) with the fact that $G(z) \cap T_C(z) \neq \emptyset$. The one-sided Lipschitz condition ensures forward uniqueness. □

Alternatively (2.9) can be seen as a special case of projected dynamical systems [89]. Let $\mathrm{Proj}_{T_C(z)}(g)$ be the projection of g onto $T_C(z)$, then (2.9) is the same as

$$\dot{z} = \mathrm{Proj}_{T_C(z)} (Mz), \tag{2.10}$$

where matrix M is defined as follows

$$M := \begin{bmatrix} A_1 & -B \\ KA_1 & -KB \end{bmatrix}.$$

[4] Outer semi-continuity of G means that for every $z^i \in C$, every $g^i \in G(z)$, if $z^i \to z$ and $g^i \to g$, then $g \in G(z)$. Local boundedness of F means that for every $x \in C$ there exists a neighborhood U of z such that the set $\bigcup_{z \in U} G(z)$ is bounded.

For (2.10) existence of local solutions established in Proposition 2.1 above follows from [63] and [89]. In this representation the state constraint $z \in C$ is implicitly included because $T_C(z) = \emptyset$ if $z \notin C$. Another possibility is to consider the following differential inclusion

$$\dot{z} \in Mz - N_C(z), \tag{2.11}$$

where $N_C(z)$ is the normal cone to C at z. This representation fits in the broader framework of sweeping processes [86, 71], where the set C depends on the state z and possibly can be controlled [40]. Sweeping processes model non-smooth mechanical systems and other dynamical systems subject to unilateral constraints, of which play and stop are special, one-dimensional, cases. The constraint $z \in C$, again, is implicit, and the right-hand side of (2.11) has unbounded values whenever $z = (z_1, z_2)$ with $z_2 = \pm 1$. Still, solutions to (2.11) exist, are unique, depend continuously on initial conditions (this follows from the one-sided Lipschitz condition) and are the slow/lazy solutions when $\dot{z}(t)$ exists (where $\dot{z}(t)$ is the element of minimal norm of the right-hand side of (2.11), and are the same as solutions to (2.10), see [42]. Furthermore, note that $N_C(z) = \partial I_C(z)$, where I_C is the indicator function of the convex set C, given by $I_C(z) = 0$ if $z \in C$, $I_C(z) = \infty$ if $z \notin C$, and where ∂I_C represents the sub-differential, in the sense of convex analysis, of the convex function I_C. Thus (2.11) is of the form $\dot{z} \in Mx - \partial h(z)$, with a convex function h. Similar, and/or more general systems of this form are studied in the literature as generalization of Lure systems, see [24] and [23]. Under some assumptions, such dynamics convert to differential equations with a maximal monotone right-hand side, and existence, uniqueness, etc. of solutions follows. The assumptions here are different, and the discussion above is independent of any monotonicity properties. Representation (2.9) has also connections with the literature of differential inequalities [123, 26], but we do not discuss this topic here. The interested reader can explore the connection between various formulations such as projected dynamics, differential inclusions, normal cones, complementarity systems in [25] and [12].

To summarize all the presented models admit a constant solution, so that the one sided Lipschitz condition implies that all solutions are bounded, and one can conclude existence of forward complete solutions. Moreover solutions are unique and depend continuously on the initial condition in an appropriate set sense.

2.4 Proof

We develop the proof of Theorem 2.1 following a few steps. A graphical representation of the relationships among the definitions and the lemmas used in the proof is shown in Figure 2.1 reported below. As a first step we consider the following coordinates transfor-

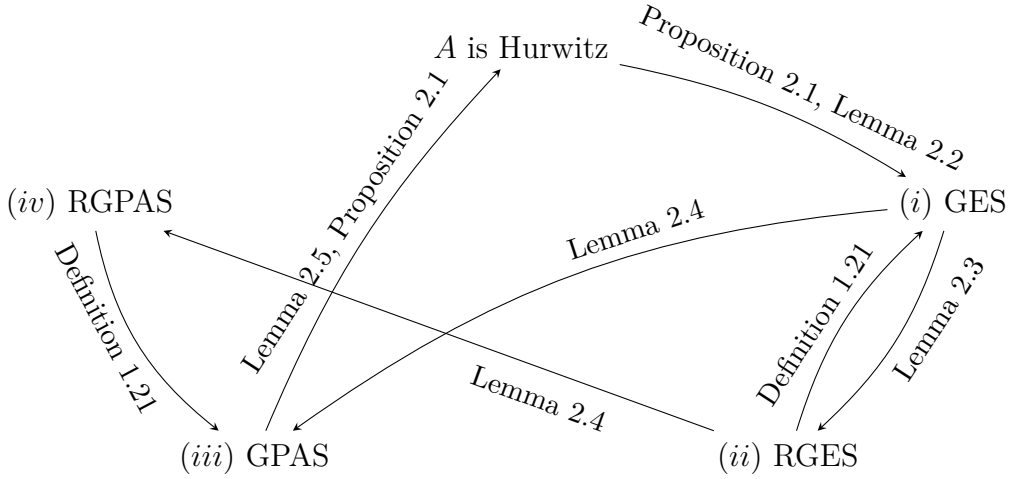

Figure 2.1: Road-map of the proof of Theorem 2.1.

mation

$$(x_1, x_2) := (z_1 - A_1^{-1} B z_2, z_2), \tag{2.12}$$

which simplifies the expression of the attractor $\mathcal{A}$. Indeed, plugging (2.12) into (2.4) yields

$$\mathcal{A} = \{(x_1, x_2) \in \mathbb{R}^m \times [-1, 1] : x_1 = 0\}, \tag{2.13}$$

so that $|x|_{\mathcal{A}}$ reduces to $|(x_1, x_2)|_{\mathcal{A}} = |x_1|$. Moreover noticing that $\dot{y} = KA_1x_1$, we can rewrite (2.3) using (2.12) as follows

$$x \in C := \mathbb{R}^m \times [-1, 1] \quad \dot{x} \in F(x) := \begin{bmatrix} A_1 x_1 - A_1^{-1} B S(x_2, KA_1x_1) \\ S(x_2, KA_1x_1) \end{bmatrix}, \tag{2.14}$$

where $F : \mathrm{dom}(F) \rightrightarrows \mathbb{R}^n$ is again a set-valued map outer semicontinuous and locally bounded. At this point it is important to notice that the restriction of the multi-valued map F to the tangent cone $T_C(x)$, results in $F(x) \cap T_C(x) := F_d(x)$, where $F_d(x)$ is a discontinuous vector field whose explicit expression is reported below

$$F_d(x) = \begin{cases} \begin{bmatrix} A_1 & 0 \\ 0 & 0 \end{bmatrix} \begin{bmatrix} x_1 \\ x_2 \end{bmatrix}, & \text{if } \begin{bmatrix} KA_1 & 0 \\ 0 & 1 \end{bmatrix} \begin{bmatrix} x_1 \\ x_2 \end{bmatrix} \leq \begin{bmatrix} 0 \\ -1 \end{bmatrix} \text{ or } \begin{bmatrix} KA_1 & 0 \\ 0 & 1 \end{bmatrix} \begin{bmatrix} x_1 \\ x_2 \end{bmatrix} \geq \begin{bmatrix} 0 \\ 1 \end{bmatrix}, \\ \begin{bmatrix} A_2 & 0 \\ KA_1 & 0 \end{bmatrix} \begin{bmatrix} x_1 \\ x_2 \end{bmatrix}, & \text{otherwise,} \end{cases} \tag{2.15}$$

where$A_2 := (I - A_1^{-1} BK)A_1 \in \mathbb{R}^{m \times m} := A_1^{-1} A A_1$. We can now prove that the attractor $\mathcal{A}$ is GES. Equation (2.15) shows that the evolution of x_1 is ruled by the pair of matrices A_1 and A_2, and because $|x|_{\mathcal{A}} = |x_1|$, we can study GES of $\mathcal{A}$ just looking at the x_1 dynamics.

By Assumption 2.2 the matrices A_1 and A_2 share a common quadratic Lyapunov function, i.e., there exists a symmetric positive definite matrix $Q = Q^\top \in \mathbb{R}^{m\times m}$ such that:

$$A_1^\top Q + QA_1 < 0, \tag{2.16a}$$
$$A_2^\top Q + QA_2 < 0. \tag{2.16b}$$

Picking $V(x) := x^\top \mathrm{diag}(Q, 0)x$ as a candidate Lyapunov function for (2.14), the following bounds hold $\lambda_{\min}(Q)|x|_{\mathcal{A}}^2 \le V(x) \le \lambda_{\max}(Q)|x|_{\mathcal{A}}^2$, $\forall x \in C$. Moreover for $c > 0$ sufficiently small we have $\langle \nabla V(x), f\rangle \le -cV(x)$, $\forall x \in C$, $f \in F(x) \cap T_C(x)$, establishing GES of the attractor $\mathcal{A}$.

Now that we have established GES we use the following Lemma 2.3 to prove that for (2.9) GES can be strengthened to RGES, showing the implication $(i) \Rightarrow (ii)$ of Theorem 2.1 (see 2.1).

Lemma 2.3
Given a compact attractor $\mathcal{A}$ suppose that there exists a function $V : \mathbb{R}^n \to \mathbb{R}$ that satisfies the following conditions:

A.1) $c_1|x|_{\mathcal{A}}^2 \le V(x) \le c_2|x|_{\mathcal{A}}^2$,

A.2) $\langle \nabla V(x), f\rangle \le -c_3|x|_{\mathcal{A}}^2$, $\forall f \in F(x)$,

A.3) $|\nabla V(x^1) - \nabla V(x^2)| \le c_4|x^1 - x^2|_{\mathcal{A}}$,

A.4) $|f| \le c_5|x|_{\mathcal{A}}$, $\forall f \in F(x)$,

for all $x^1, x^2 \in \mathbb{R}^n$, and for some positive constants c_i, $i = 1, \dots 5$, then the set $\mathcal{A}$ is RGES.

Proof. Plugging $A.1$) into $A.2$) we obtain $\langle V(x), f\rangle \le -(c_3/c_2)V(x)$, which implies $V(x(t)) \le \exp(-c_3t/c_2)V(x(0))$ for all $t \in \mathrm{dom}(x)$. Using the lower bound of $A.1$) we obtain $|x(t)|_{\mathcal{A}} \le \sqrt{c_2/c_1}\exp(-c_3t/(2c_2))|x(0)|_{\mathcal{A}} \le m\exp(-\alpha t)|x(0)|_{\mathcal{A}}$, for appropriate m, α which shows GES. To prove RGES pick a small enough $r > 0$ and let $\rho(x) = r|x|_{\mathcal{A}}$. For $x^1 \in x + \rho(x)\mathbb{B}$, one has $(1-r)|x|_{\mathcal{A}} \le |x^1|_{\mathcal{A}} \le (1+r)|x|_{\mathcal{A}}$ and $|x^1 - x| \le r|x|_{\mathcal{A}}$. Then, for $x \in C_\rho$, $x^1 \in x + \rho(x)\mathbb{B}$, and $f^1 \in F(x^1)$ we have

$$\begin{aligned}
\langle \nabla V(x), f^1\rangle &= \langle \nabla V(x^1), f^1\rangle + \langle \nabla V(x) - \nabla V(x^1), f^1\rangle \\
&\le -c_3|x^1|_{\mathcal{A}}^2 + |\nabla V(x) - \nabla V(x^1)||f^1| \\
&\le -c_3|x^1|_{\mathcal{A}}^2 + c_4c_5|x - x^1|_{\mathcal{A}}|x^1|_{\mathcal{A}} \\
&\le -c_3(1-r)^2|x|_{\mathcal{A}}^2 + c_4c_5r(1+r)|x|_{\mathcal{A}}^2.
\end{aligned}$$

For $x^1 \in C_\rho$ and $f^1 \in F_\rho(x^1)$ yields[5],

$$\begin{aligned}\langle \nabla V(x^1), f^1 \rangle &\leq -c_3(1-r)^2|x^1|^2_{\mathcal{A}} + c_4c_5r(1+r)|x^1|^2_{\mathcal{A}} + |\nabla V(x^1)|\rho(x^1) \\ &\leq -c_3(1-r)^2|x^1|^2_{\mathcal{A}} + c_4c_5r(1+r)|x^1|^2_{\mathcal{A}} + c_4r|x^1|^2_{\mathcal{A}} \\ &\leq -c_3|x^1|^2_{\mathcal{A}}/2,\end{aligned}$$

for a non zero r sufficiently small, and this completes the proof. □

Lemma 2.3 can be directly applied to (2.9) using the Lyapunov function $V(x) := x^\top \mathrm{diag}(Q, 0)x$ and selecting $c_1 = \lambda_{\min}(Q)$, $c_2 = \lambda_{\max}(Q)$, c_3 sufficiently small, $c_4 = |Q|$ and $c_5 = \max\{|A_1|, |A_2|\}$, establishing RGES for $\mathcal{A}$. The reverse implication $(ii) \Rightarrow (i)$ follows trivially by Definition 1.21. We now prove that GES plus a proper grow condition for the vector field implies GPAS, showing the implication $(i) \Rightarrow (iii)$ of Figure 2.1.

Lemma 2.4
Assume that $\mathcal{A}$ is GES and that there exists $c > 0$ such that $|f| \leq c|x|_{\mathcal{A}}$ for all $x \in C, f \in F(x)$, then $\mathcal{A}$ is GPAS.

Proof. Pick any $a \in \mathcal{A}$ and $\epsilon > 0$, from GES there exist $m > 0$, $\alpha > 0$ such that all solutions satisfy $|x(t)|_{\mathcal{A}} \leq m\exp(-\alpha t)|x(0)|_{\mathcal{A}}$. Let $\delta > 0$ be such that $(1 + \alpha^{-1}cm)\delta < \epsilon$ and pick an initial condition such that $|x(0)|_{\mathcal{A}} \leq |x(0) - a| \leq \delta$. Then, by GES, $|x(t)|_{\mathcal{A}} \leq m\exp(-\alpha t)|x(0)|_{\mathcal{A}} \leq m\delta$ for all $t \in \mathrm{dom}(x)$. Moreover by assumption we have $|\dot{x}(t)| \leq c|x(t)|_{\mathcal{A}} \leq cm\exp(-\alpha t)\delta$ and so,

$$|x(t) - x(0)| = \left|\int_0^t \dot{x}(\tau)\,\mathrm{d}\tau\right| \leq \int_0^t |\dot{x}(\tau)|\,\mathrm{d}\tau \leq mc|x(0)|_{\mathcal{A}}\int_0^t e^{-\alpha\tau}\,\mathrm{d}\tau \leq \alpha^{-1}cm\delta.$$

Consequently, $\dot{x}$ is absolutely integrable on $\mathbb{R}_{\geq 0}$ and $x(t)$ converges as $t \to \infty$. Furthermore we have $|x(t) - a| \leq |x(t) - x(0)| + |x(0) - a| \leq (1 + \alpha^{-1}cm)\delta < \epsilon$, which shows Lyapunov stability of the generic point $a \in \mathcal{A}$. Combining convergence of x and pointwise Lyapunov stability of $\mathcal{A}$ we obtain the desired result. □

Lemma 2.4 applies to (2.9) selecting $c = \max\left\{\sigma_{\max}(A_1), \sigma_{\max}\left[(A_2^\top, A_1^\top K)\right]\right\}$, showing that GES implies GPAS. Moreover Lemma 2.4 can be also applied to the ρ-inflation of (2.9) proving that the chain of implications $(ii) \Rightarrow (iv) \Rightarrow (iii)$ holds taking a perturbation $\rho = r|x|_{\mathcal{A}}$ with $r > 0$ sufficiently small. Therefore from RGES we deduce that $\mathcal{A}$ is PAS for the ρ-inflated system, or in other words $\mathcal{A}$ is RPAS. To complete the proof of Theorem 2.1 according to Figure 2.1, we show $(iii) \Rightarrow (i)$ using the following Lemma 2.5.

[5]One can pass the inequality above through the convex hull and the closure operation.

Lemma 2.5
If attractor $\mathcal{A}$ is GPAS for (2.9), then the matrix A is Hurwitz.

Proof. By GPAS of $\mathcal{A}$ solutions to (2.9) starting from an initial condition $|x(0)|_{\mathcal{A}} \leq \delta$, with δ small enough, are solutions to the linear system

$$\dot{x} = \begin{bmatrix} A_2 & 0 \\ KA_1 & 0 \end{bmatrix} x, \tag{2.17}$$

for all $t \in \mathbb{R}_{\geq 0}$. From the structure of (2.17) we notice that the one-dimensional subspace $\text{span}\{(0,1)\}$ that contains $\mathcal{A}$ is associated to a zero eigenvalue. A necessary condition for this subspace to be PAS is that all the other directions must be associated to converging and stable dynamics, we conclude that due to the very structure of (2.17) necessarily A_2 must be Hurwitz. Thus A_2 is Hurwitz and by Lemma 2.1 so is A. □

2.5 Examples

In this section, we present two examples. The first one is a parametric scalar linear system in feedback with the play. Depending on the value of the parameter $a \in \mathbb{R}$, different behaviors can be obtained. We solve this scalar example analytically. The second example comprises instead a known second order linear system in feedback with play. For this more complicated example, we numerically show that each system trajectory converges toward a point contained in the attractor $\mathcal{A}$ defined in (2.4).

2.5.1 A scalar example

Let us consider the following linear scalar systems feedback with play and stop,

$$\begin{cases} \dot{\xi} &= a\xi + \mathscr{P}[y] \\ y &= -2\xi, \end{cases} \tag{2.18}$$

$$\begin{cases} \dot{\xi} &= a_1\xi - \mathscr{S}[y] \\ y &= -2\xi. \end{cases} \tag{2.19}$$

Here a takes values in the set $\{-1, 0, 1\}$ which is designed to show possible different scenarios. The pair $(a, 1)$ is controllable and $a_1 := (a - 2) < 0$ for all $a \in \{-1, 0, 1\}$. Assume that play and stop satisfy Assumption 2.1, then $\mathcal{A} := \{0\} \times [-1, 1]$. Let us consider the stop state $v \in [-1, 1]$, and consider the change of coordinates (2.12) that results

$x = (x_1, x_2) := (\xi - a_1^{-1} v, v) \in \mathbb{R}^2$. According to the representation in (2.15) we obtain

$$\begin{bmatrix} \dot{x}_1 \\ \dot{x}_2 \end{bmatrix} = \begin{cases} \begin{bmatrix} a_1 & 0 \\ 0 & 0 \end{bmatrix} \begin{bmatrix} x_1 \\ x_2 \end{bmatrix} & \text{if} \quad \begin{bmatrix} x_1 \\ x_2 \end{bmatrix} \leq \begin{bmatrix} 0 \\ -1 \end{bmatrix} \text{ or } \begin{bmatrix} x_1 \\ x_2 \end{bmatrix} \geq \begin{bmatrix} 0 \\ 1 \end{bmatrix} \\ \begin{bmatrix} a & 0 \\ -2a_1 & 0 \end{bmatrix} \begin{bmatrix} x_1 \\ x_2 \end{bmatrix} & \text{otherwise.} \end{cases} \tag{2.20}$$

For $a = -1$ the hypotheses of Theorem 2.1 are fulfilled and $\mathcal{A}$ is GES, RGES, GPAS and RGPAS. We check these properties by directly computing the analytical solutions. Depending on the initial conditions different scenarios may arise. To simplify the presentation it is useful to partition the state space as $C := C_1 \cup C_2 \cup C_3$, where $C_1 := \{(x_1, x_2) \in \mathbb{R} \times [-1, 1] : -1 \leq 6x_1 + x_2 \leq 1\}$, $C_2 := (\mathbb{R}_{\geq 0} \times \{1\}) \cup (\mathbb{R}_{\leq 0} \times \{-1\})$ and $C_3 := \mathbb{R} \times [-1, 1] \setminus (C_1 \cup C_2)$. For any $x(0) := (x_1(0), x_2(0)) \in C_1$ a direct integration of (2.20) provides

$$x(t) = \begin{bmatrix} \mathrm{e}^{-t} & 0 \\ 6(1 - \mathrm{e}^{-t}) & 1 \end{bmatrix} x(0),$$

for all $t \in \mathbb{R}_{\geq 0}$, and the solution exponentially converges to $(0, 6x_1(0) + x_2(0)) \in \mathcal{A}$. For $x(0) \in C_2$ a direct integration of (2.20) yields

$$x(t) = \begin{bmatrix} \mathrm{e}^{-3t} & 0 \\ 0 & 1 \end{bmatrix} x(0),$$

for all $t \in \mathbb{R}_{\geq 0}$ and the solution converges to $(0, x_2(0)) \in \mathcal{A}$. Finally for $x(0) \in C_3$ the solution is piecewise-defined and yields

$$x(t) = \begin{cases} \begin{bmatrix} \mathrm{e}^{-t} & 0 \\ 6(1 - \mathrm{e}^{-t}) & 1 \end{bmatrix} x(0) & \text{for } 0 \leq t \leq t^\star \\ \begin{bmatrix} \mathrm{e}^{-3(t - t^\star)} & 0 \\ 0 & 1 \end{bmatrix} x(t^\star) & \text{for } t > t^\star \end{cases}$$

where time $t^\star = \ln(6x_1(0)/(6x_1(0) - \operatorname{sgn}(x_1(0)) + x_2(0)))$ is positive and bounded for all $x(0) \in C_3$. We conclude that the solution converges to $(0, \operatorname{sgn}(x_1(0))) \in \mathcal{A}$. Summarizing, $\mathcal{A}$ is GES and GPAS because for all $x(0) \in C$ solutions converge exponentially to one point of the attractor.

Now, let us consider $a = 0$, then the set $\mathcal{A}$ is stable and globally attractive, however the converge is not exponential. Let $C := C_1 \cup C_2$ where $C_1 := (\mathbb{R}_{\leq 0} \times \{1\}) \cup (\mathbb{R}_{\leq 0} \times \{-1\})$

and $C_2 := (\mathbb{R} \times [-1, 1]) \setminus C_1$. For $x(0) \in C_1$ the solution yields

$$x(t) = \begin{bmatrix} \mathrm{e}^{-2t} & 0 \\ 0 & 1 \end{bmatrix} x(0),$$

for all $t \in \mathbb{R}_{\geq 0}$ and the solution converges exponentially to $(0, x_2(0)) \in \mathcal{A}$, however for $x(0) \in C_2$ the solution is piecewise-defined and corresponds to

$$x(t) = \begin{cases} \begin{bmatrix} 1 & 0 \\ 4t & 1 \end{bmatrix} x(0) & \text{for } 0 \leq t \leq t^\star, \\ \begin{bmatrix} \mathrm{e}^{-2(t-t^\star)} & 0 \\ 1 & 0 \end{bmatrix} x(t^\star) & \text{for } t > t^\star \end{cases}$$

where $t^\star := (\mathrm{sgn}(x_1(0)) - x_2(0))/(4x_1(0))$. This shows that the convergence is not exponential because $t^\star$ can be made arbitrarily large by selecting $x_1(0)$ sufficiently small. Still solutions converge to $\mathcal{A}$ after a sufficiently long time. Finally for $a = 1$ the set $\mathcal{A}$ is not Lyapunov stable but globally attractive. Let $C := C_1 \cup C_2$ as in the previous case. For any initial condition $x(0) \in C_1$ we have

$$x(t) = \begin{bmatrix} \mathrm{e}^{-t} & 0 \\ 0 & 1 \end{bmatrix} x(0)$$

for all $t \in \mathbb{R}_{\geq 0}$ and the solution exponentially converges to $(0, x_2(0)) \in \mathcal{A}$. For $x(0) \in C_2$ the solution is piecewise-defined and corresponds to

$$x(t) = \begin{cases} \begin{bmatrix} \mathrm{e}^{t} & 0 \\ 2(\mathrm{e}^{t} - 1) & 1 \end{bmatrix} x(0) & \text{for } 0 \leq t \leq t^\star \\ \begin{bmatrix} \mathrm{e}^{-(t-t^\star)} & 0 \\ 0 & 1 \end{bmatrix} x(t^\star) & \text{for } t > t^\star, \end{cases}$$

where $t^\star = \ln((2x_1(0)+\mathrm{sgn}(x_1(0))-x_2(0))/(2x_1(0)))$. We can observe that in this case set $\mathcal{A}$ is not Lyapunov stable because trajectories escape from it, however it is globally attractive because trajectories approach one of the two points $x = (0, \pm 1)$. Again, the convergence toward $\mathcal{A}$ is not exponential because $t^\star$ can be made arbitrarily large by selecting $x_1(0)$ sufficiently small. Figure 2.2 shows the possible scenarios associated to $a \in \{-1, 0, 1\}$ for a few randomly generated initial conditions.

2.5.2 A bi-dimensional example

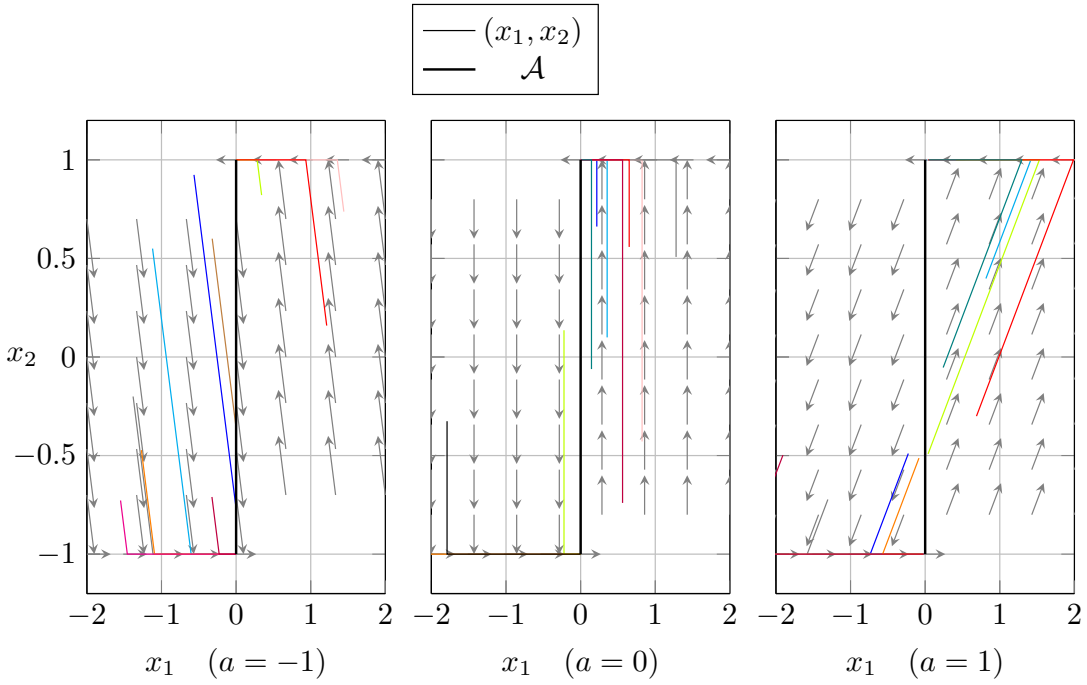

Figure 2.2: Integral curves for random initial conditions and different values of a.

Now let us consider a bi-dimensional single-input single-output linear system in feedback interconnection with a play operator that satisfies Assumption 2.1. Matrices (A, B, K) are reported below

$$\left[\begin{array}{c|c} A & B \\ \hline K & \end{array}\right] = \left[\begin{array}{cc|c} -1 & 3 & 1 \\ -3 & -1 & -2 \\ \hline 1 & 1 & \end{array}\right].$$

Matrices A and $A_1 := A + BK$ are Hurwitz and the pair (A, B) is controllable, so that Theorem 2.1 applies. The set $\mathcal{A} := \{(x_1, x_2) \in \mathbb{R}^2 \times [-1, 1] : x_2 = 0\}$ is GES, RGES, GPAS and RGPAS. A number of trajectories for randomly generated initial conditions are shown in Figure 2.3. According to Theorem 2.1 all the trajectories approach $\mathcal{A}$ with exponential convergence rate and finally stop in one point.

2.6 Conclusion

We studied a general class of linear single-input single-output systems in feedback with play and stop operators. For these systems, we showed that there exists a compact set of equilibria, and under the hypothesis of the existence of a common quadratic Lyapunov function between a special matrix pair, we show that the set is globally exponentially stable.

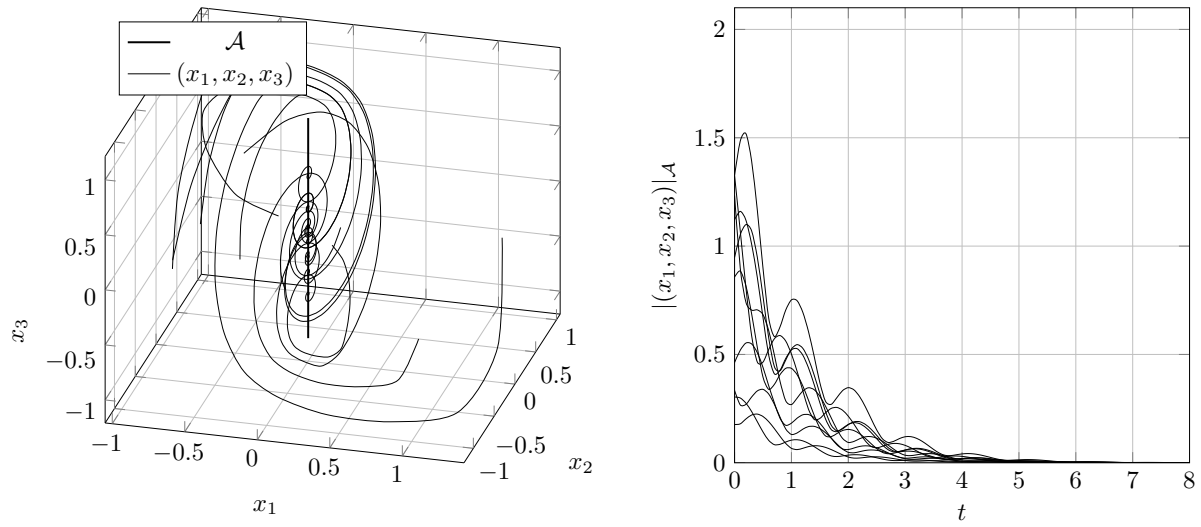

Figure 2.3: Orbits and distance to the attractor $\mathcal{A}$ for a few random initial conditions.

.

We also prove the equivalence between global exponential stability and global pointwise asymptotic stability. Determining the existence of a common Lyapunov function can be formulated as an LMI problem and solved numerically. Our result generalize those in [124] reinterpreting the frequency based condition and adding robustness. We hope that this sharp result can serve as a starting point for future investigations involving multiple-inputs multiple-outputs systems, and more general types of hysteresis operators.

Chapter 3

Hybrid Dual Stage Control

In this chapter we propose a novel hybrid controller for linear single-input single-output plants. The controller combines two linear controllers that can be tuned independently and a mechanism to switch between them. This architecture is motivated by the necessity of having different performances in different operating conditions, a situation that often arises in practice. For example, the first controller can be used to shape the transient performance, while the second to adjust the steady-state. The study of the stability properties of this scheme requires some carefulness because the switch between the two controllers may cause destabilizing transients. For this reason, the switch happens with the help of a bumpless filter and a carefully designed reset rule. The simultaneous action of these two mechanisms ensures stability under a large class of switching signals. For robustness reasons, both controllers are equipped with an integral action. The second embeds an *internal model*, while the first uses the internal state of the first controller to set the initial condition for an *external model*, see [126], [106], [30]. In this way the first controller can be calibrated to be aggressive, although not very precise, while the second one may be slower, but with better steady-state performance. The main result of the chapter is proved using modern hybrid systems tools, in particular a hybrid reduction theorem. These tools are necessary due to the discontinuous nature of the controller state. The results presented in this chapter are adapted from [46] and [36]. An experimental validation of the theoretical results reported in this chapter is presented in Chapter 5.

3.1 Introduction

Linear control is a well-developed subject and a variety of synthesis techniques are available both in the frequency and state space domain. Some well known examples are the Ziegler–Nichols tuning method, the root locus diagram, the pole placement algorithm and the Linear Quadratic Regulator (LQR). On the contrary, control techniques for nonlinear systems are less systematic and often more complicated from a mathematical point of view. For these reasons, a widely used industrial approach to control nonlinear plants is to linearize them around a set of different operating conditions and then use linear controllers. Obviously each controller is suitable for a specific region of the state space and

in principle, by switching among them, one can achieve better performance as compared to a single controller designed for the overall control task. This *switching* operation allows overcoming the intrinsic limitations of linear control, allowing to satisfy simultaneously conflicting requirements [21]. A classical example is the trade-off between the rising time and percentage of overshoot [48]. Similar results can be obtained with the use of resets, i.e. discontinuities of the controller state designed to obtain specific behaviors. However, while the design of individual controllers is simplified by their local nature, the control law that determines the switching between them can be complicated. In practice, dwell-time conditions are often used, sometimes unconsciously. These conditions ensure that if the switches are not too frequent, then the stability of the loop between the plant and the controller is preserved. More conservative approaches enforce stability under arbitrary switching using Lie algebraic conditions [73], or using in a smart way the Youla–Kucera parametrization [65, 17].

As compared to these works, an important feature of the results presented here is that they address regulation in addition to stabilization. In this chapter, we propose a scheme that embeds a bumpless filter [125], two different controllers and an observer. The scheme is also equipped with a properly designed reset rule that ensures the stability of the plant-controller loop under a large family of switching signals. The advantage of the proposed scheme is that one can freely switch between the two controllers, without fear of causing instability. Due to the presence of resets in the controller state, a systematic treatment requires a Lyapunov theory for hybrid differential equations, also known as *hybrid systems* [58].

3.2 Problem formulation

We consider a linear time invariant, single-input single-output plant of the following form

$$\mathcal{H}_{\mathrm{p}} := \begin{cases} \dot{x}_{\mathrm{p}} = Ax_{\mathrm{p}} + Bu + Gw \\ e_{\mathrm{p}} = Cx_{\mathrm{p}} + Qw \end{cases} \tag{3.1}$$

where $x_{\mathrm{p}} \in \mathbb{R}^{n_{\mathrm{p}}}$ is the state, $u \in \mathbb{R}$ is the input, $w \in \mathbb{R}$ is a disturbance/reference to be rejected/tracked and $e_{\mathrm{p}} \in \mathbb{R}$ is the tracking error. For plant (3.1) we propose an error feedback hybrid controller $\mathcal{H}_{\mathrm{c}}$ of the following form:

$$\mathcal{H}_{\mathrm{c}} := \begin{cases} \dot{x}_{\mathrm{c}} = A_{\mathrm{c}}(q)x_{\mathrm{c}} + B_{\mathrm{c}}(q)e_{\mathrm{p}} \\ x_{\mathrm{c}}^{+} = E_{\mathrm{c}}(q)x_{\mathrm{c}}, \end{cases} \tag{3.2}$$

where $x_c \in \mathbb{R}^{n_c}$ is the controller state, and $q \in \mathcal{Q} := \{1, 2\}$ is a logic variable selecting what mode of the controller is currently active. The two logic states $q = 1$ and $q = 2$ correspond to the two modes available for the controller, i.e., *transient mode* and *steady-state mode*. The logic variable q and the controller state x_c are updated synchronously during jumps. This point will be better clarified in the proof of Theorem 3.1. Controller (3.2) is interconnected to (3.1) through the following output equation:

$$u = C_c(q)x_c, \tag{3.3}$$

so that the closed-loop system between (3.1) and (3.2) through (3.3) yields,

$$\mathcal{H} := \begin{cases} \begin{bmatrix} \dot{x}_p \\ \dot{x}_c \end{bmatrix} = \begin{bmatrix} A & BC_c(q) \\ B_c(q)C & A_c(q) \end{bmatrix} \begin{bmatrix} x_p \\ x_c \end{bmatrix} + \begin{bmatrix} G \\ B_c(q)Q \end{bmatrix} w \\ \begin{bmatrix} x_p^+ \\ x_c^+ \end{bmatrix} = \begin{bmatrix} I & 0 \\ 0 & E_c(q) \end{bmatrix} \begin{bmatrix} x_p \\ x_c \end{bmatrix} \\ e_p = \begin{bmatrix} C & 0 \end{bmatrix} \begin{bmatrix} x_p \\ x_c \end{bmatrix} + Qw \end{cases} \tag{3.4}$$

It is important to stress that (3.4) represents a fully hybrid system with linear flow and jump maps. Indeed, controller (3.2) includes a reset mechanism, namely a discontinuity of the state x_c. We report below the explicit structure of the hybrid controller (3.2) for the logic value $q = 1$ corresponding to the "transient mode", and for $q = 2$ corresponding to

the "steady-state mode":

$$\left[\begin{array}{c|c} A_{\mathrm{c}}(1) & B_{\mathrm{c}}(1) \\ \hline C_{\mathrm{c}}(1) & \\ \hline E_{\mathrm{c}}(1) & \end{array}\right] := \left[\begin{array}{cccc|c} A+LC+BK_1 & B & 0 & 0 & -L \\ 0 & 0 & 0 & 0 & 0 \\ B(K_2-K_1) & -B & A+BK_2 & BK_{\mathrm{i}} & 0 \\ 0 & 0 & C & 0 & I \\ \hline K_1 & I & 0 & 0 & \\ \hline I & 0 & 0 & 0 & \\ K_2-K_1 & 0 & K_2-K_1 & K_{\mathrm{i}} & \\ 0 & 0 & I & 0 & \\ 0 & 0 & 0 & I & \end{array}\right] \tag{3.5a}$$

$$\left[\begin{array}{c|c} A_{\mathrm{c}}(2) & B_{\mathrm{c}}(2) \\ \hline C_{\mathrm{c}}(2) & \\ \hline E_{\mathrm{c}}(2) & \end{array}\right] := \left[\begin{array}{cccc|c} A+LC+BK_2 & 0 & B(K_2-K_1) & BK_{\mathrm{i}} & -L \\ 0 & 0 & 0 & 0 & 0 \\ 0 & 0 & A+BK_1 & 0 & 0 \\ 0 & 0 & C & 0 & I \\ \hline K_2 & 0 & K_2-K_1 & K_{\mathrm{i}} & \\ \hline I & 0 & 0 & 0 & \\ K_2-K_1 & 0 & K_2-K_1 & K_{\mathrm{i}} & \\ 0 & 0 & I & 0 & \\ 0 & 0 & 0 & I & \end{array}\right]. \tag{3.5b}$$

Although the structure of Equation (3.5) may seem complicated, there is a rather intuitive motivation for each block. Looking at (3.5) we can split the controller state into 4 different sub-states as follows $x_{\mathrm{c}} = (x_{\mathrm{c}1}, x_{\mathrm{c}2}, x_{\mathrm{c}3}, x_{\mathrm{c}4}) \in \mathbb{R}^{n_{\mathrm{p}}} \times \mathbb{R} \times \mathbb{R}^{n_{\mathrm{p}}} \times \mathbb{R}$. The individual role of each component of the controller state is clarified below:

1. The state $x_{\mathrm{c}1}$ is associated to a Luenberger observer that provides an estimate of the state x_{p} in (3.1);
2. The state $x_{\mathrm{c}2}$ introduces a constant input bias that plays the role of an integral action updated only during jumps (external model);
3. The state $x_{\mathrm{c}3}$ corresponds to a bumpless filter, inspired by [125], which guarantees stability under a large class of switching signals;
4. $x_{\mathrm{c}4}$ implements the integral action of the steady-state controller ($q = 2$) (internal model).

The gain $L \in \mathbb{R}^{n_{\mathrm{p}}}$ is the observer gain, while K_1 and $K_2 \in \mathbb{R}^{1\times n_{\mathrm{p}}}$ are the "proportional" gains, finally $K_{\mathrm{i}} \in \mathbb{R}$ is the integral gain. The reset mechanism for (3.2) is specified by the matrix $E_{\mathrm{c}}(q)$. The combination of resets and switches is designed to keep the solutions well

behaved across jumps and, in particular ensures that q can switch almost freely between the two modes without destabilizing the closed-loop. The only restriction that we assume for the switching signal q is that it satisfies a mild dwell-time and reverse dwell-time condition. Denoting by t_j, $j \in \mathbb{N}_{\geq 1}$ the toggle times, i.e. the times when the logic variable q changes from $q = 1$ to $q^+ = 2$ or vice-versa, we assume the following.

Assumption 3.1
There exist two positive numbers $\tau_{\min}, \tau_{\max} \in \mathbb{R}_{>0}$, *such that* $\tau_{\min} \leq |t_{j+1} - t_j| \leq \tau_{\max}$, $\forall j \in \mathbb{N}_{\geq 1}$.

Remark 3.1
We remark that no constraints on $\tau_{\min}$ and $\tau_{\max}$ are imposed, and that these values are not used in the controller synthesis. Thus Assumption 3.1 virtually allows for all the possible switching sequences that are relevant from a practical viewpoint. ⌟

Finally it is interesting to notice that when switching from $q = 2$ to $q^+ = 1$, the reset exploits the information provided by $x_{\mathrm{c}3}$, $x_{\mathrm{c}4}$ to update the bias generated through x_{c2} and asymptotically recovers zero steady-state error also in transient mode ($q = 1$).

Now let us assume that plant (3.1) satisfies the following assumptions

Assumption 3.2
Matrix A *is Hurwitz and the triple* (C, A, B) *is minimal.*

Moreover, because we are interested in set-point regulation, we restrict the class of possible reference and disturbance signals to constant ones.

Assumption 3.3
The signal w *is constant.*

Thanks to Assumption 3.3 we have that $\dot{w} = 0$ and we can consider the change of coordinates

$$x := T(q) \begin{bmatrix} x_{\mathrm{p}} \\ x_{\mathrm{c}} \end{bmatrix} \tag{3.6}$$

where matrices $T(q) \in \mathbb{R}^{n \times n}$, $n := n_{\mathrm{p}} + n_{\mathrm{c}}$ and its inverse $T(q)^{-1}$ are reported below

$$T(q) := \begin{bmatrix} (2-q)I & 0 & 0 & (1-q)I & 0 \\ 0 & 0 & I & 0 & 0 \\ I & 0 & 0 & I & 0 \\ 0 & 0 & 0 & 0 & I \\ -I & I & 0 & 0 & 0 \end{bmatrix}, \quad T(q)^{-1} = \begin{bmatrix} I & 0 & (q-1)I & 0 & 0 \\ I & 0 & (q-1)I & 0 & I \\ 0 & I & 0 & 0 & 0 \\ -I & 0 & (2-q)I & 0 & 0 \\ 0 & 0 & 0 & I & 0 \end{bmatrix}.$$

Notice that $T(q)$ is full rank for all $q \in \mathcal{Q}$ so that (3.6) is always well-defined. Thanks to (3.6) the closed-loop (3.4) takes the simplified expression

$$\mathcal{H} := \begin{cases} \dot{x} = A_{\mathrm{cl}}(q)x + G_{\mathrm{cl}}(q)w \\ x^+ = E_{\mathrm{cl}}(q)x \end{cases} \tag{3.7}$$

where $A_{\mathrm{cl}}(q) \in \mathbb{R}^{n\times n}$, $G_{\mathrm{cl}}(q) \in \mathbb{R}^n$, and $E_{\mathrm{cl}}(q) \in \mathbb{R}^{n\times n}$ are reported below. Similarly, the tracking error e_{p} yields

$$e_{\mathrm{p}} = C_{\mathrm{cl}}(q)x + D_{\mathrm{cl}}w, \tag{3.8}$$

where again $C_{\mathrm{cl}}(q) \in \mathbb{R}^{1\times n}$, $D_{\mathrm{cl}}(q) \in \mathbb{R}$ are defined next

$$\left[\begin{array}{c|c} A_{\mathrm{cl}}(q) & G_{\mathrm{cl}}(q) \\ \hline E_{\mathrm{cl}}(q) & \\ \hline C_{\mathrm{cl}}(q) & D_{\mathrm{cl}}(q) \end{array}\right] := \left[\begin{array}{ccccc|c} A+BK_1 & (2-q)B & 0 & 0 & (2-q)BK_1 & (2-q)G \\ 0 & 0 & 0 & 0 & 0 & 0 \\ 0 & 0 & A+BK_2 & BK_{\mathrm{i}} & BK_2 & G \\ 0 & 0 & C & 0 & 0 & Q \\ 0 & 0 & 0 & 0 & A+LC & -G-LQ \\ \hline I & 0 & (2q-3)I & 0 & 0 & \\ 0 & 0 & K_2-K_1 & K_{\mathrm{i}} & K_2-K_1 & \\ 0 & 0 & I & 0 & 0 & \\ 0 & 0 & 0 & I & 0 & \\ 0 & 0 & 0 & 0 & I & \\ \hline C & 0 & (q-1)C & 0 & 0 & Q \end{array}\right] \tag{3.9}$$

It is worth to notice that (3.9) has a desirable cascade structure and thus a necessary condition for stability is to ensure that the diagonal sub-blocks

$$[A+BK_1], \quad \begin{bmatrix} A+BK_2 & BK_{\mathrm{i}} \\ C & 0 \end{bmatrix}, \quad [A+LC] \tag{3.10}$$

are Hurwitz. This is not restrictive in our setup, since the triple (C, A, B) is minimal from Assumption 3.2. Then it is always possible to find a set of parameters K_1, K_2, K_{i}, L such that the matrices in (3.10) are Hurwitz. We are now ready to state the main result of the chapter.

Theorem 3.1 (Main result)
Assume that the gains K_1, K_2, K_{i}, L have been designed so that the matrices in (3.10) are Hurwitz. If Assumptions 3.2, 3.3, and 3.1 hold true, then (3.7) has the following properties:

1. *For $w = 0$ the origin of (3.7) is Globally Exponentially Stable (GES) for all switching sequences.*
2. *For any constant w the solutions to (3.7) are globally bounded and ensure asymptotic*

convergence to zero of e_{p}.

Theorem 3.1 provides a strong and desirable result because it establishes asymptotic tracking and exponential convergence for any switching signal q satisfying the mild requirements in Assumption 3.1.

Proof. To properly describe the class of switching signals defined in Assumption 3.1 we use the hybrid systems framework presented in [58] and we include as a part of the state also the logic variable q and a timer τ. The arising representation is inspired by the construction in [29, page 747] and can be shown to generate all and no more than the switching sequences characterized in Assumption 3.1, see [29, Prop. 1.1]. The resulting hybrid system has then the following structure:

$$\begin{cases} \begin{bmatrix} x \\ q \\ \tau \end{bmatrix} \in \begin{bmatrix} \mathbb{R}^n \\ \mathcal{Q} \\ [0, \tau_{\max}] \end{bmatrix}, \qquad \begin{bmatrix} \dot{x} \\ \dot{q} \\ \dot{\tau} \end{bmatrix} = \begin{bmatrix} A_{\mathrm{cl}}(q)x + G_{\mathrm{cl}}(q)w \\ 0 \\ 1 \end{bmatrix} \\ \begin{bmatrix} x \\ q \\ \tau \end{bmatrix} \in \begin{bmatrix} \mathbb{R}^n \\ \mathcal{Q} \\ [\tau_{\min}, \tau_{\max}] \end{bmatrix}, \quad \begin{bmatrix} x^+ \\ q^+ \\ \tau^+ \end{bmatrix} = \begin{bmatrix} E_{\mathrm{cl}}(q)x \\ 3 - q \\ 0 \end{bmatrix}. \end{cases} \tag{3.11}$$

Using the above representation, we proceed to proving the two items of the theorem. Proof of item (1). Because we are interested in studying the stability properties of the origin of (3.7) and in (3.11) there are additional states (q, τ) we consider the compact attractor $\mathcal{A} := \{0\} \times \mathcal{Q} \times [0, \tau_{\max}]$ and the distance function $|x|_{\mathcal{A}} := \inf_{a \in \mathcal{A}}(|x - a|)$, so that $|(x, q, \tau)|_{\mathcal{A}} = |x|$, and we equivalently study the stability property of $\mathcal{A}$. According to the representation in (3.9) we split the state $x = (x_1, \ldots, x_5) \in \mathbb{R}^{n_{\mathrm{p}}} \times \mathbb{R} \times \mathbb{R}^{n_{\mathrm{p}}} \times \mathbb{R} \times \mathbb{R}^{n_{\mathrm{p}}}$ and we apply the recursive reduction theorem reported in [82, Thm 4] with the following sets: $\Gamma_4 := \{(x, q, \tau) : x_5 = 0\}$, $\Gamma_3 := \{(x, q, \tau) \in \Gamma_4 : (x_3, x_4) = 0\}$, $\Gamma_2 := \{(x, q, \tau) \in \Gamma_3 : x_2 = 0\}$, $\Gamma_1 := \{(x, q, \tau) \in \Gamma_2 : x_1 = 0\} = \mathcal{A}$. To apply [82, Thm 4] we first observe that for the case $w = 0$ (addressed in item 1), the following holds:
1) Γ_4 is asymptotically stable because the flow dynamics of x_5 is independent of the other states and governed by a Hurwitz linear time-invariant flow matrix $A + LC$, see (3.10), while the jump matrix is the identity. Asymptotic stability of Γ_4 then follows from the persistent flowing results of [58, Prop. 3.27] ensured by the fact that jumps are inhibited in (3.11) until $\tau \geq \tau_{\min}$. The same argument can be repeated to prove that Γ_i is asymptotically stable relative to Γ_{i+1}, for $i = 3, 1$, because both $\begin{bmatrix} A + BK_2 & BK_{\mathrm{i}} \\ C & 0 \end{bmatrix}$ and $A + BK_1$ are Hurwitz by assumption, see (3.10). To prove that Γ_2 is asymptotically stable relative to Γ_3, we first project the dynamics on a reduced state space where $x_1 = 0$ (this is possible due to the upper triangular structure of A_{cl} and E_{cl}). Then we observe that this projection of

Γ_2 is forward invariant and globally uniformly attractive (because the persistently flowing solutions from Γ_3 converge to zero after the first jump in at most $\tau_{\max}$ ordinary time). Using the fact that the projection of Γ_2 on the $x_1 = 0$ hyperplane is compact, GAS of Γ_2 relative to Γ_3 follows from[1] [58, Prop. 7.5].
2) All solutions are bounded. Indeed, pick an arbitrary initial condition and note that *a)* state x_5 is bounded because it does not change across jumps and converges to zero following a linear exponentially convergent transient during flows; *b)* state (x_3, x_4) follows analogous dynamics, also being perturbed by a bounded input during flows, which cannot drive the state unbounded from Bounded Input Bounded State (BIBS) stability properties of linear exponentially stable continuous-time dynamics; *c)* boundedness of x_2 follows from the fact that it remains constant along flows and jumps to some linear combinations of bounded quantities (x_3, x_4, x_5) across jumps; *d)* state x_1 is then bounded by a straightforward application of [93, Lemma 1], because the linear time-invariant dynamics is governed by an exponentially stable LTI dynamics along (persistent) flows (see the assumption on $A+BK_1$ in (3.10)) and by the identity map across jumps, whereas the forcing inputs acting along flows and across jumps come as linear combinations of bounded variables (x_1, x_2, x_3). The above properties (1) and (2) imply that we can invoke [82, Thm 4] and global asymptotic stability of $\mathcal{A}$ follows. Proof of item (2). We start proving that there exists a q-dependent vector $\Pi(q) \in \mathbb{R}^n$ that satisfies the following conditions

$$\begin{bmatrix} A_{\mathrm{cl}}(q) & G_{\mathrm{cl}}(q) \\ C_{\mathrm{cl}}(q) & D_{\mathrm{cl}} \end{bmatrix} \begin{bmatrix} \Pi(q) \\ I \end{bmatrix} = 0, \quad \forall q \in \mathcal{Q} \tag{3.12a}$$

$$\Pi(q^+) - E_{\mathrm{cl}}(q)\Pi(q) = 0, \quad \forall q \in \mathcal{Q}, \tag{3.12b}$$

which are a generalization of the classical regulator equations [52]. The conditions in (3.12) can be intuitively derived noticing that $x(\infty) := \Pi(q)w(\infty)$, and $e(\infty) := C_{\mathrm{cl}}(q)x(\infty) + D_{\mathrm{cl}}w(\infty)$, so that the flow properties $(\dot{x}(\infty), e(\infty)) = (0, 0)$ can be derived by imposing $\Pi(q^+)w(\infty) = x(\infty)^+ = E_{\mathrm{cl}}(q)x(\infty)$, and where we used the notation (∞) to denote the asymptotic value.

In order to prove feasibility of (3.12) we split the subspace $\Pi(q)$ according to the partitioning in (3.9) as follows $\Pi(q) := (\Pi_1(q), \Pi_2, \Pi_3, \Pi_4, \Pi_5)$, and considering (3.12a) we obtain the following set of equalities

$$0 = (A + BK_1)\Pi_1(q) + (2 - q)\left(B\Pi_2 + BK_1\Pi_5 + G\right) \tag{3.13a}$$

$$0 = (A + BK_2)\Pi_3 + BK_{\mathrm{i}}\Pi_4 + BK_2\Pi_5 + G \tag{3.13b}$$

$$0 = C\Pi_3 + Q \tag{3.13c}$$

$$0 = (A + LC)\Pi_5 - G - LQ, \tag{3.13d}$$

[1]The statement in [58, Prop. 7.5] is only local but a global version of it trivially follows from picking increasingly large values of the scalar μ therein characterized.

where we omitted equations that are trivially satisfied. By the internal model principle [52] we know that (3.13b), (3.13c) and (3.13d) are automatically satisfied. Now, we can easily verify that, with the selection

$$\begin{aligned} \Pi_1(q) &= (2-q)\Pi_3 \\ \Pi_2 &= K_{\mathrm{i}}\Pi_4 + (K_2 - K_1)(\Pi_3 + \Pi_5), \end{aligned} \tag{3.14}$$

equation (3.13a) reduces to (3.13b) and it is automatically satisfied by the internal model principle. It is not hard to check that with the selection (3.14) also (3.12b) is satisfied. Finally, plugging the change of coordinates $\tilde{x} = x - \Pi(q)w$ into (3.11), and using (3.12), we obtain a hybrid system equivalent to (3.11) where w has been set to zero and whose stability has already been proved, which concludes the proof. □

3.3 Conclusion

In this chapter we presented a hybrid controller that combines a reset and a switching mechanism. The proposed structure allows to simultaneously combine two controllers with almost no restriction on the switching between the two (thanks to the bumpless filter). For robustness reasons the scheme is equipped with an internal model and an external model. The external model is updated only at jumps using the information collected by the internal model and the observer during the flow. An experimental application showing satisfactory performance in controlling a wet clutch is reported in Chapter 5.

Chapter 4

Dead-zone observers

In this chapter we propose an adaptive dead-zone mechanism to robustify observers against high-frequency noise. The construction applies to Luenberger observers and high-gain observers for plants in strict feedback form. The dead-zone improves performances by trimming a portion of the output injection term and trapping the high frequency noise in the dead band. The dead-zone levels are dynamically adapted obtaining global convergence, establishing a trade-off between speed of convergence and noise sensitivity. We show that the observer gain and the adaptation parameters can be obtained by solving a linear matrix inequality, whose feasibility only requires detectability of the plant. The parameters obtained through this optimization ensure (in the absence of noise) global exponential stability of the estimation error dynamics, and input-to-state stability (ISS) from the measurement noise to the estimation error. The results presented in this chapter are extracted from the conference paper [35] and the journal paper [34].

4.1 Introduction

Robustly reconstructing the state of a plant from input-output measurements is one of the most fundamental problems in control theory. The first milestone has been obtained by David Luenberger in [80] and [79], where the problem of state estimation for linear plants has been solved by means of a dynamic filter, today called Luenberger observer. The need for robust observation laws motivated nonlinear extensions of the linear loop transfer recovery approach [47] leading to high-gain solutions that appeared in the early nineties [55], [50], and later became popular tools solving nonlinear control problems ranging from output stabilization to tracking and regulation. This great impact was also possible thanks to the output stabilization techniques developed in [116] and to the semiglobal separation principle obtained in [115, 10]. These results allow designing feedback laws as if the state were available and then use an estimate provided by a sufficiently fast observer. The prices to pay for this flexibility are essentially twofold: first, peaking phenomena, and second high sensitivity to measurements noise. The latter was already well known in the framework of linear observers [72] and entails the classical trade-off between bandwidth and noise rejection.

Despite this high sensitivity, high-gain observers are ISS from the measurement noise to the estimation error [122, 101, 9]. To reduce peaking and noise sensitivity, observation schemes with improved rejection may comprise a bank of different observers (a multi-observer) as in [84], where each observer has a different sensitivity to noise and convergence speed. Then, a supervisor chooses which observer is providing the best estimate at any given time. See also [33] where robustness with respect to an uncertain plant is studied (each observer is designed for a different value of the uncertain parameter). Alternatively, one may use an aggressive observer gain for transient estimation and a more relaxed one for steady-state performance [1]. However, there are many design challenges in using this approach, e.g., it is hard to properly select the switching time/mechanism (like trigger or threshold based mechanism) and the intrinsic discontinuous behavior of the observer is dangerous when combined with phenomena as peaking. A similar, but simpler, approach has been also proposed in [100] where a piecewise linear gain function is used. The limiting case of arbitrarily fast switching among different observers or different gains can be thought of as continuous adaptation, as in [103, 2, 18], where the observer gain is dynamically adapted according to the difference $(\hat{y} - y)$.

Nonlinear, time-varying or adaptive output injection/correction terms can also be considered, as in [5, 4, 6], to obtain superior performance or to deal with nonlinear plants that do not have special normal forms or do not satisfy Lipschitz-like conditions. Finally, recently the so-called *low-power approach* has been proposed [7, 8], which increases the dimension of the observer state but reduces the sensitivity to noise and the peaking phenomena.

In this chapter we propose here to apply an artificial dead-zone to the output injection term $(\hat{y} - y)$. The resulting "dead-zonated" observer better rejects high-frequency noise by cutting the part of it falling inside the dead-band. The dead-band amplitude is dynamically adapted according to the noise level, providing another useful information.

The dead-zone has a destabilizing effect on the estimation error dynamics, indeed in a ball around the zero estimation error the observer runs in open loop. However if the adaptation mechanism is carefully designed, the dead-zone rapidly converges to the identity function and in the absence of noise retrieves the classical output injection term $(\hat{y} - y)$. We show here that both the synthesis of the observer gain and of the adaptation mechanism can be cast as Linear Matrix Inequality (LMI), whose feasibility only requires detectability of the plant.

The use of the dead-zone is motivated by results developed for linear systems subject to sector bounded nonlinearities, such as global and local sector conditions [44, 67]. These tools have been extensively used in combination with LMIs in the context of anti-windup design, but rarely employed for observers, even if there are a few remarkable exceptions [118, 3, 6]. Our solution is indeed somewhat inspired by [3], where similar adaptations

are adopted to preserve stability in the presence of a saturated (rather than dead-zonated) output injection term, geared towards efficiently dealing with measurement outliers.

4.2 LTI problem formulation

In this work we consider a continuous-time LTI system ("the plant") of the following form,

$$\begin{cases} \dot{x} = Ax + Bu \\ y = Cx + Du + v, \end{cases} \tag{4.1}$$

where $x \in \mathbb{R}^n$ is the state, $u \in \mathbb{R}^m$ is the input, $y \in \mathbb{R}^p$ is the measured output and $v \in \mathbb{R}^p$ is a measurement noise. Following the preliminary work in [35], for dealing with high-frequency noise affecting the plant output, we introduce a Luenberger observer whose output injection is "dead-zonated" as follows

$$\begin{cases} \dot{\hat{x}} = A\hat{x} + Bu + L\mathrm{dz}_{\sqrt{\sigma}}(\hat{y} - y) \\ \hat{y} = C\hat{x} + Du, \end{cases} \tag{4.2}$$

where $\hat{x} \in \mathbb{R}^n$ is the estimated state, $\hat{y} \in \mathbb{R}^p$ is the estimated output and $\sigma \in \mathbb{R}^p_{\geq 0}$ is a vector whose entries are non-negative and define the amplitude of the dead-zone on the corresponding output channel. Matrix $L \in \mathbb{R}^{n \times p}$ is the classical observer gain. Function $\mathrm{dz}_{\sqrt{\sigma}} : \mathbb{R}^p \to \mathbb{R}^p$ is a decentralized vector-valued dead-zone defined as follows

$$\mathrm{dz}_{\sqrt{\sigma}}(y) := \begin{bmatrix} \mathrm{dz}_{\sqrt{\sigma_1}}(y_1) \\ \dots \\ \mathrm{dz}_{\sqrt{\sigma_p}}(y_p) \end{bmatrix}, \tag{4.3}$$

where $\sqrt{\sigma} := \left(\sqrt{\sigma_1}, \dots, \sqrt{\sigma_p}\right) \in \mathbb{R}^p$ is a component-wise square root. For σ we propose the following adaptation law

$$\dot{\sigma} = -\Lambda\sigma + \begin{bmatrix} (\hat{y} - y)^\top R_1 (\hat{y} - y) \\ \vdots \\ (\hat{y} - y)^\top R_p (\hat{y} - y) \end{bmatrix}, \quad \sigma \in \mathbb{R}^p_{\geq 0} \tag{4.4}$$

where $\Lambda \in \mathrm{Diag}^p_{>0}$ is a diagonal positive definite matrix, and $R_1, \dots, R_p \in \mathrm{Sym}^p_{\geq 0}$ are symmetric positive semi-definite matrices. The constraint $\sigma \in \mathbb{R}^p_{\geq 0}$ means that σ belongs to the closed p-dimensional positive orthant, which is an invariant set for (4.4). It is worth to notice that non-negativity of σ makes the square root $\sqrt{\sigma}$ always well defined.

The idea behind observer (4.2) is that the dead-zone provides a zero output correction

term around $(\hat{y}-y)=0$ so that high frequency noise is filtered out. However, the dead-zone also has a destabilizing effect on the error dynamics so that a fast enough adaptation of σ is necessary to ensure convergence to zero. Indeed, for a fixed dead-zone amplitude $\sqrt{\sigma}$, signals $\hat{y}$ and y which are close enough would never synchronize. The adaptive mechanism (4.4) is designed to weigh two antagonistic effects: first, the "adaptation speed" selected by Λ, and second, the "filtering action" tuned by $R_1,\dots,R_p$. Intuitively speaking, selecting Λ large enough, and $R_1,\dots,R_p$ sufficiently small we can recover a classical Luenberger observer. On the other hand, setting Λ small and $R_1,\dots,R_p$ large we slow down the convergence rate while increasing the filtering capability.

Remark 4.1
The initial condition $\sigma(0)$ for (4.4) can be taken small or zero if we expect measurement with a low noise level. On the contrary, if large amplitude noise is expected, then larger values of $\sigma(0)$ may lead to improved transient responses. ⌟

4.3 Main results

In this section we prove a few good properties for the dead-zone observers in (4.2). We show that for a detectable plant, the parameters Λ and R_i, can always be designed to obtain GES of the error dynamics in the absence of measurement noise, and ISS from the measurement noise to the estimation error.

4.3.1 Global Exponential Stability (GES)

Given (4.2) and the adaptation law (4.4) we cast the synthesis of the parameters L, Λ, $R_1,\dots,R_p$ as an LMI problem. In the absence of noise, this tuning procedure ensures GES of the estimation error dynamics and of the adaptive dynamics σ. To this end, define the estimation error as $e=\hat{x}-x$ and the vector-valued saturation function as $\mathrm{sat}_{\sqrt{\sigma}}(y):=y-\mathrm{dz}_{\sqrt{\sigma}}(y)$, where the vector-valued dead-zone is defined in (4.3). Then, after few manipulations, we obtain the following representation for the error arising from (4.2), (4.4),

$$\begin{cases} \dot{e}=(A+LC)e-Lv-L\mathrm{sat}_{\sqrt{\sigma}}(Ce-v) \\ \dot{\sigma}=-\Lambda\sigma+\begin{bmatrix}(Ce-v)^\top R_1(Ce-v)\\ \vdots \\ (Ce-v)^\top R_p(Ce-v)\end{bmatrix} \quad \sigma\in\mathbb{R}^p_{\geq 0}. \end{cases} \tag{4.5}$$

Equation (4.5) represents the error dynamics of a classical Luenberger observer plus a perturbation term whose amplitude is ruled by $\sqrt{\sigma}$. What follows is the main result of this

paper for the LTI case, namely for the class of systems (4.1).

Theorem 4.1
Consider the following LMI in the optimization variables $P \in \mathrm{Sym}^n_{>0}$, $X \in \mathbb{R}^{n\times p}$, $\Lambda \in \mathrm{Diag}^p_{>0}$, $R \in \mathrm{Sym}^p_{\geq 0}$, $U \in \mathrm{Diag}^p_{\geq 0}$,

$$\mathrm{He}\begin{bmatrix} PA + XC + C^\top RC & -X \\ UC & -U - \Lambda \end{bmatrix} < 0. \tag{4.6}$$

Any feasible solution to (4.6), together with the choice

$$L := P^{-1}X, \quad R := \sum_{j=1}^{p} R_j, \tag{4.7}$$

makes (4.5) globally exponentially stable to the origin for $v = 0$ *and ISS from* v *to* $(e, \sqrt{\sigma})$.

Remark 4.2
The adaptation law in (4.4) allows for a completely decentralized form where the amplitude of each dead-zone is adapted independently. This can be done by solving (4.6) for a diagonal R and then associating each diagonal element r_{ii} to the corresponding σ_i dynamics. The resulting adaptation law yields $\dot{\sigma}_i = -\lambda_{ii}\sigma_i + r_{ii}(\hat{y}_i - y_i)^2$. ⌟

Proof. Strict negativity of (4.6) implies that there exists a sufficiently small $c_0 \in \mathbb{R}_{>0}$ such that,

$$H := \mathrm{He}\begin{bmatrix} PA + XC + C^\top RC & -X \\ UC & (c_0 - 1)\Lambda - U \end{bmatrix} \leq -2c_0 I \tag{4.8}$$

Then, let us consider the candidate Lyapunov function $V(e, \sigma) := e^\top Pe + 2\mathbf{1}^\top\sigma$, where $P \in \mathrm{Sym}^n_{>0}$. The function $V(e, \sigma)$ is positive definite and radially unbounded on $\mathbb{R}^n \times \mathbb{R}^p_{\geq 0}$ and satisfies the following bounds,

$$\alpha_1 \left|(e, \sqrt{\sigma})\right|^2 \leq V(e, \sigma) \leq \alpha_2 \left|(e, \sqrt{\sigma})\right|^2, \tag{4.9}$$

where $\alpha_1 := \min\{\lambda_{\min}(P), 2\}$, and $\alpha_2 := \max\{\lambda_{\max}(P), 2\}$, so that the Lie derivative along the flow of (4.5) yields

$$\begin{aligned} \dot{V}(e, \sigma) = {} & e^\top (A + LC)^\top Pe + e^\top P(A + LC)e \\ & - 2e^\top PL\mathrm{sat}_{\sqrt{\sigma}}(Ce - v) - 2v^\top L^\top Pe - 2\mathbf{1}^\top \Lambda\sigma \\ & + 2\sum_{j=1}^{p} (Ce - v)^\top R_j (Ce - v) \end{aligned} \tag{4.10}$$

To enforce (strict) negativity of (4.10) we first consider a global sector condition for cone

bounded nonlinearities [44] and then use the fact that the saturation levels are proportional to $\sqrt{\sigma}$ and thus $\mathrm{sat}^\top_{\sqrt{\sigma}}(Ce)\mathrm{sat}_{\sqrt{\sigma}}(Ce)$ never exceeds $\mathbf{1}^\top\sigma$. These observations translate into the following inequalities

$$\mathrm{sat}^\top_{\sqrt{\sigma}}(Ce-v)U(Ce-v-\mathrm{sat}_{\sqrt{\sigma}}(Ce-v))\geq 0, \tag{4.11a}$$
$$\mathbf{1}^\top\Lambda\sigma-\mathrm{sat}^\top_{\sqrt{\sigma}}(Ce-v)\Lambda\mathrm{sat}_{\sqrt{\sigma}}(Ce-v)\geq 0, \tag{4.11b}$$

for any matrices $U\in\mathrm{Diag}^p_{\geq 0}$, $\Lambda\in\mathrm{Diag}^p_{>0}$. Multiplying (4.11a) by two and (4.11b) by $2(1-c_0)$, and adding them to (4.10), we obtain the following upper-bound, which uses $X=PL$ and $R:=\sum_{j=1}^p R_j$,

$$\begin{aligned}\dot V(e,\sigma)\leq&\begin{bmatrix}e\\ \mathrm{sat}_{\sqrt{\sigma}}(Ce-v)\end{bmatrix}^\top H\begin{bmatrix}e\\ \mathrm{sat}_{\sqrt{\sigma}}(Ce-v)\end{bmatrix}\\&-2c_0\mathbf{1}^\top\Lambda\sigma-2v^\top L^\top Pe+2v^\top Rv\\&-4v^\top RCe-2\mathrm{sat}^\top_{\sqrt{\sigma}}(Ce-v)Uv.\end{aligned} \tag{4.12}$$

To prove GES in the absence of disturbances, let us set $v=0$ and plug (4.8) into (4.12) to obtain the following inequality

$$\begin{aligned}\dot V(e,\sigma)&\leq-2c_0|(e,\mathrm{sat}_{\sqrt{\sigma}}(Ce))|^2-2c_0\mathbf{1}^\top\Lambda\sigma\\&\leq-2c_1\left|(e,\sqrt{\sigma})\right|^2\leq-\frac{2c_1}{\alpha_2}V(e,\sigma),\end{aligned}$$

where we used the rightmost bound in (4.9) and $c_1:=c_0\min\{1,\lambda_{\min}(\Lambda)\}$. Applying the comparison lemma and using the leftmost bound in (4.9) we immediately obtain $|(e,\sqrt{\sigma})|\leq\sqrt{\alpha_2/\alpha_1}\exp(-c_1/\alpha_2)\left|(e_0,\sqrt{\sigma_0})\right|$, which proves global exponential stability for $(e,\sqrt{\sigma})$. The exponential bound can then be easily extended to (e,σ), see [3].

To prove the ISS statement, let us define $c_2:=|R|$, $c_3:=\left|PL+2C^\top R\right|$, $c_4:=|U|$, so that (4.12) can be compactly rewritten as

$$\begin{aligned}\dot V(e,\sigma)&\leq-2c_1\left|(e,\sqrt{\sigma})\right|^2+2c_2\left|v\right|^2+2c_3\left|e\right|\left|v\right|+2c_4\left|\sqrt{\sigma}\right|\left|v\right|\\&\leq-c_1\left|(e,\sqrt{\sigma})\right|^2+c_1^{-1}(2c_1c_2+c_3^2+c_4^2)\left|v\right|^2\\&\leq-c_1\left|(e,\sqrt{\sigma})\right|^2<0,\end{aligned} \tag{4.13}$$

which holds for all $\left|(e,\sqrt{\sigma})\right|^2>c_1^{-2}(2c_1c_2+c_4^2+c_3^2)\left|v\right|^2:=c_5^2\left|v\right|^2$ and we conclude that (4.5) is ISS from v to $(e,\sqrt{\sigma})$ with an ISS gain proportional to c_5. In (4.13) we used the Young inequalities $2\left|e\right|\left|v\right|\leq\frac{c_1}{c_3}\left|e\right|^2+\frac{c_3}{c_1}\left|v\right|^2$ and $2\left|v\right|\left|\sqrt{\sigma}\right|\leq\frac{c_1}{c_4}\left|\sqrt{\sigma}\right|^2+\frac{c_4}{c_1}\left|v\right|^2$. □

Theorem 4.1 ensures exponential convergence of the estimation error in the absence

of disturbances, and its boundedness in the presence of bounded disturbances. This is desirable for nonlinear observers, because in a nonlinear setting diverging solutions may arise with arbitrarily small measurement noise [107]. Moreover the ISS property ensures graceful performance degradation, another desirable property for (4.5).

4.3.2 Feasibility

Theorem 4.1 provides only a sufficient condition to enforce GES, however feasibility of (4.6) can be exactly characterized.

Proposition 4.1
The LMI (4.6) is feasible if and only if pair (C, A) is detectable.

Proof. Necessity follows from standard detectability results. Indeed, if pair (C, A) is not detectable, no asymptotic observer exists and thus (4.6) must be infeasible from Theorem 4.1. To prove sufficiency we use [64, Thm 16.6] to get that detectability of (C, A) implies the existence of a matrix $P \in \mathrm{Sym}^n_{>0}$ satisfying

$$A^\top P + PA - C^\top C < 0. \tag{4.14}$$

Consider (4.6) and select $X = -3C^\top$, $\Lambda = U = I$ and $R = I/2$. Pre/post multiplying by the congruence transformation matrix

$$\begin{bmatrix} I & C^\top \\ 0 & I \end{bmatrix} \begin{bmatrix} PA + A^\top P - 5C^\top C & 4C^\top \\ 4C & -4I \end{bmatrix} \begin{bmatrix} I & 0 \\ C & I \end{bmatrix} = \begin{bmatrix} A^\top P + PA - C^\top C & 0 \\ 0 & -4I \end{bmatrix} < 0, \tag{4.15}$$

it follows that (4.15) is feasible thanks to (4.14). □

Remark 4.3
Under the detectability assumption, condition (4.6) is always feasible even when a stabilizing gain L is a priori fixed. In this case we can think of (4.2) as a dead-zone augmentation, i.e., an adaptive output injection mechanism enhancing the performance of a pre-designed observer. The LMI in (4.6) can still be used as a design tool fixing a stabilizing L (i.e., such that $(A+LC)$ is Hurwitz) and replacing X by PL. The arising LMI is always feasible and provides a convenient way to design the adaptation parameters Λ and R. ⌟

4.4 High-gain dead-zone observers for nonlinear plants

In this section we extend the dead-zone design to multi-input, single-output nonlinear plant in the following *strict feedback* form

$$\begin{cases} \dot{x}_1 = x_2 + f_1(x_1, u) \\ \quad \vdots \\ \dot{x}_{n-1} = x_n + f_{n-1}(x_{1\dots n-1}, u) \\ \dot{x}_n = f_n(x_{1\dots n}, u) \\ y = x_1 + v, \end{cases} \tag{4.16}$$

where $x := (x_1, \dots, x_n) \in \mathbb{R}^n$ is the state, $u \in \mathbb{R}^m$ is the input, $y \in \mathbb{R}$ is the output. We use the shorthand notation $x_{1\dots i} := (x_1, \dots, x_i) \in \mathbb{R}^i$ to stress that f_i depends only on the first i components of the state vector x. The functions f_i are assumed to be continuous. Conditions for the existence of a local or global diffeomorphism that maps a generic nonlinear system into the strict feedback form (4.16) are analyzed in [56, Thm 4.1] and are related to the existence of *uniform full relative degree*. For the sake of compactness we rewrite (4.16) as follows

$$\begin{cases} \dot{x} = Ax + f(x, u) \\ y = Cx + v, \end{cases} \tag{4.17}$$

where pair (C, A) is in prime form, therefore observable, and $f : \mathbb{R}^n \times \mathbb{R}^m \to \mathbb{R}^n$ is a continuous vector-valued map obtained stacking the functions f_i for $i = 1, \dots, n$. Following the construction of Section 4.2 consider the following high-gain dead-zone observer for (4.17)

$$\begin{cases} \dot{\hat{x}} = A\hat{x} + \hat{f}(\hat{x}, u) + \mathscr{E}^{-1}(\epsilon) L \mathrm{dz}_{\sqrt{\sigma}}(\hat{y} - y) \\ \hat{y} = C\hat{x} \\ \epsilon\dot{\sigma} = -\Lambda\sigma + R(\hat{y} - y)^2, \end{cases} \tag{4.18}$$

where $\hat{x} \in \mathbb{R}^n$ is the estimated state, $\hat{y} \in \mathbb{R}$ is the estimated output, and $\hat{f}_i$ are some approximations of functions f_i. The vector $L \in \mathbb{R}^n$ is the observer gain and matrix $\mathscr{E}(\epsilon) := \mathrm{diag}(\epsilon, \dots, \epsilon^n) \in \mathbb{R}^{n\times n}$ contains the powers of the high-gain parameter $\epsilon \in \mathbb{R}_{(0,1)}$, which is assumed to be small. For the analysis that follows it is convenient to define a re-scaled version of the error coordinates as follows

$$e = \epsilon^{-1}\mathscr{E}(\epsilon)(\hat{x} - x), \tag{4.19}$$

so that combining (4.18) and (4.17) the error dynamics results

$$\begin{cases} \epsilon\dot{e} = (A+LC)e + \mathscr{E}(\epsilon)(\hat{f}(\hat{x},u) - f(x,u)) \\ \qquad - Lv - L\mathrm{sat}_{\sqrt{\sigma}}(Ce - v) \\ \epsilon\dot{\sigma} = -\Lambda\sigma + R(Ce - v)^2. \end{cases} \tag{4.20}$$

From the upper-triangular structure of $\hat{f} - f$, we may select ϵ sufficiently small to dominate this mismatch and also speed up the observer dynamics. We ensure global convergence of the error by assuming the following [70].

Assumption 4.1
The difference $\hat{f}_i - f_i$ satisfies globally the Lipschitz-like condition

$$|\hat{f}_i(\hat{x}_{1\dots i}, u) - f_i(x_{1\dots i}, u)| \leq \mu_i^\circ + \mu_i \sum_{j=1}^{i} |\hat{x}_j - x_j|, \tag{4.21}$$

for all $x_{1\dots i} \in \mathbb{R}^i$ with μ_i°, μ_i independent of u.

From the structure of (4.21) and (4.19), follows that

$$\begin{aligned} |\mathscr{E}(\epsilon)(\hat{f}(\hat{x},u) - f(x,u))| &\leq \epsilon \sum_{i=1}^{n} \epsilon^{i-1}(\mu_i^\circ + \mu_i \sum_{j=1}^{i} \epsilon^{1-j}|e_j|) \\ &\leq \epsilon \sum_{i=1}^{n} \epsilon^{i-1}\mu_i^\circ + \epsilon \sum_{i=1}^{n} \mu_i |e| \\ &\leq \epsilon\mu^\circ + \epsilon\mu|e|, \end{aligned} \tag{4.22}$$

where we defined $\mu^\circ := \sum_{i=1}^{n} \mu_i^\circ$ and $\mu := \sum_{i=1}^{n} \mu_i$ and we used the fact that $\epsilon \in \mathbb{R}_{(0,1)}$. This upper bound will be useful in the proof of Theorem 4.2.

Remark 4.4
As usually done in the high-gain observers literature, the global Lipschitz property in Assumption 4.1 can be relaxed to local Liscphitzness if we assume that the state of the plant evolves inside a known compact set. If this is the case, we can saturate functions $\hat{f}_i$ outside such a compact set, and still obtain a globally convergent observer. ⌟

Remark 4.5
Global observers for nonlinear systems that do not satisfy global Lipschitz conditions can be still constructed using homogenization tools, see for example [5], [15]. ⌟

Theorem 4.2
Suppose that L, Λ, R have been designed according to (4.6) and that Assumption 4.1 holds,

then (4.20) is ISS from (v, μ°) to $(e, \sqrt{\sigma})$ and for $\mu^\circ = 0$, $v = 0$ the origin is GES for (4.20).

Proof. We follow similar steps as in Theorem 4.1. Consider a scaled candidate Lyapunov function $V(e, \sigma) := \epsilon e^\top P e + 2\epsilon\sigma$ so that the Lie derivative along the flow of (4.20) yields,

$$\begin{aligned}\dot{V}(e,\sigma) \leq & -c_1|(e,\sqrt{\sigma})|^2 + c_5|v|^2 + 2e^\top P\mathscr{E}(\epsilon)(\hat{f}(\hat{x},u) - f(x,u)) \\ \leq & -c_1|(e,\sqrt{\sigma})|^2 + c_5|v|^2 + 2|e||P||\mathscr{E}(\epsilon)(\hat{f}(\hat{x},u) - f(x,u))|,\end{aligned} \tag{4.23}$$

where c_1 and c_5 are defined in the proof of Theorem 4.1. Plugging (4.19) into (4.21) and using (4.22) we can upper-bound equation (4.23) as follows

$$\begin{aligned}\dot{V}(e,\sigma) \leq & -c_1|(e,\sqrt{\sigma})|^2 + c_5|v|^2 + 2\epsilon\mu^\circ|P||e| + 2\epsilon\mu|P||e|^2 \\ \leq & -(c_1 - 2\epsilon\mu|P|)|(e,\sqrt{\sigma})|^2 + c_5|v|^2 + 2\epsilon\mu^\circ|P||e| \\ \leq & -(c_1 - 2\epsilon\mu|P| - \epsilon c_1)|(e,\sqrt{\sigma})|^2 + c_5|v|^2 + \epsilon c_1^{-1}|P|^2(\mu^\circ)^2\end{aligned}$$

so that, for ϵ sufficiently small, system (4.20) is ISS in the sense defined in Theorem 4.2 and for $\mu^\circ = 0$, $v = 0$, GES. □

4.5 An academic example

We propose an example that compares a high-gain observer with and without the dead-zone mechanism proposed in Section 4.4. We show through simulations that the dead-zone mechanism successfully improves the noise rejection capability. Let us consider the Van der Pol oscillator,

$$\begin{cases}\dot{x}_1 = x_2 \\ \dot{x}_2 = -x_1 + \gamma(1 - x_1^2)x_2 + u \\ \ \ y = x_1 + v,\end{cases} \tag{4.24}$$

where $\gamma = 5$. Equation (4.24) is in *strict feedback form*, but does not satisfy Assumption 4.1. However, assuming u bounded the solutions to (4.24) evolve in a compact set and according to Remark 4.4 we can saturate the nonlinear part of the observer obtaining global practical convergence. We propose the following dead-zonated high-gain observer

$$\begin{aligned}\dot{\hat{x}}_1 &= \hat{x}_2 + \epsilon^{-1}\ell_1 \mathrm{dz}_{\sqrt{\sigma}}(\hat{x}_1 - y) \\ \dot{\hat{x}}_2 &= \mathrm{sat}_M\left(-\hat{x}_1 + \hat{\gamma}(1 - \hat{x}_1^2)\hat{x}_2 + u\right) + \epsilon^{-2}\ell_2 \mathrm{dz}_{\sqrt{\sigma}}(\hat{x}_1 - y) \\ \epsilon\dot{\sigma} &= -\Lambda\sigma + R(\hat{x}_1 - y)^2,\end{aligned}$$

R	1.9	3.0	4.1	5.3	6.4	7.5
ENR High-gain	32.6	32.6	32.6	32.6	32.6	32.6
ENR Dead-zone	19.2	16.1	13.7	11.8	10.2	8.9

Table 4.1

where $\hat{\gamma} = 7$ and $M = 20$. Parameters $L := [\ell_1, \ell_2]^\top \in \mathbb{R}^2$, $\Lambda \in \mathbb{R}_{>0}$, $R \in \mathbb{R}_{\geq 0}$ have been designed according to the following convex optimization problem that maximizes the effect of the noise on the adaptation dynamics σ,

$$\begin{aligned} &\sup_{P,X,\Lambda,R} \ \mathrm{tr}(R) \ \text{ subject to:} \\ &\mathrm{He}\begin{bmatrix} PA + XC + C^\top RC & -X \\ UC & -U - \Lambda \end{bmatrix} < 0 \\ &\mathrm{He}\Big[PA + XC + \alpha_{\min} P\Big] < 0 \\ &\mathrm{He}\Big[PA + XC + \alpha_{\max} P\Big] > 0 \\ &0 < \Lambda \leq \Lambda_{\max}, \ R = R^\top \geq 0, \ P = P^\top > I. \end{aligned} \tag{4.25}$$

In addition to the LMI condition (4.6) we impose an interval for the possible convergence rates, so that $-\alpha_{\max} \leq \mathrm{Re}(\lambda_k(A + LC)) \leq -\alpha_{\min}$ where $\alpha_{\min} = 1$, $\alpha_{\max} = 100 \in \mathbb{R}_{>0}$ for this specific example. Finally, we select $\Lambda_{\max} = 10 \in \mathbb{R}_{>0}$, to avoid an excessive time scale separation among the observer and the adaptation dynamics. Solving (4.25) we obtain the following values $L = \begin{bmatrix} -68.36 & -68.06 \end{bmatrix}^\top$, $\Lambda = 9.98$, and $R = 7.51$. The high-gain parameter has been selected as $\epsilon = 0.1$.

Numerous simulations have been performed for the values of R reported in Table 4.1, a sinusoidal input $u(t) = 3\sin(2t)$, initial condition $x(0) = [0, 0]^\top$ for the plant, $\hat{x}(0) = [5, -5]^\top$ for the observer and $\sigma(0) = 5$ for the adaptation dynamics. The output measurement y is corrupted by noise generated by the Simulink block Uniform Random Number with sampling time and output range equal to $t_{\mathrm{s}} = 0.001$s, and ± 1. During the simulation, the noise starts at time $t_{\mathrm{start}} = 10$ and ends at $t_{\mathrm{end}} = 20$.

A comparison among the true and the estimated state for the two observers ($R = 7.5$) is shown in Figure 4.1. Figure 4.2 shows the estimation error, where the benefit of the dead-zone mechanism can be better appreciated, and the adaptation of the dead-zone level $\sqrt{\sigma}$. To compare the two observers we propose a tracking Error to Noise Ratio (ENR) which is inspired by the classical concept of Signal to Noise Ratio (SNR). The ENR is formally defined as $\mathrm{ENR} := \frac{\mathbb{E}\{e^\top e\}}{\mathbb{E}\{v^\top v\}}$, where $\mathbb{E}\{\cdot\}$ denotes the expectation operator. The value of the expectations has been obtained simply computing the average of the signals

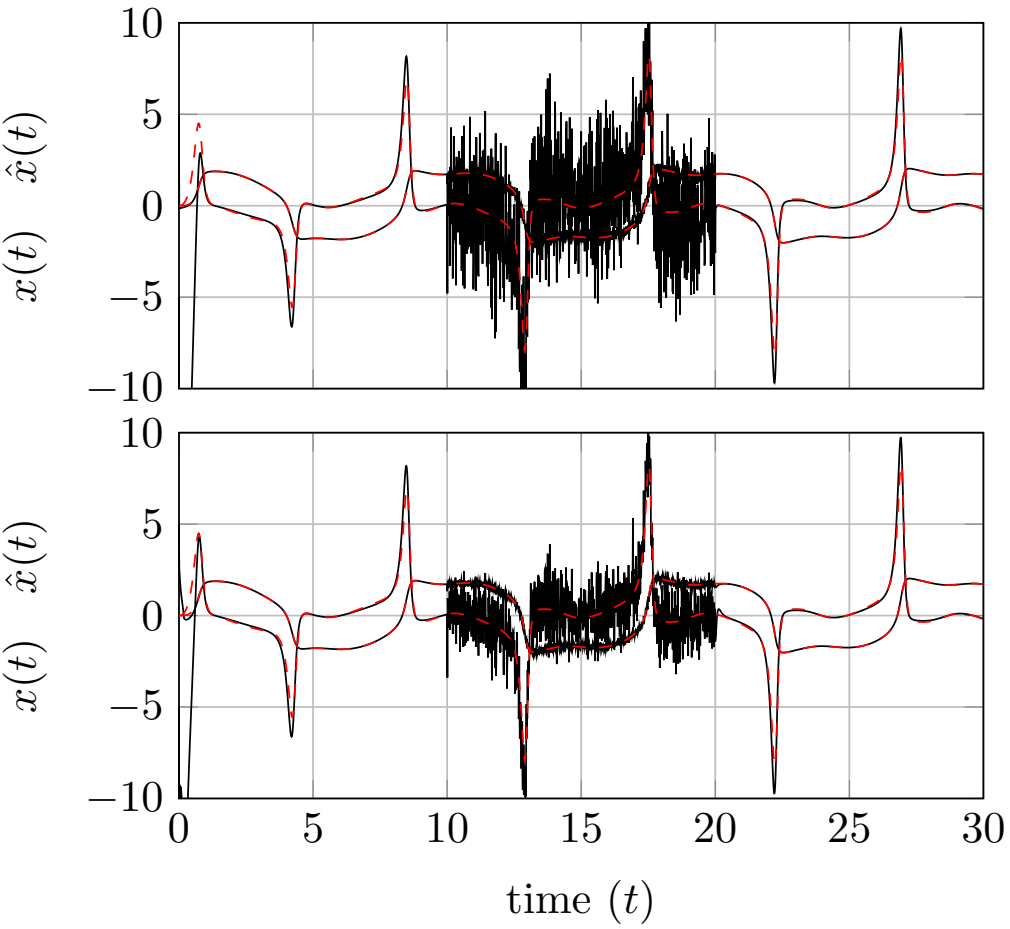

Figure 4.1: Estimated (black) and true (red) state with the bare high-gain observer (above) and the dead-zonated high-gain Observer (below) ($R = 7.5$). Notice the significant estimation error reduction in the lower trace.

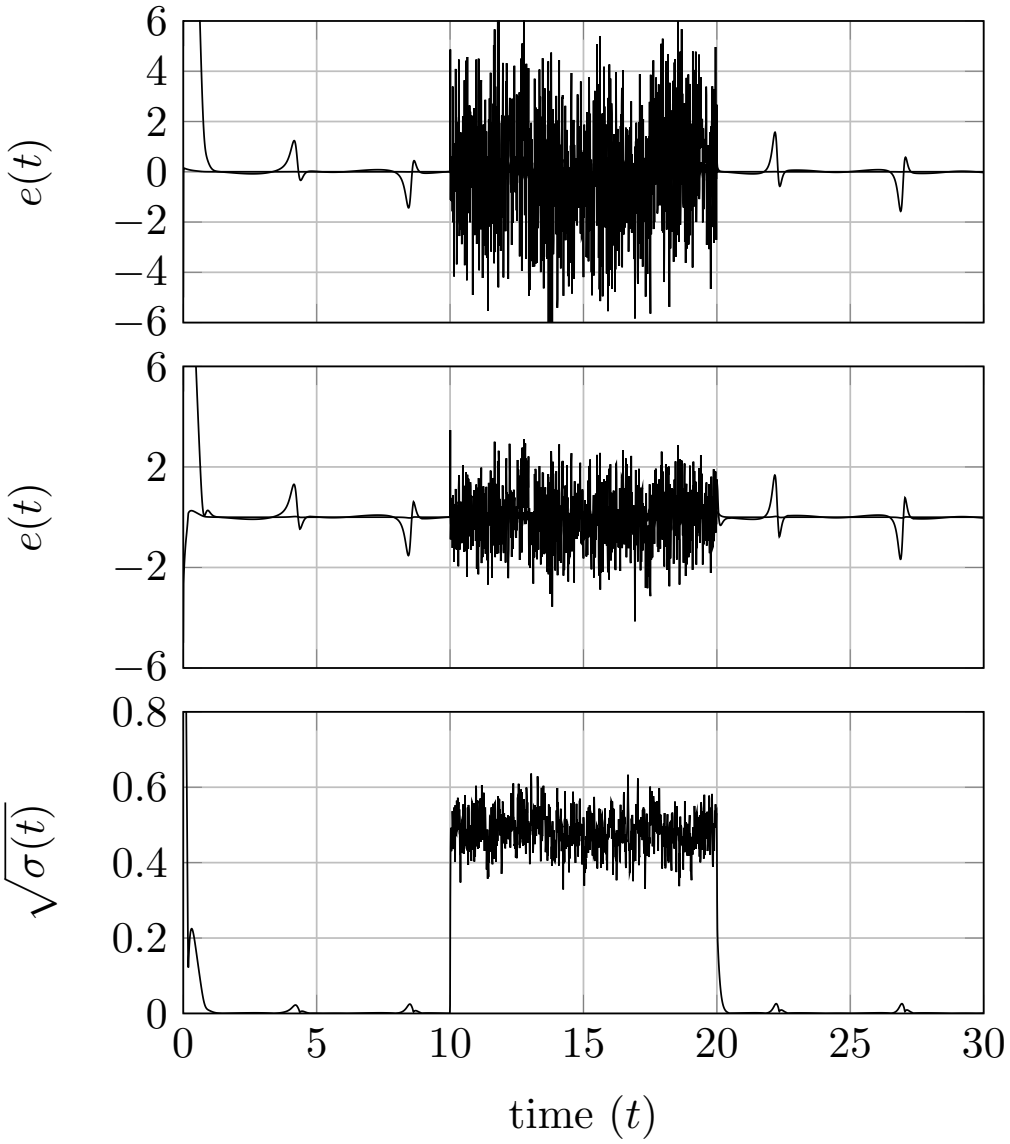

Figure 4.2: Estimation error for the high-gain observer (top), dead-zonated high-gain observer (middle) ($R = 7.5$), and adaptation of the σ level (bottom).

over the interval $[t_{\text{start}}, t_{\text{end}}]$. The ENRs for the two observers, and for different values of R, are reported in the Table 4.1. We can notice that the dead-zone mechanism reduces the tracking error to noise ratio (ENR) and that this reduction is more consistent when the value of R is large.

4.6 Conclusion

We proposed a dead-zonated output injection term that robustifies Luenberger and high-gain observers against high frequency noise. We proved that the resulting dead-zone observers are not restrictive for LTI plants and can always be designed under standard (and necessary) detectability assumption. Numerical studies within the nonlinear high-gain setting clearly reveal potential to reduce the ISS from the measurement noise and the estimation error. The quantitative characterization of this ISS gain appears to be a nontrivial task due to the convoluted nonlinear effect of the dynamic dead-zone, and it is seen as a future work.

Part II
Applications

Chapter 5

Hybrid Non-overshooting Set-point Pressure Regulation for a Wet Clutch

In this chapter we present a technological application of the hybrid controller presented in Chapter 3. We consider the problem of precisely controlling the oil pressure inside a wet clutch without overshoot. To achieve this objective we propose a control-oriented Wiener model for wet-clutches in filled conditions and we discuss the associated identification technique. We adapt the hybrid controller presented in Chapter 3, so that it ensures zero steady-state error and a fast non-overshooting response. We show that the controller parameters can be conveniently obtained by solving a set of Linear Matrix Inequalities (LMIs). Finally, we test the proposed control strategy on the Hydromechanical Variable Transmission (HVT) developed by Dana-Rexroth Transmission Systems (DRTS). The experiments show good performance and robustness with respect to modeling errors and noise. The material presented in this chapter is adapted from the conference paper [46] and the journal paper [36].

5.1 Introduction

The main goals for the next generation of transmission systems are an improved fuel economy and a better productivity. Toward these goals the automotive industry has developed numerous solutions, such as automatic and dual clutch transmissions, which can automatically shift among different drive ranges, thus improving both vehicle drivability and fuel economy. These technologies are now mature enough to be employed also in the off-highway, agricultural and working machines industry. However, it is particularly challenging to adapt these technologies for the off-highway market due to the rather different requirements. For example, mechanical Continuous Variable Transmissions (CVTs) are efficient, but they operate in a too narrow power range. This problem can be partially solved using Hydrostatic Transmissions (HTs), but their efficiency is low. Ideally, the best solution should combine the efficiency of the mechanical CVT and the power range of a HT. This marriage between the hydrostatic and the mechanical world is the Hydromechanical

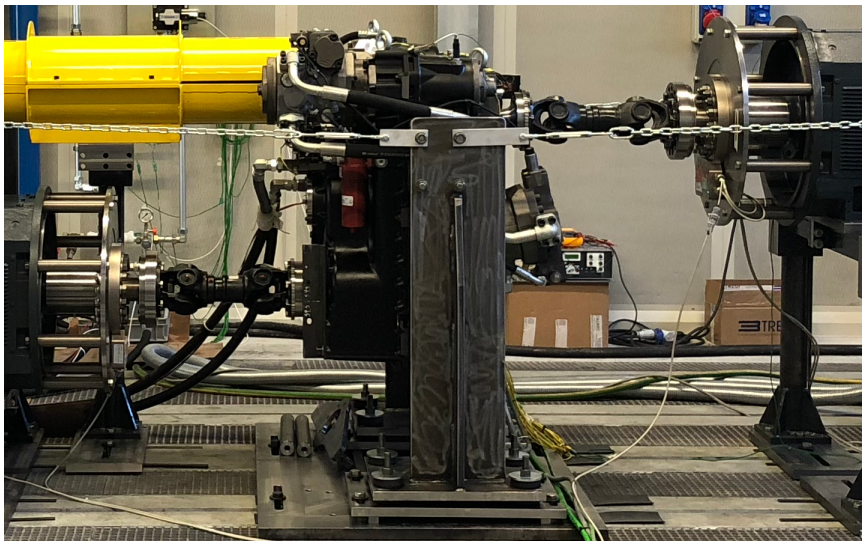

Figure 5.1: The Hydromechanical Variable Transmission (HVT).

Variable Transmission (HVT) that has been introduced by Dana-Rexroth Transmission Systems (DRTS) in [88] and references therein.

In the HVT architecture, see Figure 5.1, the engine power is split into two different pathways: the first one is mechanical and is highly efficient, while the second one is hydrostatic and preserves the continuous variable transmission characteristic. The powers coming from each pathway are then combined by means of a planetary gear. Moreover, in order to extend the range of possible speeds, the HVT can also shift among several drive ranges. This shift is performed by coordinating several wet-clutches, suitably actuated by electro-proportional valves. Ideally, during a clutch shift, the transmitted torque should remain constant to ensure a comfortable and smooth transition. Clutch control is an active area of research, and numerous control techniques have been proposed in the literature. In [66, 62] the authors propose a combination of differential flatness and feedback linearization, while in [109] a robust sliding-mode controller is presented. These approaches are rather elegant, but they are usually hard to implement in a digital form due to discretization issues or poorly known dynamics. This is especially true in our setup, where the actuation system of the HVT is difficult to identify precisely, due to non-linear effects, hysteresis and dependence on the oil temperature. Consequently, complex controllers may fail to work properly. Moreover, in contrast to [66] and [62], we do not assume the knowledge of the piston position, because for wet clutches it is technologically hard to place sensors inside a chamber with a rotating shaft soaked into oil. For this reason, the only available measurement for feedback is the oil pressure. A similar setup has been already considered in [60], where the authors propose a linear model for a twin-clutch transmission and they design a pressure feedback controller inducing a desirable clutch shift.

In this work we follow a similar spirit, but compared to [60], we consider a more complete model and we propose a novel hybrid controller. The main differences are highlighted below. First, in our setup the clutch shows a non-constant DC gain and a small variable delay in the actuation. We include these effects by adding a non-linear invertible map and considering a non-minimum phase approximation of the delay. The resulting model is the cascade of a non-minimum phase Single-Input Single-Output (SISO) Linear Time Invariant (LTI) system and an invertible non-linear output map, a so-called Wiener model.

Second, since a large amount of power is transmitted by the HVT, the closed-loop specifications are tight and somehow conflicting. The step response of the pressure in the chamber must be fast, non-overshooting, and with zero steady-state error. However, it is well-known that using linear controllers, non-overshoot and zero steady-state error are conflicting goals, and (in general) they cannot be simultaneously achieved. To overcome this limitation, we propose a novel hybrid controller that combines a switching and a resetting mechanism, thus providing the desired response. The controller synthesis is conveniently formulated as a Linear Matrix Inequality (LMI) problem, which is an efficient and systematic way to tune controllers.

Moreover, we study the robustness properties of the proposed solution considering constant (or slowly varying) disturbances acting on the model. Finally, we provide new and more convincing experimental results, showing the advantages of the proposed controller. For reasons of confidentiality all the units of measure are normalized and the technological details are omitted.

5.2 Setup description and goals

In the HVT architecture, wet-clutches are actuated by the hydraulic circuit sketched in Figure 5.2. The current in the valve regulates the oil pressure inside the clutch chamber, and controls in an indirect way the piston movement. Through this mechanism we can open and close the clutch, and by increasing or decreasing the contact force we modulate the transmitted torque. The standard actuation sequence is the following one: first, the current in the valve increases opening the orifice between the clutch chamber and the supply high pressure line. The oil flows pushing the clutch piston towards the end of the stroke, causing the transmission of a small torque due to drag effects. This phase is known as Filling Phase (FP), and it is usually performed in an open-loop fashion. During the FP, the pressure measurements are not reliable due to the pressure gradient associated to the flow. Secondly, when the piston reaches the end of the stroke, the gap between the clutch plates is zero and the flow stops. At this pressure, known as (mechanical) Kiss Point (KP) [49], the piston remains in equilibrium, thanks to the balancing of forces coming from the oil

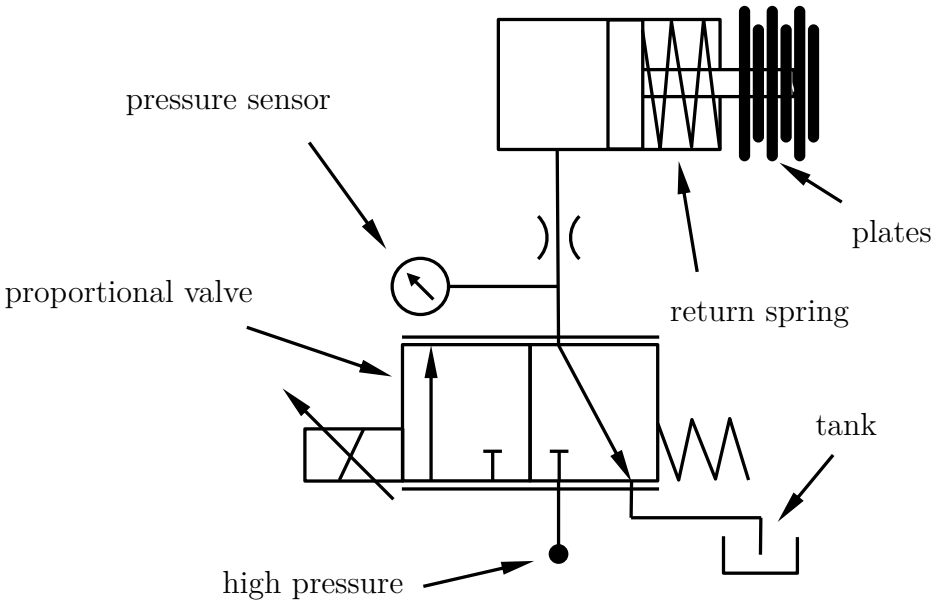

Figure 5.2: Hydraulic actuation scheme.

pressure and the return spring. Thirdly, when the KP is overcome, the plates push against each other and they transmit a considerable amount of torque. This operative condition is known as Modulation Range (MR), and is characterized by an affine relationship between the oil pressure and the transferred torque.

In order to obtain a smooth clutch shift, the Filling Phase (FP), the Kiss Point (KP), and the Modulation Range (MR), need to be properly controlled and synchronized. This translates into three key ingredients: 1) a correct timing and synchronization of the clutches, 2) a well prepared on-coming clutch (filled with oil and ready to engage), 3) a precise oil pressure control during the MR. A correct timing and synchronization can be obtained through a properly designed high level control and a time-scheduling algorithm, while the preparation of the clutch is performed in the FP. All these aspects are highly relevant, but in this work we focus on controlling the oil pressure in the MR. Because in the MR there is an affine relationship between the oil pressure and the transmitted torque, the task of controlling the torque is indeed equivalent to controlling the pressure. Here we assume that the electrical dynamics of the valve is negligible, i.e., much faster than the mechanical one, because a high performance current control has been implemented [41].

Even under the above simplifying assumptions, precisely controlling the oil pressure is a challenging task. The nonlinear interaction between the valve and the oil, and the viscosity that changes with the temperature, make the task non trivial.

For this application it is also fundamental that the closed-loop satisfies the following tight performance goals, whose motivations are discussed next.

Problem 5.1 (Control problem)
Design an oil pressure controller for the HVT such that the closed-loop response satisfies the following conditions:

1. *Non-overshooting step response.*
2. *Small rise time.*
3. *Zero steady-state error for constant reference signals.*

The precise value of the rise time is not specified for confidentiality reasons. These goals are all equally important to achieve a smooth clutch-shift because items 2) and 3) are key to ensuring that the driver does not experience any perturbation during the shift operation. Moreover, among all, the non-overshooting constraint is especially critical. Because, overshoot in the pressure response causes an excess of dissipated power that could burn the clutch friction discs. Problem 5.1 is difficult because requirements 1) and 3) are conflicting, and 2) imposes to use an aggressive controller.

In addition to the goals defined in Problem 5.1, it is desirable that the controller is robust w.r.t. 1) small delays in the loop, 2) possible slow unmodeled dynamics, 3) variations of the oil temperature and clutch aging. Moreover, due to the limited electronic hardware in the automotive industry, the proposed controller must be "easy enough" to be implemented with a limited computational power.

5.3 Modeling and identification

5.3.1 Model selection

In this section we discuss a control-oriented model for wet clutches in the MR. A good model must be accurate enough to capture the interplay among the different elements of the clutch, i.e., the valve, the line and the piston, but at the same time should be "simple", so that consolidated control techniques can be used. We consider as input the current in the valve, and as output the oil pressure inside the clutch chamber.

We performed a series of experiments, using a staircase like input current, as shown in Figure 5.3. The response at the first step differs from the others due to the presence of flowing oil (the clutch is still in the FP). When the clutch reaches the MR, the oscillating behavior recalls a second-order linear system with complex conjugate poles, however, a closer look reveals some nonlinear effects.

First, the DC gain is not constant, and second there is a small variable input-output delay, probably associated to a non-constant computational time. We capture the non-constant DC gain through a static output nonlinearity ϕ, for which we assume the following property.

Assumption 5.1
The output non-linearity ϕ is a continuous strictly increasing function on $\mathbb{R}_{\geq 0} := [0, +\infty)$.

For the input delay d, we introduced a non-minimum phase behavior in the response, which approximates the delay by way of a small undershoot. This is not surprising since the first-order Padé approximation of delay d yields,

$$e^{-i\omega d} \approx \frac{1 - i\omega d/2}{1 + i\omega d/2} \quad \forall \omega \ll 1/d, \tag{5.1}$$

where i is the imaginary unit and $\omega \in \mathbb{R}$ the pulsation. This approximation shows that for a large range of frequencies, ($1/d$ is large), a small time delay is equivalent to a zero in the open right-half plane plus a pole in the open left-half. We can disregard the pole, because it is much faster than the clutch dynamics, and we keep the zero. With slight abuse of notation, we mix time and Laplace domain. Given a signal $u(\cdot)$ defined for $t \in \mathbb{R}_{\geq 0}$, we denote by $u(t) \in \mathbb{R}$ the value at time t, and by $u(s) \in \mathbb{C}$ the value of its Laplace transform at $s \in \mathbb{C}$. Based on the considerations above, we propose a *Wiener* model [76], of the following form

$$y(s) := \left(\frac{1 + a_3 s}{1 + a_1 s + a_2 s^2}\right) u(s) = H(s)u(s) \tag{5.2a}$$

$$z(t) := \phi(y(t)), \tag{5.2b}$$

where $u \in \mathbb{R}$ is the input, $z \in \mathbb{R}$ is the measured output, $y \in \mathbb{R}$ is an equivalent "linear output" and $\phi : \mathbb{R}_{\geq 0} \to \mathbb{R}_{\geq 0}$ an invertible nonlinear map.

The transfer function $H(s) \in \mathbb{C}$ is strictly proper and non-minimum phase due to the delay approximation in (5.1).

Remark 5.1
Without loss of generality we assume that the DC gain of (5.2a) is unitary, $\lim_{s \to 0} H(s) = 1$. Indeed, a different DC gain can be easily absorbed into the nonlinearity ϕ. ⌟

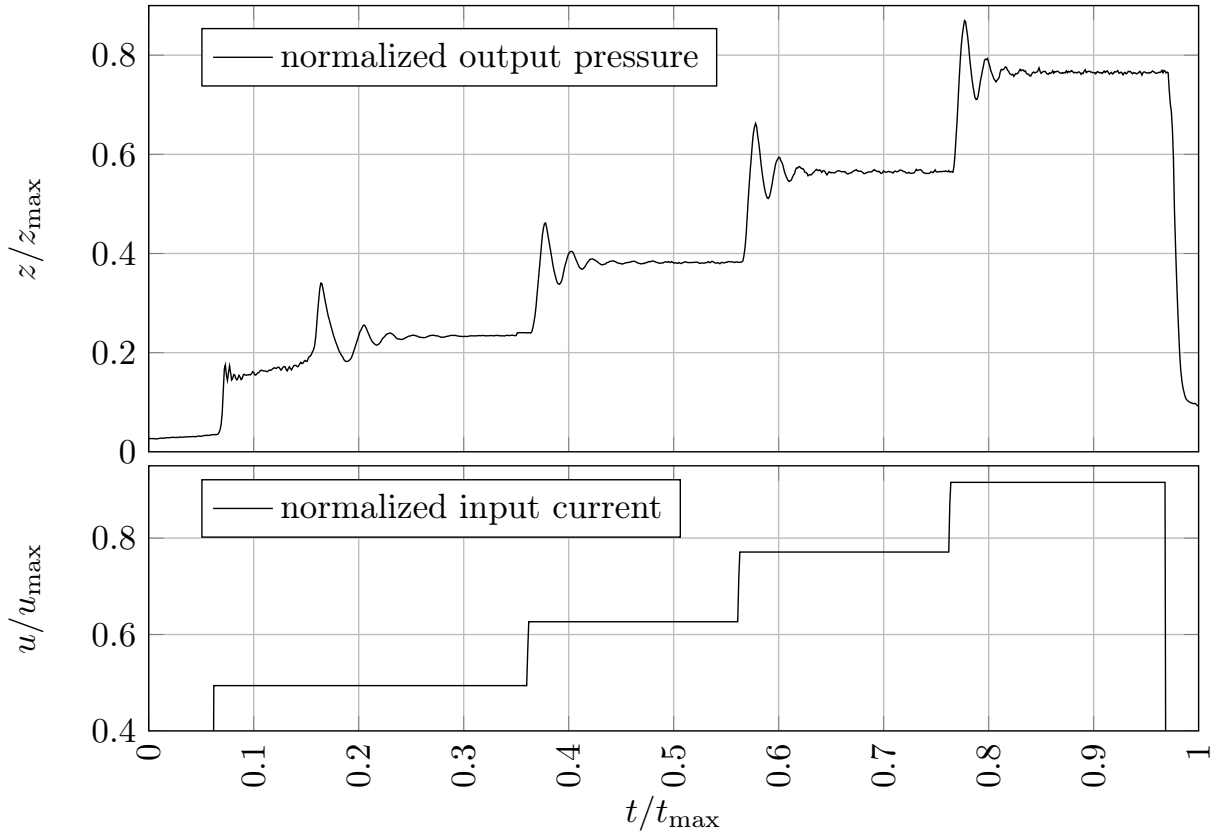

Figure 5.3: Experimental pressure response to a staircase input current. Here $z \in \mathbb{R}$ denotes the pressure and $u \in \mathbb{R}$ the commanded current, while $z_{\max}$, $u_{\max}$ and $t_{\max}$ are normalization factors. The sampling rate of the data has been decreased for graphical reasons.

5.3.2 Model identification

The identification technique that we propose for (5.2) comprises two steps. First we identify the output nonlinearity ϕ, and secondly we estimate the coefficients $a := (a_1, a_2, a_3) \in \mathbb{R}^3$.

For the first step, let us consider a sufficiently large set of steady-state input-output pairs $\{(u^i, z^i)\}_{i=1}^N \subset \mathbb{R}^2$ (where $N \gg 1$). Because the transfer function (5.2a) has unitary DC gain, the pairs (u^i, z^i) are related through ϕ, and the identification of the output nonlinearity reduces to an interpolation problem. Experimental data are reported in Figure 5.4, where we can observe that a second order polynomial of the form

$$z^i = \phi(u^i) := p_0 + p_1 u^i + p_2 (u^i)^2 + \epsilon^i, \quad i = 1, \dots, N, \tag{5.3}$$

provides good fitting results. The coefficients $p_0, p_1, p_2 \in \mathbb{R}$ can be easily obtained by solving a standard Least Squares (LS) problem.

In general, a quadratic function is not globally invertible, as required in Assumption 5.1. However (5.3) is invertible with the identified parameters when the domain is restricted to $\mathbb{R}_{\geq 0}$.

Once ϕ is known, Assumption 5.1 ensures that we can virtually access the linear output y as $y = \phi^{-1}(z)$. Then any standard identification techniques for linear systems can be applied, see for example [76].

5.3.3 Balanced realization

In Section 5.5 we will describe an LMI-based procedure for the controller synthesis, and because LMIs are naturally formulated in state space, we consider a minimal realization of (5.2a) as follows

$$\mathcal{H}_{\mathrm{p}} := \begin{cases} \dot{x}_{\mathrm{p}} = A x_{\mathrm{p}} + B u + G w \\ y = C x_{\mathrm{p}} + Q w \\ z = \phi(y), \end{cases} \tag{5.4}$$

where $x_{\mathrm{p}} \in \mathbb{R}^2$ is the state, and $w \in \mathbb{R}$ is a disturbance. Matrices G and Q cannot be directly obtained from (5.2a), but can be freely designed to "shape" the effect of the disturbance w on the measurement and the state. For (5.4), we used a balanced realization [85], which guarantees that equally "important" states have similar magnitude. This improves numerical stability and makes the LMIs in Section 5.4 better conditioned from a numerical viewpoint. The balanced realizations provides also a few advantage from an implementation point of view, e.g., since the Control Unit (CU) works at a fixed-point precision, having balanced internal states of the controller helps in working out the correct numerical

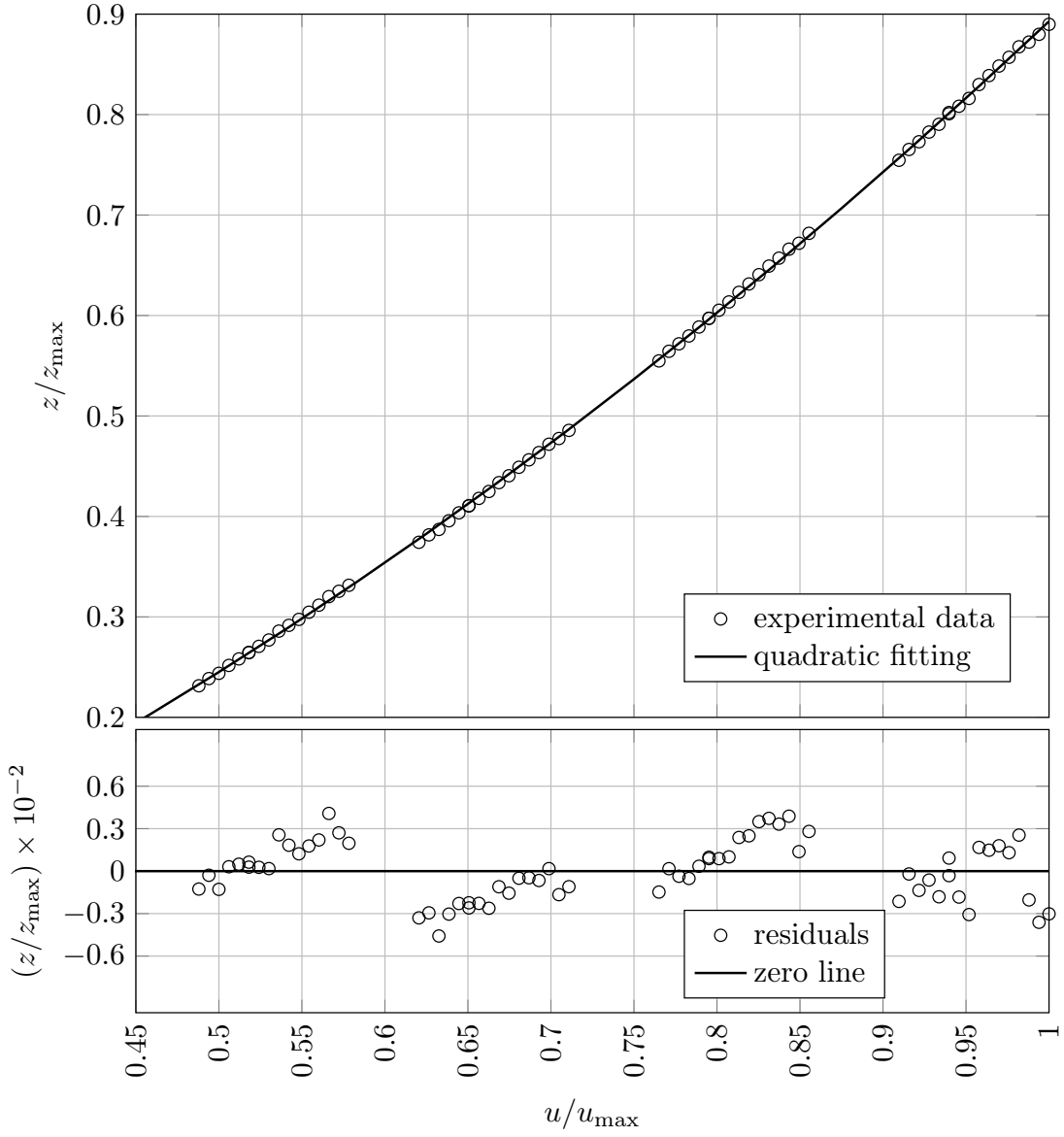

Figure 5.4: Interpolation of the steady-state pairs (top) and residuals (bottom) normalized with respect to the maximum pressure $z^{\max}$.

bounds to use in the integration process. According to Remark 5.1, we assume that (5.4) satisfies the following:

Assumption 5.2
Matrix A is Hurwitz, the triple (C, A, B) is minimal, balanced and satisfies $-CA^{-1}B = 1$.

According to the goal of set-point regulation defined in Problem 5.1, we restrict the class of possible reference and disturbance signals to constant ones.

Assumption 5.3
The signals r and w are constant.

Remark 5.2
Assumptions 5.2, 5.3 are not restrictive for the experimental system under consideration, and the presence of the output nonlinearity ϕ adds no conceptual difficulties, because thanks to Assumption 5.1 we can always access y through ϕ^{-1}. It is important to stress that an imperfect knowledge of the output non-linearity ϕ produces a constant steady-state error that can be thought of as part of w. Therefore, from this point over, and especially in Section 5.4, we consider to have full access to signal y. ⌟

5.4 Hybrid controller

In this section, we adapt the hybrid controller presented in Chapter 3 in order to satisfy the objectives defined in Problem 5.1. The central idea is to switch among the two different modes of the hybrid controller. The first mode corresponds to a "transient mode" that shapes the transient providing a fast non-overshooting step response. The second mode is a "steady-state mode" that activates an integral action able to zeroing out the steady-state error.

As already discussed in Chapter 3, switching has been recognized as an effective way to overcome intrinsic limitations of linear control and obtain superior performance [87]. However, it is well-known that the transients caused by switching may result in instability of the closed loop. To overcome the problem of destabilizing transients we equip our controller with a bumpless filter [125], and because of the presence of a feed-forward action we also re-design the reset rule. The interplay between the bumpless dynamics and the resets guarantees stability under a large class of switching signals. This strong property leaves complete freedom in the design of the high-level switching logic.

A graphical representation of model (5.2) in feedback interconnection with the hybrid controller is shown in Figure 5.5. We may notice that controller $\mathcal{H}_c$ now requires two inputs:

$$\left[\begin{array}{c|c} A_{\mathrm{c}}(1) & B_{\mathrm{c}}(1) \\ \hline C_{\mathrm{c}}(1) & D_{\mathrm{c}}(1) \\ \hline E_{\mathrm{c}}(1) & F_{\mathrm{c}}(1) \end{array}\right] := \left[\begin{array}{cccc|cc} A+LC+BK_1 & B & 0 & 0 & -L & 0 \\ 0 & 0 & 0 & 0 & 0 & 0 \\ B(K_2-K_1) & -B & A+BK_2 & BK_{\mathrm{i}} & 0 & -(A+BK_2)A^{-1}B \\ 0 & 0 & C & 0 & I & I \\ \hline K_1 & I & 0 & 0 & 0 & I \\ \hline I & 0 & 0 & 0 & 0 & 0 \\ K_2-K_1 & 0 & K_2-K_1 & K_{\mathrm{i}} & 0 & (K_1-K_2)A^{-1}B \\ 0 & 0 & I & 0 & 0 & -A^{-1}B \\ 0 & 0 & 0 & I & 0 & 0 \end{array}\right] \tag{5.5a}$$

$$\left[\begin{array}{c|c} A_{\mathrm{c}}(2) & B_{\mathrm{c}}(2) \\ \hline C_{\mathrm{c}}(2) & D_{\mathrm{c}}(2) \\ \hline E_{\mathrm{c}}(2) & F_{\mathrm{c}}(2) \end{array}\right] := \left[\begin{array}{ccc|cc} A+LC+BK_2 & 0 & B(K_2-K_1) & BK_{\mathrm{i}} & -L & 0 \\ 0 & 0 & 0 & 0 & 0 & 0 \\ 0 & 0 & A+BK_1 & 0 & 0 & 0 \\ 0 & 0 & C & 0 & I & 0 \\ \hline K_2 & 0 & K_2-K_1 & K_{\mathrm{i}} & 0 & I \\ \hline I & 0 & 0 & 0 & 0 & 0 \\ K_2-K_1 & 0 & K_2-K_1 & K_{\mathrm{i}} & 0 & 0 \\ 0 & 0 & I & 0 & 0 & A^{-1}B \\ 0 & 0 & 0 & I & 0 & 0 \end{array}\right] \tag{5.5b}$$

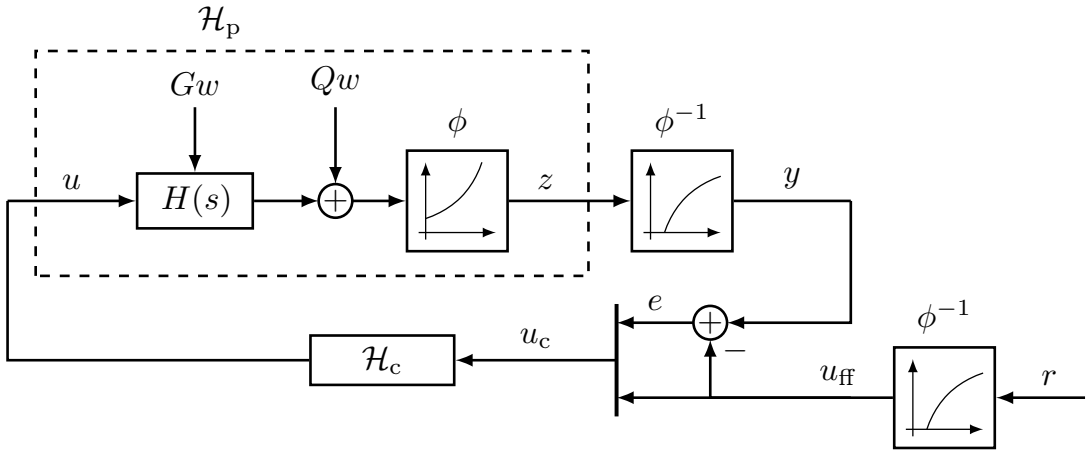

Figure 5.5: Block diagram of the model-controller loop. Please notice the presence of ϕ^{-1} and the error feedback hybrid controller.

the "tracking error" $e \in \mathbb{R}$ and the "feed-forward" control $u_{\text{ff}} \in \mathbb{R}$. The "feed-forward" control u_{ff} is obtained by inverting the Wiener non-linearity ϕ as follows

$$u_{\text{ff}} := \phi^{-1}(r), \tag{5.6}$$

where r is the reference signal for z. Because by Assumption 5.2 the DC gain of (5.2a) is unitary, u_{ff} can be interpreted also as a reference signal for y and it makes sense to define the tracking error e as

$$e := y - u_{\text{ff}}. \tag{5.7}$$

We notice that thanks to Assumption 5.1, the non-overshooting requirement for $(z - r)$ can be equivalently considered on e. The proposed hybrid controller $\mathcal{H}_{\text{c}}$ has the following structure:

$$\mathcal{H}_{\text{c}} := \begin{cases} \dot{x}_{\text{c}} = A_{\text{c}}(q)x_{\text{c}} + B_{\text{c}}(q)u_{\text{c}} \\ x_{\text{c}}^{+} = E_{\text{c}}(q)x_{\text{c}} + F_{\text{c}}(q)u_{\text{c}} \end{cases} \tag{5.8}$$

where $x_{\text{c}} \in \mathbb{R}^6$ is the controller state, $u_{\text{c}} := (e, u_{\text{ff}}) \in \mathbb{R}^2$ is the controller input, and $q \in \mathcal{Q} := \{1, 2\}$ is a logic variable selecting what mode is currently active. Moreover, controller (5.8) is interconnected to (5.4) through the following output equation:

$$u = C_{\text{c}}(q)x_{\text{c}} + D_{\text{c}}(q)u_{\text{c}}. \tag{5.9}$$

The logic value $q = 1$ is associated to the "transient mode", while $q = 2$ is associated to the "steady-state mode". Explicit expressions for the matrices in (5.8), (5.9) for each mode are reported in (5.5).

Remark 5.3
Notice that (5.8) includes a reset mechanism, namely a discontinuity of the controller state x_{c}. This discontinuity is imposed when the logic variable q toggles between values 1 and 2, and it is designed to keep the solutions well behaved across jumps. In particular, it ensures that the feed-forward signal u_{ff} enters only in the sub-block of the controller relative to the active mode. ⌟

As already discussed in Chapter 3 the properties of the hybrid loop arising from the interconnection between (5.4) and (5.8) through (5.9) and (5.7), are more evident in a different set of coordinates. Thanks to Assumption 5.3 we have that $\dot{u}_{\text{ff}} = 0$ and we can consider the change of coordinates

$$x := T(q)(x_{\text{p}}, x_{\text{c}}) + U(q)u_{\text{ff}}, \tag{5.10}$$

where matrices $T(q) \in \mathbb{R}^{8\times 8}$ and $U(q) \in \mathbb{R}^{8\times 1}$ are reported below

$$(T(q),\ U(q)) := \left[\begin{array}{ccccc|c} (2-q)I & 0 & 0 & (1-q)I & 0 & (2-q)A^{-1}B \\ 0 & 0 & I & 0 & 0 & 0 \\ I & 0 & 0 & I & 0 & (q-1)A^{-1}B \\ 0 & 0 & 0 & 0 & I & 0 \\ -I & I & 0 & 0 & 0 & -A^{-1}B \end{array}\right].$$

Notice that $T(q)$, $U(q)$ are full rank for all $q \in \mathcal{Q}$ so that (5.10) is always well-defined. Thanks to (5.10) the closed-loop takes the simplified expression

$$\mathcal{H} := \begin{cases} \dot{x} = A_{\mathrm{cl}}(q)x + G_{\mathrm{cl}}(q)w \\ x^+ = E_{\mathrm{cl}}(q)x, \end{cases} \tag{5.11}$$

where $A_{\mathrm{cl}}(q) \in \mathbb{R}^{8\times 8}$, $G_{\mathrm{cl}}(q) \in \mathbb{R}^{8\times 1}$, and $E_{\mathrm{cl}}(q) \in \mathbb{R}^{8\times 8}$ are fully reported in Equation (5.14). Similarly, the tracking error e yields

$$e = C_{\mathrm{cl}}(q)x + D_{\mathrm{cl}}w, \tag{5.12}$$

where again $C_{\mathrm{cl}}(q) \in \mathbb{R}^{1\times 8}$, $D_{\mathrm{cl}} \in \mathbb{R}^{1\times 1}$ are defined in Equation (5.14). Equation (5.14) has a desirable cascade structure and a necessary condition for stability is to ensure that the diagonal sub-blocks

$$[A + BK_1], \quad \begin{bmatrix} A + BK_2 & BK_{\mathrm{i}} \\ C & 0 \end{bmatrix}, \quad [A + LC] \tag{5.13}$$

are Hurwitz. This is not restrictive in our setup, since the triple (C, A, B) is minimal from Assumption 5.2. Then it is always possible to find a set of parameters K_1, K_2, K_{i}, L such that the matrices in (5.13) are Hurwitz. We illustrate a possible design procedure in Sections 5.5.1, 5.5.2 and 5.5.3. Under a direct and a reverse dwell-time condition, see Assumption 3.1, a result similar to Theorem 3.1 holds also for this controller. A formal statement is reported below.

Theorem 5.1 (Main result)
Assume that the gains K_1, K_2, K_{i}, L have been designed so that the matrices in (5.13) are Hurwitz. If Assumptions 5.1, 5.2, 5.3, and 3.1 hold true, then (5.11) has the following properties:

1. *For $w = 0$ the origin of (5.11) is Globally Exponentially Stable (GES) for all switching sequences defined in Assumption 3.1.*

$$\left[\begin{array}{c|c} A_{\mathrm{cl}}(q) & G_{\mathrm{cl}}(q) \\ \hline E_{\mathrm{cl}}(q) & \\ \hline C_{\mathrm{cl}}(q) & D_{\mathrm{cl}}(q) \end{array}\right] := \left[\begin{array}{ccccc|c} A+BK_1 & (2-q)B & 0 & 0 & (2-q)BK_1 & (2-q)G \\ 0 & 0 & 0 & 0 & 0 & 0 \\ 0 & 0 & A+BK_2 & BK_{\mathrm{i}} & BK_2 & G \\ 0 & 0 & C & 0 & 0 & Q \\ 0 & 0 & 0 & 0 & A+LC & -G-LQ \\ \hline I & 0 & (2q-3)I & 0 & 0 & \\ 0 & 0 & K_2-K_1 & K_{\mathrm{i}} & K_2-K_1 & \\ 0 & 0 & I & 0 & 0 & \\ 0 & 0 & 0 & I & 0 & \\ 0 & 0 & 0 & 0 & I & \\ \hline C & 0 & (q-1)C & 0 & 0 & Q \end{array}\right] \tag{5.14}$$

2. *For any constant w the solutions to (5.11) are globally bounded and ensure asymptotic convergence to zero of e.*

Proof. The proof follows the same steps reported in the proof of Theorem 3.1. □

5.5 Controller tuning

In this section we propose an LMI-based technique to tune the controller parameters K_1, K_2, K_{i}, and L. These procedures are designed to meet the tight requirements defined in Problem 5.1. We remark that, due to the special cascaded structure of (5.11), all these parameters can be tuned independently.

5.5.1 Transient mode tuning

We propose to choose K_1 following a two-step procedure generalizing the results of [46]. As a first step we characterize the maximum achievable convergence rate $\alpha \in \mathbb{R}_{>0}$ by imposing constraints on the aggressiveness of the feedback gain K_1 (a bound on its norm) and on the closed-loop damping factor. Specifically, we aim at solving the following optimization

problem:

$$\max_{W,X,\alpha} \alpha \quad \text{subject to:}$$

$$W = W^\top \geq I \tag{5.15a}$$

$$M + M^\top \leq -2\alpha W \tag{5.15b}$$

$$\begin{bmatrix} (M + M^\top)\sin\theta & (M - M^\top)\cos\theta \\ (M^\top - M)\cos\theta & (M + M^\top)\sin\theta \end{bmatrix} \leq 0 \tag{5.15c}$$

$$\begin{bmatrix} W & X^\top \\ X & I\kappa^2 \end{bmatrix} \geq 0, \tag{5.15d}$$

where $M := AW + BX \in \mathbb{R}^{2\times 2}$ and $\theta \in [0, \pi/2]$.

It is worth to notice that the optimization problem (5.15) is non convex due to the product αW, however it can still be solved efficiently because it is a so-called (quasi-convex) generalized eigenvalue problem, see [22]. The next proposition establishes a few useful properties for (5.15).

Proposition 5.1
Under Assumption 5.2, for any value of $\kappa \in \mathbb{R}_{>0}$, there exists a large enough $\theta \in [0, \pi/2]$ such that (5.15) is feasible. Moreover, for any feasible solution to (5.15) together with the choice $K_1 = XW^{-1}$, the following properties hold: i) the norm $|K_1| \leq \kappa$, ii) the closed-loop matrix $(A + BK_1)$ has eigenvalues with real part less than $-\alpha$, iii) the damping factors of the poles is larger than $\cos\theta$.

Proof. Feasibility follows from the fact that, with $\theta = \pi/2$, constraint (5.15c) reduces to $M + M^\top \leq 0$. Then the assumption that A be Hurwitz implies that $X = 0$ is a feasible solution for any non-negative value of κ. To show that $|K_1| \leq \kappa$ we perform a Schur complement on (5.15d) and we use $X = K_1 W$ and (5.15a) to obtain

$$I\kappa^2 \geq XW^{-1}X^\top = K_1 W K_1^\top \geq K_1 K_1^\top,$$

which implies $|K_1| \leq \kappa$. The eigenvalues of $(A + BK_1)$ having real part less than $-\alpha$ is a straightforward consequence of (5.15b), and the damping factor greater than $\cos\theta$ is a direct application of the results in [32, Equation (13)]. □

The optimization problem (5.15) provides a convenient way to trade-off between speed of convergence, imposed by α, and level of aggressiveness of the arising controller, tuned by κ.

The second step of the proposed synthesis procedure consists in reducing the overshoot associated to the gain selection obtained with (5.15). Toward this goal we heuristically im-

pose the non-overshooting condition by forcing a small constant of proportionality between the derivative of the tracking error $\dot{e}$ and the partial state x_1, when $e = 0$. This condition captures the intuitive idea that a nice non-overshooting response must be flat in a neighborhood of the set-point. We formalize this idea by imposing the following conservative bound

$$e = 0 \qquad \Rightarrow \qquad |\dot{e}| \leq \rho \, |x_1| \,, \tag{5.16}$$

and we minimize $\rho \in \mathbb{R}_{>0}$. Since x_1 is the only non-zero element of the state x whenever $e = 0$, Equation (5.16) can be equivalently re-written in the following way

$$|C(A + BK_1)x_1| \leq \rho \, |x_1| \,, \quad \forall x_1 : Cx_1 = 0. \tag{5.17}$$

Equation (5.17) can be formulated in an LMI form and included in the following optimization problem with the goal of providing reduced values of ρ.

$$\begin{aligned}
&\min_{W,S,X,\rho^2} \rho^2 \quad \text{subject to:} \\
&M + M^\top \leq -\eta^{-1}\alpha W && \text{(5.18a)} \\
&M + M^\top \geq -\eta\alpha W && \text{(5.18b)} \\
&\begin{bmatrix} 2W & MC^\top & I \\ CM & \rho^2 I & 0 \\ I & 0 & I + C^\top S C \end{bmatrix} > 0 && \text{(5.18c)} \\
&S = S^\top > 0 && \text{(5.18d)} \\
&(5.15a), (5.15c), (5.15d),
\end{aligned}$$

with $M := AW + BX$.

Remark 5.4
Constraints (5.18a), (5.18b) and (5.15c) correspond to imposing that the closed-loop poles belong to a conic region in the left half plane, represented by the shaded gray area in Figure 5.6. We can observe that the shape of this region depends on the parameters η and α. ⌟

Proposition 5.2
Under Assumption 5.2, assume that α, θ, κ are parameters for which (5.15) is feasible; then there exists a large enough $\eta \in \mathbb{R}_{\geq 1}$ such that (5.18) is feasible as well.

Moreover, for any feasible solution to (5.18), selecting $K_1 = XW^{-1}$ the following properties hold: i) the norm $|K_1| \leq \kappa$, ii) the closed-loop matrix $(A + BK_1)$ has eigenvalues with real part less than $-\alpha\eta^{-1}$, iii) the damping factors of the poles is greater than $\cos\theta$,

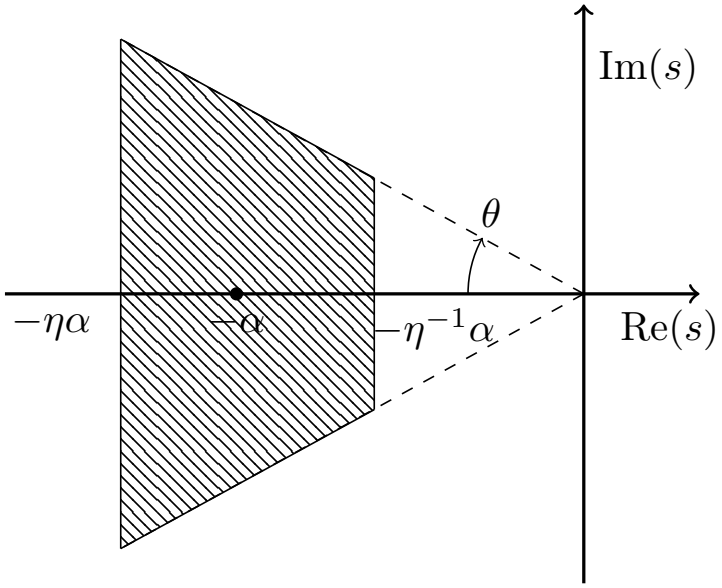

Figure 5.6: The shaded conic region represents the region in the complex plane where the closed-loop poles are constrained.

iv) the relation in (5.16) holds.

Proof. Feasibility follows from the fact that there exists η sufficiently large such that the shaded region in Figure 5.6 contains the positions of the poles obtained by the feasible solution for (5.15), assumed in Proposition 5.2. Then that solution is also a feasible solution for (5.18) as long as ρ^2 is selected sufficiently large. Properties i)–iii) are a straightforward consequence of constraints (5.15a), (5.15c), (5.15d), which imply the stated properties from Proposition 5.1. We finish the proof by showing property iv). Performing a Schur complement on (5.18c), and using (5.18d), we obtain:

$$\begin{bmatrix} 2W - (I + C^\top SC)^{-1} & M^\top C^\top \\ CM & \rho^2 I \end{bmatrix} > 0, \tag{5.19}$$

where $I + C^\top SC$ is clearly invertible. Consider now the following inequality

$$(W - (I + C^\top SC)^{-1})^\top (I + C^\top SC)(W - (I + C^\top SC)^{-1}) \geq 0,$$

which implies $2W - (I + C^\top SC)^{-1} \leq W(I + C^\top SC)W$. From (5.19), pre/post multiplying by $\mathrm{diag}(W^{-1}, I)$ and using $M = (A + BK_1)W$, we obtain

$$\begin{bmatrix} I + C^\top SC & (A + BK_1)^\top C^\top \\ C(A + BK_1) & \rho^2 I \end{bmatrix} > 0,$$

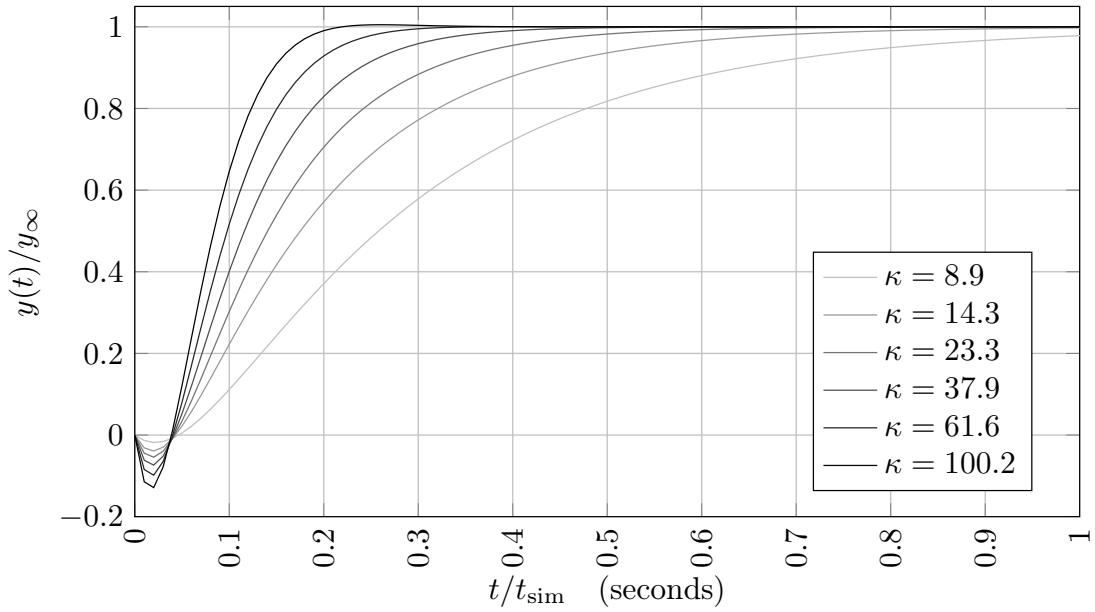

Figure 5.7: Simulated step responses for increasing values of κ. The time scale is normalized.

which, after being multiplied by ρ^2 and after a Schur complement, implies:

$$|C(A + BK_1)x_1|^2 < \rho^2 |x_1|^2 + \rho^2 \left|\sqrt{S}Cx_1\right|^2 .$$

Finally, when $Cx_1 = 0$, we apply the square root and we retrieve (5.17). □

The properties established in Propositions 5.1 and 5.2 suggest that the feedback gain K_1 be selected as follows: first a set of different levels of aggressiveness are fixed, spanning an experimentally reasonable range. Then for each one of them we solve the optimization problem in (5.15), possibly adjusting the parameter θ if the LMIs are infeasible (feasibility is guaranteed by Proposition 5.1 for a large enough θ). This first step provides a number of values for α, each of them corresponding to a different selection of κ. As a second step, optimization (5.18) is solved for each one of the (κ, α) pairs with the same value of θ, possibly adjusting parameter η (feasibility is guaranteed by Proposition 5.2 for a large enough η).

For the model identified in this work, the values of κ are shown in Figure 5.7 with the resulting step responses. The corresponding values for α have been obtained by applying optimization (5.15) after fixing $\theta = \pi/4$ and $\eta = 5$.

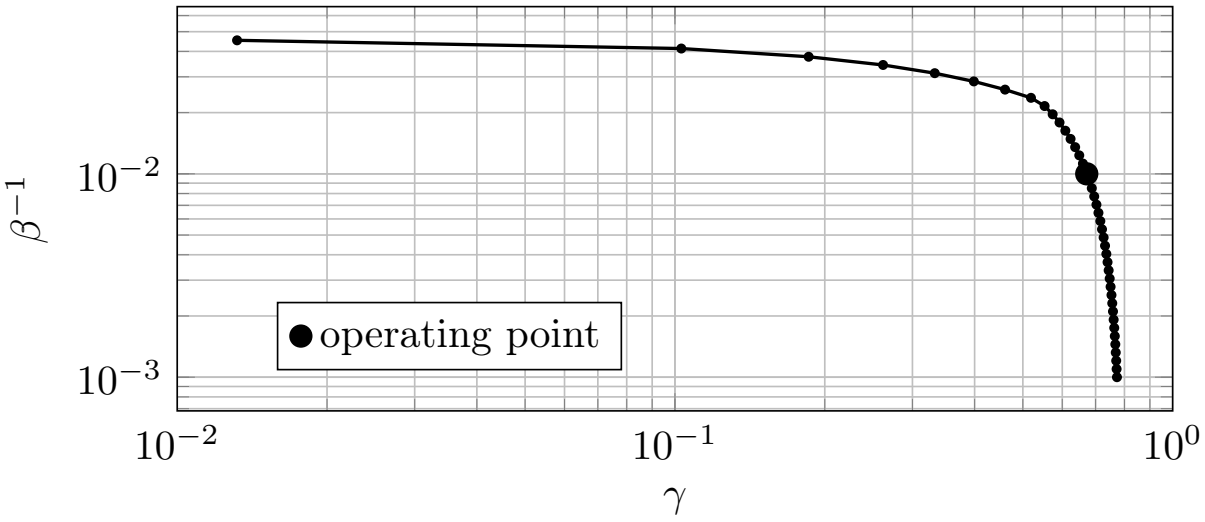

Figure 5.8: Trade-off curve between β and γ. The curves have been obtained by solving the optimization problem (5.21) for model (5.4), considering increasing values of β.

5.5.2 Steady-state mode tuning

In this section we provide the details of the synthesis of the controller gains K_2 and K_{i}. In practice we tuned these gains, associated with the dynamics of the second matrix in (5.13), in such a way that its convergence rate is larger than the convergence rate α obtained by the optimization problem (5.18). In this way, when switching from the transient mode to the steady-state mode, the integral action associated to state $x_{\mathrm{c}4}$ is already almost constant. We also remark that, for the steady-state dynamics, no special non-overshooting requirements are imposed. Indeed, from (5.5) we can observe that these gains have no effect during the transient mode. Consequently, the convergence rate of this dynamics can be made arbitrarily large without affecting the transient performance.

5.5.3 Observer design

In this section we tune the observer gain L as a convenient trade-off between convergence rate of the estimation error and noise rejection capability. For the estimation error dynamics

$$\dot{x}_5 = (A + LC)x_5 - Gw - LQw, \tag{5.20}$$

which emerges from (5.14), we propose to optimize the observer gain L in order to reduce the effect of disturbance w on the estimation error in the $\mathcal{L}_2$ sense. Following the well-known Lyapunov formulations of the bounded real lemma (see, e.g, [22]), we select L according

to the following LMI-based convex optimization problem, parametrized by $\beta \in \mathbb{R}_{>0}$,

$$\begin{aligned}
&\min_{P,Y,\gamma} \gamma \quad \text{subject to:} \\
&P = P^\top > 0 && \text{(5.21a)} \\
&\text{He}\begin{bmatrix} PA + YC & -YQ - PG & 0 \\ 0 & -\gamma I/2 & 0 \\ I & 0 & -\gamma I/2 \end{bmatrix} < 0 && \text{(5.21b)} \\
&\text{He}\Big[PA + YC\Big] \leq -2\beta P. && \text{(5.21c)}
\end{aligned}$$

Proposition 5.3
Given any $\beta \in \mathbb{R}_{>0}$, the set of LMIs (5.21) is feasible under Assumption 5.2. Moreover, for any feasible solution to (5.21), selecting $L := P^{-1}Y$ the following properties hold: i) the $\mathcal{L}_2$ gain from w to x_5 for (5.20) is smaller than γ, ii) matrix $A + LC$ has eigenvalues with real part smaller than or equal to $-\beta$.

Proof. Feasibility of (5.21c) follows from standard pole placement theory combined with minimality, see Assumption 5.2. The remaining part of the proof is a standard application of the bounded real lemma and the use of quadratic Lyapunov functions. In particular, defining $V(x_5) := x_5^\top P x_5$, where $P = P^\top > 0$ by constraint (5.21a), performing a Schur complement on (5.21b), left-right-multiplying by (x_5, w) and substituting $Y = PL$, we obtain $\langle \nabla V(x_5), \dot{x}_5 \rangle + \frac{1}{\gamma} x_5^\top x_5 - \gamma w^\top w < 0$.

Integrating both sides, we obtain the desired bound on the $\mathcal{L}_2$ gain from w to x_5 (or equivalently on the $\mathcal{H}_\infty$ norm). Regarding the speed of convergence β, this follows from noticing that (5.21c) implies $\text{He}\,[P(A + LC + \beta I)] < 0$, which only holds with a positive definite P if $A + LC$ has convergence abscissa smaller than $-\beta$. □

Proposition 5.3 emphasizes that the LMI-based design tool corresponding to (5.21) can be an effective means for performing the design of L, while establishing a trade-off between the guaranteed speed of convergence of the observer dynamics (corresponding to β) and the level of disturbance rejection γ from the noise w to the estimation error x_5. The suggested use of this tool is to fix increasing values of β and then determine the trade-off curve reported in Figure 5.8. This curve provides a range of optimal selections of the observer gain L. For our specific identified model, Figure 5.8 reports the selected operating point, corresponding to a black dot. Such a selection is performed by fixing a sufficiently large convergence rate β once the state feedback gains have been designed.

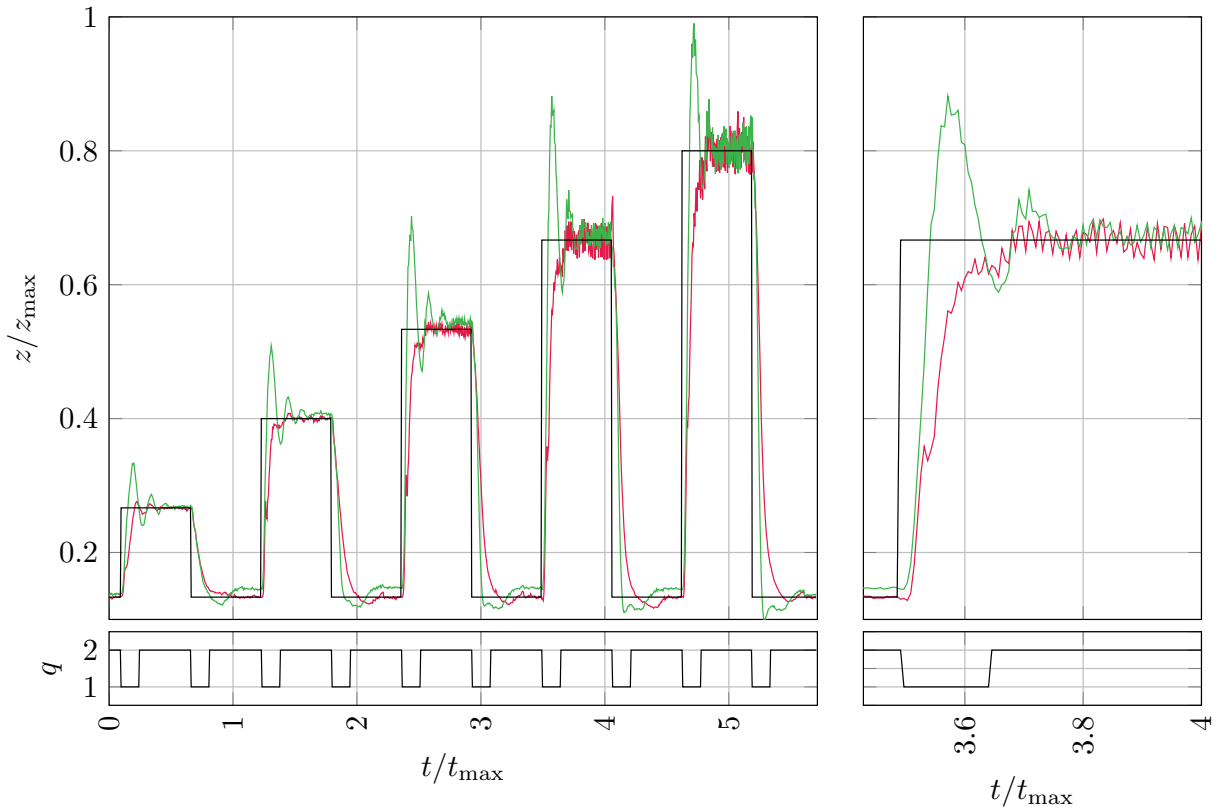

Figure 5.9: Open-loop vs. closed-loop step response. In green open-loop, in red closed-loop and in black the reference. On the left a sequence of increasing amplitude steps and on the right a zoom of the fourth step.

5.6 Experimental validation

All the experiments have been conducted on the testing facilities provided by DRTS. The hybrid controller (5.8) has been implemented using TargetLink®on an Electronic Control Unit provided by Bosch®, and controller (5.8) has been discretized using Tustin's method.

Tests have been conducted over a range of clutches that differ in dimensions, transmissible torque, stiffness and hydraulic properties. For each one of these clutches, we performed the identification procedure described in Section 5.3 and the controller tuning procedure reported in Section 5.5.

Several experimental tests have been performed, providing excellent results for a large variety of working conditions. Figure 5.9 shows the comparison between the closed-loop (in red), and the open loop (in green). The controller successfully removes the overshoot and ensures a zero steady-state error. The switch among controller 1 and 2 is ruled by the

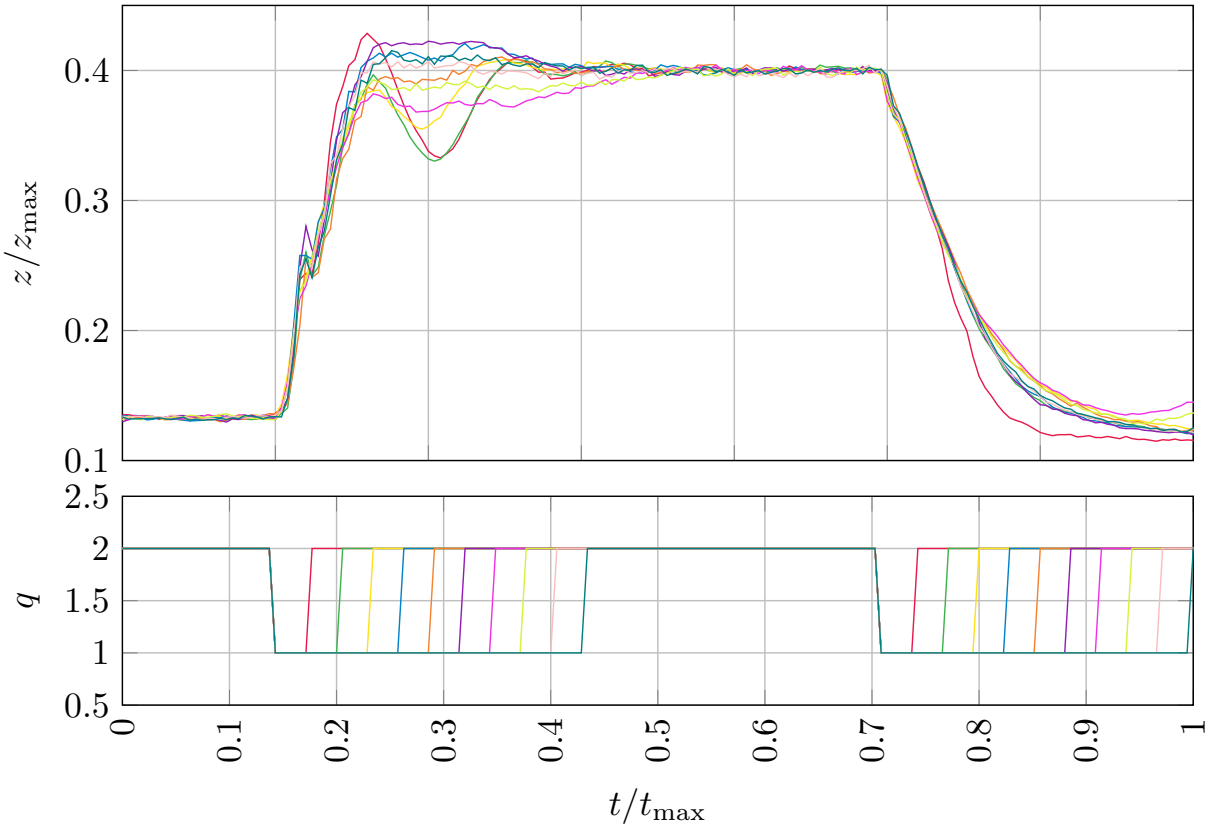

Figure 5.10: Step responses for different t_{switch}. In the graph above the pressure, below the logic variable q.

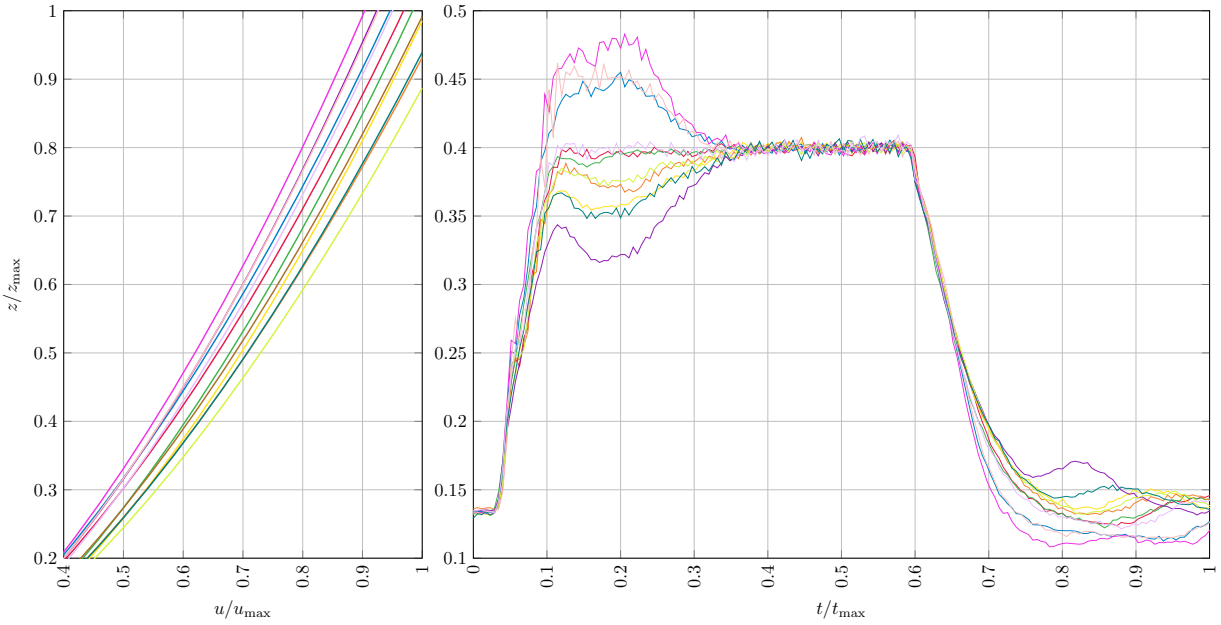

Figure 5.11: Step responses for different t_{switch}. In the graph above the pressure response, below the logic variable q.

logic variable q reported in Figure 5.9 as well.

The value of q toggles according to a timer that is reset to zero at each rising/falling of the reference signal. Therefore after a time $t_{\text{switch}} \in \mathbb{R}_{>0}$ from the last reference change, the variable q toggles from 1 to 2 and the controller switches from the *transient mode* to the *steady-state* one. The time t_{switch} can be easily calibrated experimentally through a bisection procedure. In Figure 5.10 we show the set of responses obtained by varying t_{switch} between 0 and the settling time of the closed-loop. We can observe that, for a reasonable range of values around the optimum, the closed-loop response remains sufficiently non-overshooting.

It is important to stress that the variable q toggles according to a timer, but in principle more complicated strategies are possible, thanks to the stability properties proved in Theorem 5.1.

Finally, we tested the robustness of the proposed controller against large perturbations of the nonlinear map ϕ, such as those due to oil aging and temperature variations. Those perturbations are reported on the left in Figure 5.11, while on the right the corresponding step responses are reported.

We notice that for large variations of ϕ, the non-overshooting property is no longer preserved, but the integral action is still able to zero out the steady-state error.

Those perturbation are large, compared to the ones experienced in practice (roughly three times larger), and it is important to stress that the degradation of performance is graceful. This shows a desirable level of robustness.

We conclude that the experimental tests have proved the validity of the proposed control technique for achieving a non-overshooting and fast pressure response. Moreover, we experimentally tested robustness with respect to perturbations of the nonlinear map ϕ and of the switching time t_{switch}.

5.7 Conclusions

In this chapter we addressed the problem of set-point regulation of the oil pressure in wet clutches. We developed a control-oriented model for a filled clutch in the modulation range and we proposed a novel hybrid controller. The controller can operate in two modes, a transient mode and a steady-state mode, and may freely switch among these modes without compromising stability. The transient mode provides a nice non-overshooting response, while the steady-state mode compensates for constant disturbances and unmodeled dynamics. The controller synthesis is conveniently formulated as an LMI problem.

We implemented and tested the proposed hybrid controller on the HVT developed by DRTS. Experiments show excellent performance and good robustness with respect to modeling errors and noise. Future research directions will involve the design of a high-level switching strategy and the control of the oil pressure in conditions of clutch only partially filled.

Chapter 6

The Kinematic Dead-zone Observer

In this chapter we apply the adaptive dead-zone mechanism presented in Chapter 4 to the Farrelly and Wellstead kinematic observer. We extend the result in Theorem 4.1 to cover a special class of linear parameter varying systems. As already presented in Chapter 4 the dead-zone mechanism maintains the structure of the kinematic observer, but inserts an adaptive dead-zone at the output injection term. This dead-zone partially "cuts" the noise and increases the noise rejection performance allowing for the selection of a larger observer gain. We use this degree of freedom to increase the observer gain to attenuate constant bias errors in the acceleration measurements. The proposed solution is easy to implement and requires only measurements acquired from standard on-board sensors. Once again, the adaptation parameters are selected by solving a suitable Linear Matrix Inequality (LMI). We show the effectiveness of the proposed solution through numerical simulations. This chapter is adapted from the conference paper [45].

6.1 Introduction

Control of vehicle dynamics is a firmly established field in the automotive industry. The possibility to change the dynamical behavior of a vehicle using an electronic control unit (ECU) leads to tremendous improvement in passengers safety and comfort. Remarkable examples are the Traction Control (TC), the Longitudinal Slip Control (LSC) [105], and the Electronic Stability Control (ESC) [102].

In the latter the side-slip angle plays a crucial role, because it is a direct measure of the instability of the vehicle. The side-slip angle identifies the orientation of the vehicle with respect to the longitudinal direction and is representative of the lateral velocity component.

An accurate measurement of the lateral velocity requires expensive devices such as optical sensors [111], two-antenna GPS [57] or lateral tire forces sensors [90]. Those sensors are usually not available on commercial cars and for this reason, many techniques have been proposed to reconstruct the lateral velocity based on measurements provided by accelerometers, gyroscopes and wheel encoders. Two approaches are popular in the

literature: the first one employs an observer based on a "physical" linearized model of the vehicle, while the second one is an observer based on a purely kinematic model [120].

Observers based on physical models have good robustness properties; they reject sensor noise and biases, but require a precise knowledge of the parameters of the vehicle. The most critical parameter is the cornering stiffness, whose value may largely vary with time, thus making its prediction hard during fast maneuvers. To fix this issue a vast number of solutions have been proposed, see for example [75], [19], and [20, 121] just to cite a few. The performance of physically based observers can be further improved using non-linear models for the tire-road contact forces [68, 31, 98], but once again a good knowledge of the parameters is necessary.

Observers built upon the kinematic model are instead more appealing, because they do not depend on the physical parameters [97, 51, 96]. However, they provide reliable estimates only for high yaw-rates and in the absence of biases on the acceleration measurements (e.g. when the vehicle travels on a flat road). Because acceleration biases are frequent, numerous techniques have been proposed, see for example the road angle approach [119, 99], or the disturbance observer technique [54, 53, 91]. Robustness to acceleration bias can also be improved by increasing the observer gain, but with the drawback of increasing sensitivity to high-frequency noise. To reduce this sensitivity, we propose a modified version of the well-known kinematic observer [51], where we introduce the adaptive dead-zone mechanism presented in Chapter 4.

The noise reduction attained with the dead-zone mechanism allows for a selection of a larger observer gain, which attenuates the deterioration of the estimate caused by the bias on the acceleration measurements. The effectiveness of the proposed observer is shown by means of numerical simulations on a eight degrees of freedom non-linear vehicle model.

6.1.1 The Farrelly and Wellstead kinematic observer

One of the simplest models that we can consider to relate longitudinal and lateral velocities with measured accelerations is the kinematic model. The kinematic model is a Linear Parameter Varying (LPV) system of the form

$$\begin{cases} \dot{x} = A(r)x + u \\ y = Cx, \end{cases} \tag{6.1}$$

where $u = (a_{\mathrm{x}}, a_{\mathrm{y}}) \in \mathbb{R}^2$ is the acceleration vector, $x = (v_{\mathrm{x}}, v_{\mathrm{y}}) \in \mathbb{R}^2$ is the vector of longitudinal and lateral velocities, and $r \in \mathbb{R}$ is a time varying parameter representing the yaw-rate. We assume that the vector u is available, since directly sensed by the

accelerometers mounted on the chassis.

It is worth to notice that in this model the velocity vector is the state, the acceleration is the input and $y = v_{\mathrm{x}} \in \mathbb{R}$ is the measured output. The explicit expression for matrices in (6.1) is given below:

$$A(r) := \begin{bmatrix} 0 & r \\ -r & 0 \end{bmatrix}, \quad C := \begin{bmatrix} 1 & 0 \end{bmatrix}.$$

It is important to remark that the pair $(C, A(r))$ is detectable if and only if r is different from zero. For the kinematic model (6.1) Farrelly and Wellstead [51] proposed a Luenberger-like observer of the following form,

$$\begin{cases} \dot{\hat{x}} = A(r)\hat{x} + u + L(r)(\hat{y} - y) \\ \hat{y} = C\hat{x}, \end{cases} \tag{6.2}$$

where the yaw-dependent observer gain is defined as $L(r) := [-2\alpha|r|, (1-\alpha^2)r]^\top$, with $\alpha \in \mathbb{R}_{>0}$ being a tunable parameter that assigns the observer speed of converge. Indeed, for a constant yaw-rate, the two eigenvalues associated to $(A(r) + L(r)C)$ are both located at $-\alpha|r|$.

Remark 6.1
The observer (6.2) is a Linear Parameter Varying (LPV) system, therefore eigenvalues with negative real part do not imply stability nor convergence. ⌟

In [51] it is shown that through a suitable Lyapunov function, Uniform Global Asymptotic Stability is guaranteed for all uniformly non-zero evolutions of r.

Since its proposal, the kinematic-observer has been widely used [97], [120], and many tests have been made to evaluate its performance. It turns out that, despite its simplicity, the kinematic-observer provides good estimates even during driving conditions where the vehicle dynamics is far from being linear. However, as pointed out in [96], the selection of the parameter α is especially critical, as it entails the well-known trade-off between bandwidth (speed of converge of the error dynamics) and sensitivity to noise. For example a bank angle $\vartheta \in \mathbb{R}$ introduces a lateral acceleration bias $a_{\mathrm{y}} \in \mathbb{R}$ in the input measurement as follows

$$\Delta a_{\mathrm{y}} = -g \sin(\vartheta), \tag{6.3}$$

with $g \in \mathbb{R}$ being the gravitational constant. With constant yaw-rate the presence of this bias introduces a steady-state estimation error $e := (\hat{x} - x)$ of

$$e = (A(r) + L(r)C)^{-1} \begin{bmatrix} 0 \\ \Delta a_{\mathrm{y}} \end{bmatrix} = -\frac{1}{r} \begin{bmatrix} \alpha^{-2} \\ 2\alpha^{-1}\mathrm{sign}(r) \end{bmatrix} \Delta a_{\mathrm{y}}. \tag{6.4}$$

As expected, larger values of α and r lead to smaller estimation errors, and this is consistent with the intuition that when r approaches zero, the kinematic model (6.1) is increasingly less observable.

By increasing α we improve robustness to bias and noise at the input, but we also deteriorate the rejection of high-frequency affecting the measurement output y, and for this reason, in the following section, we propose a dead-zone modification of observer (6.2).

6.2 The Dead-zone Kinematic Observer

We propose to augment the kinematic observer (6.2) with the dead-zone mechanism illustrated in Chapter 4. The resulting *dead-zone kinematic observer* has the following form

$$\begin{cases} \dot{\hat{x}} = A(r)\hat{x} + u + L(r)\mathrm{dz}_{\sqrt{\sigma}}(\hat{y} - y) \\ \hat{y} = C\hat{x}. \end{cases} \tag{6.5}$$

For this observer, the matrix $A(r)$ and the observer gain $L(r)$ are parameter varying, and the results presented in Chapter 4 cannot be immediately applied. Moreover, for small values of $|r|$ the observer gain $L(r)$ is small as well, and the observer (6.5) is already less sensitive to measurement noise. For this reason, we propose to scale the adaptation dynamics σ according to $|r| \in \mathbb{R}_{\geq 0}$ as follows

$$\dot{\sigma} = -\lambda|r|\sigma + \gamma|r|(\hat{y} - y)^2, \quad \sigma \in \mathbb{R}_{\geq 0} \tag{6.6}$$

Defining the estimation error as $e := \hat{x} - x$, and using (6.6), we obtain the following LPV system with adaptive dead-zone

$$\begin{cases} \dot{e} = A_{\mathrm{CL}}(r)e - L(r)\mathrm{sat}_{\sqrt{\sigma}}(Ce) \\ \dot{\sigma} = -\lambda|r|\sigma + \gamma|r|(Ce)^2 \qquad\qquad \sigma \in \mathbb{R}_{\geq 0}. \end{cases} \tag{6.7}$$

Here, for simplicity of notation, we defined the closed-loop matrix $A_{\mathrm{CL}}(r) := A(r) + L(r)C$, whose explicit expression is reported below

$$\left[\begin{array}{c|c} A_{\mathrm{CL}}(r) & L(r) \end{array}\right] := \left[\begin{array}{cc|c} -2\alpha|r| & r & -2\alpha|r| \\ -\alpha^2 r & 0 & (1-\alpha^2)r \end{array}\right]. \tag{6.8}$$

To retrieve the LMI-based tuning procedure presented in Chapter 4, we assume that the yaw rate is uniformly bounded away from zero, i.e., that $|r(t)| \geq \epsilon$ for all $t \in \mathbb{R}_{\geq 0}$ where $\epsilon \in \mathbb{R}_{>0}$ is not necessarily known. This is restrictive, but in practice it is not possible to

obtain reliable estimates of the lateral velocity when the yaw rate is too small, due the very nature of the kinematic model (6.1). We are now ready to state the main result of the chapter.

Theorem 6.1
Consider the observer (6.7). Assume that the following LMI in the optimization variables $0 < P = P^\top \in \mathbb{R}^{2\times 2}$, $\gamma \in \mathbb{R}_{\geq 0}$, $\lambda, \mu \in \mathbb{R}_{>0}$ *is feasible:*

$$\mathrm{He}\begin{bmatrix} PA_{\mathrm{CL}}(1) + \gamma C^\top C & -PL(1) \\ \mu C & -\mu - \lambda \end{bmatrix} < 0. \tag{6.9}$$

Then for any $\epsilon \in \mathbb{R}_{>0}$ *and for any value of* $r \in (-\infty, -\epsilon]$, *or* $r \in [\epsilon, \infty)$, *the error dynamics (6.7) is Globally Asymptotically Stable (GAS) to the origin.*

Proof. The proof is carried out in two steps. First we show that (6.9) implies GAS of the origin for (6.7) as long as $r \in [\epsilon, \infty)$. Second, we show that the GAS property holds also when $r \in (-\infty, -\epsilon]$. Let us start considering the following candidate Lyapunov function $V(e, \sigma) := e^\top P e + 2\sigma$. We remark that $P = P^\top > 0$ and that $\sigma \in \mathbb{R}_{\geq 0}$ so that $V(e, \sigma)$ is proper and positive definite. Differentiating with respect to time yields

$$\dot{V}(e,\sigma) = e^\top A_{\mathrm{CL}}(r)^\top P e + e^\top P A_{\mathrm{CL}}(r) e - 2e^\top P L(r) \mathrm{sat}_{\sqrt{\sigma}}(Ce) - 2\lambda|r|\sigma + 2\gamma|r|(Ce)^2. \tag{6.10}$$

Let us consider the following inequalities

$$2\mu|r|\mathrm{sat}_{\sqrt{\sigma}}(Ce)(Ce - \mathrm{sat}_{\sqrt{\sigma}}(Ce)) \geq 0 \tag{6.11a}$$
$$2\lambda|r|(\sigma - \mathrm{sat}^2_{\sqrt{\sigma}}(Ce)) \geq 0, \tag{6.11b}$$

where (6.11a) is a global sector condition for the saturation function and (6.11b) simply states that σ is always greater than the square of a saturation function whose amplitude is $\sqrt{\sigma}$. Summing up (6.11) to (6.10) we obtain the following upper-bound

$$\dot{V}(e,\sigma) \leq \begin{bmatrix} e \\ \mathrm{sat}_{\sqrt{\sigma}}(Ce) \end{bmatrix}^\top \begin{bmatrix} \mathrm{He}(PA_{\mathrm{CL}}(r)) + 2\gamma|r|C^\top C & -PL(r) + \mu|r|C^\top \\ -L(r)^\top P + \mu|r|C & -2|r|(\mu+\lambda) \end{bmatrix} \begin{bmatrix} e \\ \mathrm{sat}_{\sqrt{\sigma}}(Ce) \end{bmatrix} \leq 0, \tag{6.12}$$

for all $(e, \sigma) \neq 0$. Equation (6.12) can be strengthened and conveniently re-written in a strict LMI like form as follows

$$\mathrm{He}\begin{bmatrix} PA_{\mathrm{CL}}(r) + \gamma|r|C^\top C & -PL(r) \\ \mu|r|C & -|r|(\mu+\lambda) \end{bmatrix} < 0, \tag{6.13}$$

where r ranges in the interval $[\epsilon, \infty)$. It is important to notice that inequality (6.13) does not imply asymptotic convergence, but only stability; however we can represent the LPV

model as a differential inclusion and invoke the invariance principle presented in [104] to conclude that if (6.13) holds for all $r \in [\epsilon, \infty)$, then (6.7) is Globally Asymptotically Stable (GAS).

Now recalling that $r \in [\epsilon, \infty)$ notice that the entries of (6.8) are homogeneous of degree one with respect to r, so that $A_{\mathrm{CL}}(r) = rA_{\mathrm{CL}}(1)$ and $L(r) = rL(1)$. Collecting a scaling factor $|r|$ from Equation (6.13), this last one reduces to (6.9), showing GAS for uniformly positive yaw-rates. We conclude the proof by showing that any feasible solution to (6.13) with $r = r^\star \in [\epsilon, \infty)$ is also a feasible solution to (6.13) with $r = -r^\star \in (-\infty, \epsilon]$. This idea is formally stated in Lemma 6.1 below, which concludes the proof of the case $r \in (-\infty, -\epsilon]$. □

Lemma 6.1
Assume that $(P^\star, \gamma^\star, \mu^\star, \lambda^\star)$ is a feasible solution to (6.13) associated to a positive yaw-rate $r = r^\star \in [\epsilon, \infty)$, and consider the non-singular diagonal matrix $T := \mathrm{diag}(1, -1) \in \mathbb{R}^{2\times 2}$. Then $(TP^\star T, \gamma^\star, \mu^\star, \lambda^\star)$ is a feasible solution to (6.13) with $r = -r^\star \in (-\infty, -\epsilon]$.

Proof. First we notice that feasibility of the LMI (6.13) is not affected by congruence transformations. We pre/post-multiply (6.13) by $\mathrm{diag}(T, 1) \in \mathbb{R}^{3\times 3}$ and we obtain the equivalent condition

$$\mathrm{He}\begin{bmatrix} TPA_{\mathrm{CL}}(r)T + \gamma|r|TC^\top CT & -TPL(r) \\ \mu|r|CT & -|r|(\mu+\lambda) \end{bmatrix} < 0. \tag{6.14}$$

Using the expression in (6.8) it is easy to verify that the following equalities hold

$$A_{\mathrm{CL}}(r)T = TA_{\mathrm{CL}}(-r) \tag{6.15a}$$
$$TC^\top CT = C^\top C \tag{6.15b}$$
$$L(r) = TL(-r). \tag{6.15c}$$

Plugging (6.15) into (6.14) we retrieve (6.13) with parameters $(TP^\star T, \gamma^\star, \mu^\star, \lambda^\star)$ and following the same steps as in the proof of Theorem 6.1 we conclude GAS for $r \in (-\infty, \epsilon]$. It is interesting to notice that matrix $TP^\star T \in \mathbb{R}^{2\times 2}$ has the same elements as P but with a sign inversion of the off-diagonal terms, namely

$$P^\star := \begin{bmatrix} p_{11} & p_{12} \\ p_{12} & p_{22} \end{bmatrix} \Leftrightarrow TP^\star T := \begin{bmatrix} p_{11} & -p_{12} \\ -p_{12} & p_{22} \end{bmatrix},$$

where we remark that $TP^\star T > 0$ if and only if $P^\star > 0$. □

The combination of Theorem 6.1 and Lemma 6.1 provides a desirable unified design strategy, which is independent of the sign of r, and provides guarantees for any value

of r uniformly bounded away from zero. We do not include the defective point $r = 0$ (where we know that the system is not detectable), even if Theorem 6.1 suggests that the same observer can also be used for cases where r keeps changing sign and spends little time around zero. However a rigorous stability analysis for that scenario is not carried out in this preliminary work. We also remark that LMI (6.9) is always feasible because pair $(C, A(1))$ is detectable: the proof of this fact follows similar steps to those reported in Chapter 4. As a consequence, we can think of the dead-zone mechanism as an augmentation of the original observer (6.2), which improves its performance.

6.3 Optimization and simulations

In this section we use the LMI constraint (6.9) to formulate an optimization problem similar to the one presented in Section 4.5, with the goal to optimize the noise rejection capability of the dead-zone observer (6.5).

In general there are infinitely many solutions to (6.9) and we propose to choose the one that maximizes the effect of noise on the adaptation dynamics. A good idea is to select the largest possible value of γ, once an upper bound $\lambda_{\max} \in \mathbb{R}_{>0}$ has been fixed for the σ-adaptation speed λ. The resulting optimization problem can be cast as follows

$$\begin{aligned} &\sup_{\gamma,\lambda,\mu,P} \gamma, \qquad \text{subject to:} \\ &\mathrm{He}\begin{bmatrix} PA_{\mathrm{CL}}(1) + \gamma C^\top C & -PL(1) \\ \mu C & -\mu - \lambda \end{bmatrix} < 0 \\ &P = P^\top > 0, \quad \lambda_{\max} \geq \lambda > 0 \\ &\mu \geq 0, \quad \gamma \geq 0. \end{aligned} \tag{6.16}$$

The upper-bound $\lambda_{\max} \in \mathbb{R}_{>0}$ avoids an excessive mismatch between the plant and the dead-band adaptation dynamics.

What follows is a comparison, based on simulations, between the standard Farrelly and Wellstead observer reported in (6.2), and the modified version with the adaptive dead-zone presented in this chapter, see (6.5). Simulations have been performed adding a high frequency noise ν at the measurement, i.e., $y = Cx + \nu$. We show that the dead-zone observer allows for a selection of larger values of α, without increased sensitivity to measurement noise. We quantify sensitivity using two indicators: the Signal to Noise Ratio (SNR) and the Normalized Root Mean Squared Error (NRMSE). The SNR is defined as

$$\mathrm{SNR}_{\mathrm{dB}} := 10 \log \left(\frac{\mathbb{E}\{\hat{x}^\top \hat{x}\}}{\mathbb{E}\{\nu^\top \nu\}} \right),$$

while the NRMSE is defined as

$$\text{NRMSE} := 1 - \frac{\| x - \hat{x} \|}{\| x - \mathbb{E}\{x\} \|}.$$

For NRMSE $= 1$ we have a perfect match between the estimate $\hat{x}$ and the real value x. Our simulations show that for a similar value of the SNR the parameter α for the dead-zone observer is roughly twice the one without dead-zone. Numerical simulations have been performed with a double track model setting a longitudinal speed of $v_{\text{x}} = 13.9\,\text{m/s}$, and a step-like steering angle at the front wheels. The output measurement $y = v_{\text{x}} + \nu$ is corrupted by a uniform high-frequency noise (500 Hz) with amplitude $\pm 0.034\,\text{m/s}$. At time $t = 10\,\text{s}$ the vehicle encounters a banked road with inclination $\vartheta = 1.4°$, which introduces a lateral acceleration bias, see (6.3). The parameters for the dead-zone adaptation have been obtained by solving the convex optimization problem (6.16), with the selection $\lambda_{\max} = 300$. The obtained parameters are $\gamma = 225.37$ and $\lambda = 299.9$ and thanks to Lemma 6.1, those are valid design parameters also for negative yaw rates. The simulations are are reported

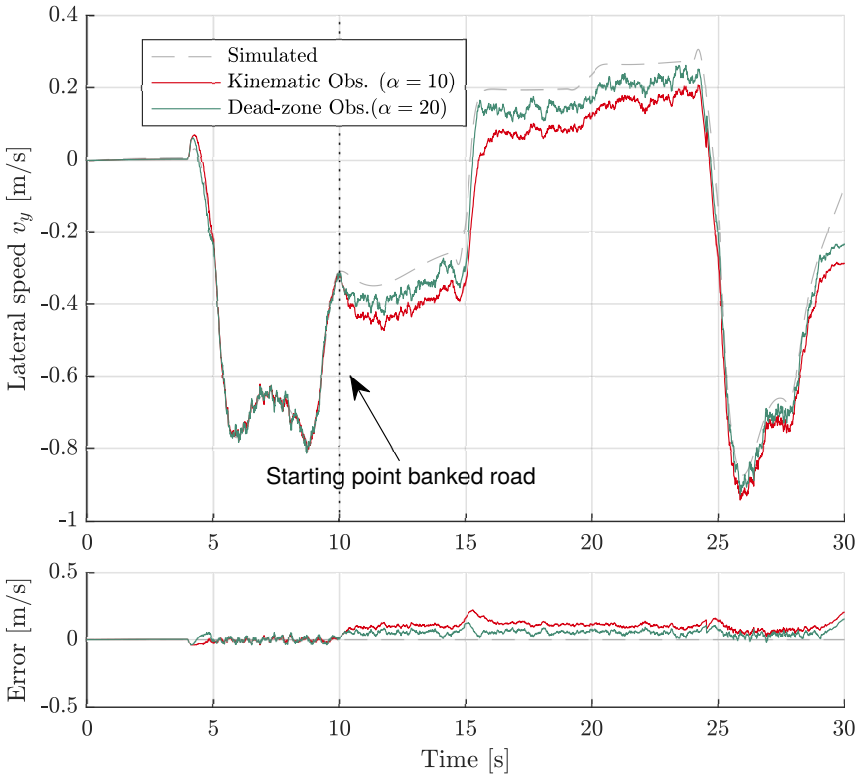

Figure 6.1: Comparison between the simulated (dashed line) and the estimated lateral velocity with the kinematic observer (green solid line) and the dead-zone observer (red solid line) during a step-like steering maneuver on the double track model.

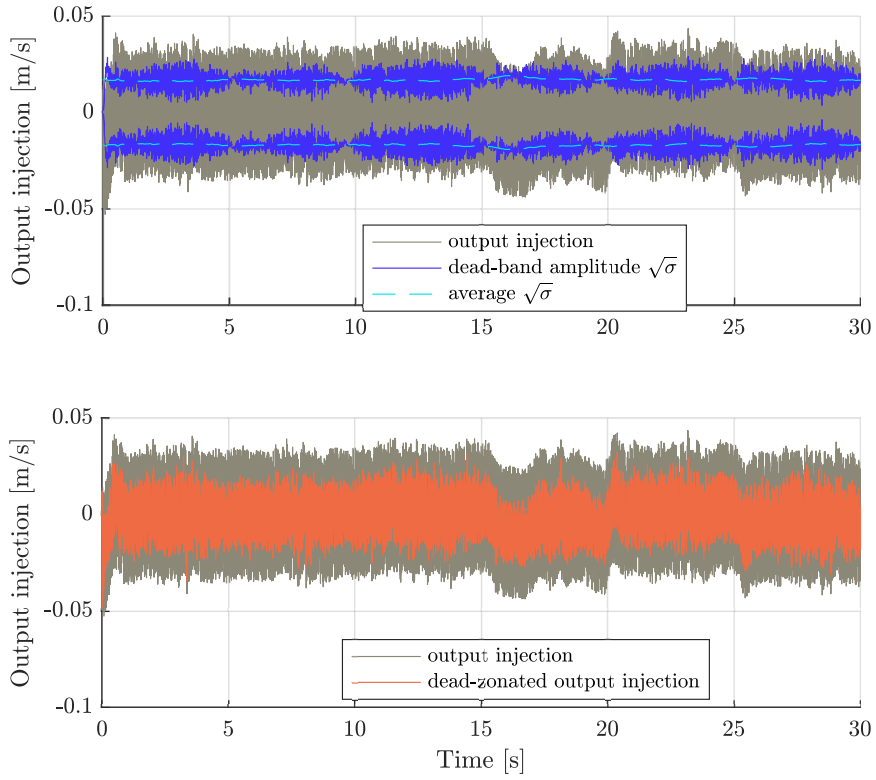

Figure 6.2: Dead-zone "tube" overlapped to the output injection term (top) and filtering action of the dead-zone (bottom).

	α	SNR	NRMSE
Kinematic Observer	10	42.5 dB	75.50 %
Dead-zone Observer	20	40.3 dB	86.93 %

Table 6.1: Parameter α and performance indicator for the sinusoidal steering test on the double track model.

in Fig. 6.1. We can observe that for $t \leq 10\,\text{s}$, both observers provide roughly the same estimate. At time $t = 10\,\text{s}$ the vehicle encounters the banked road, and the estimates start to deteriorate. However, since the dead-zone observer has a larger α, it provides a better estimate. This intuition is also supported by the values of the NRMSE reported in Table 6.1. In Figure 6.2 we can visually interpret the action of the dead-zone mechanism. The output injection term (gray line in the top plot) is trapped inside the dead-band (blue lines in the top plot) and the resulting dead-zonated output injection is reported in orange in the bottom plot.

6.4 Conclusion

In this chapter we presented an application of the adaptive dead-zone mechanism discussed in Chapter 4, to the Farrelly and Wellstead kinematic observer. The adaptive dead-zone reduces the sensitivity to high frequency noise and allows for larger values of the observer gain. We have shown that the stability of the resulting LPV error dynamics can be cast as an LMI problem and we have shown its feasibility, under the necessary detectability condition for the linearized plant. We characterized the effectiveness of the proposed solution for positive and negative yaw rates. Finally, we tested the effectiveness of our approach by means of numerical simulations on a non-linear double-track vehicle model. The implementation of the proposed estimation scheme on an experimental setup will be the subject of future investigations.

Part III
Conclusions

Chapter 7

Conclusions and perspectives

In this dissertation we studied problems involving linear time-invariant systems in feedback with three different types of nonlinearities; a play/stop operator, a switching-reset mechanism, and an adaptive dead-zone. From a control point of view the arising nonlinear loops show a few interesting behaviors, e.g., compact sets of equilibria, state constraints, discontinuities of the vector field, resets of the state, and adaptation mechanisms. To consider all these possibilities within a unique framework we adopted the hybrid systems formalism, which easily allows for the integration of all these phenomena. In the first part of the thesis, we studied the stability properties of these loops mainly through Lyapunov techniques, while in the second part these properties are exploited to solve real problems arising in mechatronic applications (in particular related to the automotive world). We paid particular attention to the numerical tractability of the results, making them broadly applicable to real world applications. Many designs and stability conditions have been formulated as linear matrix inequalities, which can be efficiently solved through convex optimization techniques, and this has been useful to optimize the performance of the applications presented in the second part of the thesis.

In Chapter 2 we studied a linear single-input single-output system in feedback with a play/stop operator. We have shown that this operator creates a compact set of equilibria (an attractor) that can be explicitly characterized. Global exponential stability and global pointwise asymptotic stability have been proved under the hypothesis of the existence of a common quadratic Lyapunov function. We also established the equivalence between global exponential stability, global pointwise asymptotic stability, and their robust counterparts for this class of systems. We believe that these results open many interesting research directions. First, it would be interesting to complete the analysis of the single-input single-output case including the cases of purely imaginary and unstable poles. Simulations suggest that for this scenario, a nonlinear oscillating regime is reached by the loop. Secondly, the extension of the current results to the multiple-input multiple-output case also deserves attention. However, this direction seems to be quite challenging because the equilibrium set is more complicated, and the existence of a quadratic Lyapunov is a way more restrictive condition in this case. With high probability, only sufficient conditions can be obtained, and the equilibrium set can only be approximated. Nonetheless, from a practical viewpoint, it might still be desirable to provide numerically tractable sufficient stability conditions.

In Chapter 3 we proposed a reset-switching controller to improve the transient and the steady-state performance of linear plants. The resulting loop is a full hybrid system, where a differential equation with a discontinuous right-hand side is coupled with a state reset law. Roughly speaking, the proposed hybrid mechanism switches between two different linear controllers, and the reset action keeps the transients between the two well behaved. Indeed the controller achieves set-point regulation under a large class of switching signals (essentially all those that satisfy a direct and reverse dwell-time condition), and the two linear controllers can be designed to meet different performance and activated when needed. For this hybrid control scheme, many different extensions are possible. Firstly, it would be interesting to consider more complicated references and disturbances, casting the problem in the output regulation framework and modeling these signals as the output of a neutrally stable exosystem. In this scenario, the steady-state response would be a nontrivial function of the exosystem output, and of the switching signal, making if necessary to use a set of generalized regulation equations. Linear output regulation for hybrid systems is already a promising research direction, but to the best of the authors' knowledge, currently only periodic switching signals are considered, and the proposed direction appears to be new. Secondly, it would be interesting to explore the potential of discontinuous control laws coupled with reset mechanisms.

In Chapter 4 we studied an adaptive dead-zone mechanism that improves the noise rejection capability of classical Luenberger and high-gain observers, leading to what we called dead-zone observers. The adaptation parameter is constrained to the positive orthant, and using this property we have been able to prove stability using a Lyapunov function that is positive definite only on a restricted subset of the overall state space. For these dead-zone observers, it would be interesting to remove the full relative degree assumption and consider a larger class of nonlinear plants. Nonlinear systems with a uniform relative degree are good candidates because they can be transformed (with a proper change of coordinates) into the upper-triangular form used by the standard high-gain construction. Another interesting direction would be to consider other nonlinear functions as output correction terms. Saturation has already been used in the literature to mitigate the effect of outliers at the measured output, but different functions could be used to optimize different performances. Dead-zone observers could also be combined with the recently proposed low-power observers to obtain an improved noise rejection capability.

To conclude, we want to say that all the presented results have potentially interesting applications and in the future, we hope to have the possibility to test their performance in more realistic scenarios.

Bibliography

[1] Jeffrey H. Ahrens and Hassan K. Khalil. "High-gain observers in the presence of measurement noise: A switched-gain approach." In: *Automatica* 45.4 (2009), pp. 936–943.

[2] Angelo Alessandri and Anna Rossi. "Increasing-gain observers for nonlinear systems: Stability and design." In: *Automatica* 57 (2015), pp. 180–188.

[3] Angelo Alessandri and Luca Zaccarian. "Stubborn State Observers for Linear Time-invariant Systems." In: *Automatica* 88 (Feb. 2018), pp. 1–9.

[4] Vincent Andrieu, Laurent Praly, and Alessandro Astolfi. "High gain observers with updated gain and homogeneous correction terms." In: *Automatica* 45.2 (2009), pp. 422–428.

[5] Vincent Andrieu, Laurent Praly, and Alessandro Astolfi. "Homogeneous approximation, recursive observer design, and output feedback." In: *SIAM Journal on Control and Optimization* 47.4 (2008), pp. 1814–1850.

[6] Daniele Astolfi, Angelo Alessandri, and Luca Zaccarian. "Stubborn ISS redesign for nonlinear high-gain observers." In: *IFAC-PapersOnLine* 50.1 (2017), pp. 15422–15427.

[7] Daniele Astolfi and Lorenzo Marconi. "A high-gain nonlinear observer with limited gain power." In: *IEEE Transactions on Automatic Control* 60.11 (2015), pp. 3059–3064.

[8] Daniele Astolfi, Lorenzo Marconi, and Andrew R. Teel. "Low-power peaking-free high-gain observers for nonlinear systems." In: *Control Conference (ECC), 2016 European*. IEEE. 2016, pp. 1424–1429.

[9] Daniele Astolfi, Lorenzo Marconi, Laurent Praly, and Andrew Teel. "Sensitivity to high-frequency measurement noise of nonlinear high-gain observers." In: *10th IFAC Symposium on Nonlinear Control Systems, Monterey, CA*. 2016, pp. 276–278.

[10] Ahmad N. Atassi and Hassan K. Khalil. "A separation principle for the stabilization of a class of nonlinear systems." In: *IEEE Transactions on Automatic Control* 44.9 (1999), pp. 1672–1687.

[11] Jean Pierre Aubin. *Viability theory*. Birkhauser, 1991.

[12] Jean Pierre Aubin and Arrigo Cellina. "Differential Inclusions: Set-Valued Maps and Viability Theory." In: (1984).

[13] Fabio Bagagiolo. "Dynamic programming for some optimal control problems with hysteresis." In: *Nonlinear Differential Equations and Applications NoDEA* 9.2 (2002), pp. 149–174.

[14] Antonio Barreiro and Alfonso Baños. "Input–output stability of systems with backlash." In: *Automatica* 42.6 (2006), pp. 1017–1024.

[15] Pauline Bernard, Laurent Praly, and Vincent Andrieu. "Observers for a non-Lipschitz triangular form." In: *Automatica* 82 (2017), pp. 301–313.

[16] Sanjay P. Bhat and Dennis S. Bernstein. "Nontangency-based Lyapunov tests for convergence and stability in systems having a continuum of equilibria." In: *SIAM Journal on Control and Optimization* 42.5 (2003), pp. 1745–1775.

[17] F. Blanchini, S. Miani, and F. Mesquine. "A Separation Principle for Linear Switching Systems and Parametrization of All Stabilizing Controllers." In: *IEEE Transactions on Automatic Control* 54.2 (Feb. 2009), pp. 279–292.

[18] Nicolas Boizot, Eric Busvelle, and Jean-Paul Gauthier. "An adaptive high-gain observer for nonlinear systems." In: *Automatica* 46.9 (2010), pp. 1483–1488.

[19] Jerome Bosche and Ahmed El Hajjaji. *An output feedback controller design for lateral vehicle dynamic*. Vol. 41. 2. Elsevier, 2008, pp. 5670–5675.

[20] Stefano Bottelli, Mara Tanelli, Ivo Boniolo, and Sergio Matteo Savaresi. "Online estimation of vehicle load and mass distribution for ground vehicles." In: *IFAC Proceedings Volumes* 47.3 (2014), pp. 8439–8444.

[21] Stephen Boyd and Craig Barratt. *Linear controller design: limits of performance*. Tech. rep. Stanford University Stanford United States, 1991.

[22] Stephen Boyd, Laurent El Ghaoui, Eric Feron, and Venkataramanan Balakrishnan. *Linear matrix inequalities in system and control theory*. 1994.

[23] Bernard Brogliato and Daniel Goeleven. "Existence, uniqueness of solutions and stability of nonsmooth multivalued Lur'e dynamical systems." In: *Journal of Convex Analysis* 20.3 (2013), pp. 881–900.

[24] Bernard Brogliato and Daniel Goeleven. "Well-posedness, stability and invariance results for a class of multivalued Lur'e dynamical systems." In: *Nonlinear Analysis: Theory, Methods & Applications* 74.1 (2011), pp. 195–212.

[25] Bernard Brogliato, Aris Daniilidis, Claude Lemarechal, and Vincent Acary. "On the equivalence between complementarity systems, projected systems and differential inclusions." In: *Systems & Control Letters* 55.1 (2006), pp. 45–51.

[26] Martin Brokate and Pavel Krejčí. "Optimal control of ODE systems involving a rate independent variational inequality." In: *Discrete & Continuous Dynamical Systems-Series B* 18.2 (2013).

[27] Martin Brokate and Jürgen Sprekels. *Hysteresis and phase transitions*. Vol. 121. Springer Science & Business Media, 2012.

[28] Chaohong Cai and Andrew R. Teel. "Characterizations of input-to-state stability for hybrid systems." In: *Systems & Control Letters* 58.1 (2009), pp. 47–53.

[29] Chaohong Cai, Andrew R. Teel, and Rafal Goebel. "Smooth Lyapunov Functions for Hybrid Systems Part II: (Pre)Asymptotically Stable Compact Sets." In: *IEEE Transactions on Automatic Control* 53.3 (Apr. 2008), pp. 734–748.

[30] Daniele Carnevale, Sergio Galeani, Mario Sassano, and Andrea Serrani. "External Models for Output Regulation based on Moment Estimation from Input-Output Data." In: *IFAC-PapersOnLine* 50.1 (2017). 20th IFAC World Congress, pp. 7777–7782.

[31] B-Chien Chen and F-C. Hsieh. "Sideslip angle estimation using extended Kalman filter." In: *Vehicle System Dynamics* 46.S1 (2008), pp. 353–364.

[32] Mahmoud Chilali and Pascal Gahinet. "$\mathcal{H}_\infty$ design with pole placement constraints: an LMI approach." In: *IEEE Transactions on Automatic Control* 41.3 (1996), pp. 358–367.

[33] Michelle S. Chong, Dragan Nesic, Romain Postoyan, and Levin Kuhlmann. "Parameter and state estimation of nonlinear systems using a multi-observer under the supervisory framework." In: *IEEE Transactions on Automatic Control* 60.9 (2015), pp. 2336–2349.

[34] Matteo Cocetti, Sophie Tarbouriech, and Luca Zaccarian. "High-gain dead-zone observers for linear and nonlinear plants." In: *IEEE Control Systems Letters* (2018).

[35] Matteo Cocetti, Sophie Tarbouriech, and Luca Zaccarian. "On dead-zone observers for linear plants." In: *American Control Conference (ACC)*. June 2018.

[36] Matteo Cocetti, Silvia Donnarumma, Luca De Pascali, Matteo Ragni, Francesco Biral, Fabrizio Panizzolo, Pier Paolo Rinaldi, Alex Sassaro, and Luca Zaccarian. "Hybrid non-overshooting set-point pressure regulation for a wet clutch." In: *accepted on Transaction on Mechatronics* (2019).

[37] Matteo Cocetti, Rafal Goebel, Luca Zaccarian, Fabio Bagagiolo, and Enrico Bertolazzi. "Necessary and sufficient conditions for GES/GPAS equilibria in linear SISO systems feedback with play/stop operators." In: *submitted to SIAM Journal on Control and Optimization* (2019).

[38] Matteo Cocetti, Luca Zaccarian, Fabio Bagagiolo, and Enrico Bertolazzi. "Necessary and sufficient stability conditions for equilibria of linear SISO feedbacks with a play operator." In: *IFAC-PapersOnLine* 49.18 (2016), pp. 211–216.

[39] Bernard D Coleman and Marion L Hodgdon. "A constitutive relation for rate-independent hysteresis in ferromagnetically soft materials." In: *International Journal of Engineering Science* 24.6 (1986), pp. 897–919.

[40] Giovanni Colombo, René Henrion, D Hoang Nguyen, and Boris S Mordukhovich. "Optimal control of the sweeping process over polyhedral controlled sets." In: *Journal of Differential Equations* 260.4 (2016), pp. 3397–3447.

[41] Matteo Cordioli, M Mueller, Fabrizio Panizzolo, Francesco Biral, and Luca Zaccarian. "An adaptive reset control scheme for valve current tracking in a power-split transmission system." In: *2015 European Control Conference (ECC)*. IEEE. 2015, pp. 1884–1889.

[42] Bernard Cornet. "Existence of slow solutions for a class of differential inclusions." In: *Journal of Mathematical Analysis and Applications* 96.1 (1983), pp. 130–147.

[43] Letizia M. Corradini and Giuseppe Orlando. "Robust stabilization of nonlinear uncertain plants with backlash or dead zone in the actuator." In: *IEEE Transactions on Control Systems Technology* 10.1 (2002), pp. 158–166.

[44] J.M. Gomes Da Silva and Sophie Tarbouriech. "Antiwindup design with guaranteed regions of stability: an LMI-based approach." In: *IEEE Transactions on Automatic Control* 50.1 (2005), pp. 106–111.

[45] Luca De Pascali, Francesco Biral, Matteo Cocetti, Luca Zaccarian, and Sophie Tarbouriech. "A kinematic observer with adaptive dead-zone for vehicles lateral velocity estimation." In: *2018 IEEE 15th International Workshop on Advanced Motion Control (AMC)*. Mar. 2018, pp. 511–516.

[46] Luca De Pascali, Matteo Cocetti, Francesco Biral, Andrea Palazzetti, Fabrizio Panizzolo, Pier Paolo Rinaldi, Alex Sassaro, and Luca Zaccarian. "LMI-based non-overshooting pressure control design for a wet clutch." In: *Control Applications (CCA), 2016 IEEE Conference on*. IEEE. 2016, pp. 329–334.

[47] John Doyle and Gunter Stein. "Robustness with observers." In: *IEEE Transactions on Automatic Control* 24.4 (Aug. 1979), pp. 607–611.

[48] Johan Eker and Jorgen Malmborg. "Design and implementation of a hybrid control strategy." In: *IEEE control systems* 19.4 (1999), pp. 12–21.

[49] Lars Eriksson and Lars Nielsen. *Modeling and control of engines and drivelines*. John Wiley & Sons, 2014.

[50] Farzad Esfandiari and Hassan K. Khalil. "Output feedback stabilization of fully linearizable systems." In: *International Journal of control* 56.5 (1992), pp. 1007–1037.

[51] Jim Farrelly and Peter Wellstead. "Estimation of vehicle lateral velocity." In: (1996), pp. 552–557.

[52] Bruce A Francis. "The linear multivariable regulator problem." In: *SIAM Journal on Control and Optimization* 15.3 (1977), pp. 486–505.

[53] Hiroshi Fujimoto and Naoki Takahashi. *Cornering stiffness and slip angle estimation of electric vehicle for direct yaw-moment control*. Vol. 39. 16. IFAC, 2004, pp. 496–501.

[54] Hiroshi Fujimoto, Take Saito, Akio Tsumasaka, and Toshihiko Noguchi. "Motion Control and Road Condition Estimation of Electric Vehicles with Two In-wheel Motors." In: (2004).

[55] Jean-Paul Gauthier, Hassan Hammouri, and Sami Othman. "A simple observer for nonlinear systems applications to bioreactors." In: *IEEE Transactions on automatic control* 37.6 (1992), pp. 875–880.

[56] Jean-Paul Gauthier and Ivan Kupka. *Deterministic observation theory and applications*. Cambridge university press, 2001.

[57] J. Christian Gerdes. "Estimation of Vehicle Roll and Road Bank Angle." In: (2004), pp. 2110–2115.

[58] Rafal Goebel, Ricardo G. Sanfelice, and Andrew R Teel. *Hybrid Dynamical Systems: modeling, stability, and robustness*. 2012.

[59] Rafal Goebel and Andrew R Teel. "Solutions to hybrid inclusions via set and graphical convergence with stability theory applications." In: *Automatica* 42.4 (2006), pp. 573–587.

[60] Martin Goetz, Martin Levesley, and David Crolla. "Dynamics and control of gearshifts on twin-clutch transmissions." In: *Proceedings of the institution of mechanical engineers, Part D: Journal of Automobile Engineering* 219.8 (2005), pp. 951–963.

[61] Wassim M. Haddad, VijaySekhar Chellaboina, and JinHyoung Oh. "Linear controller analysis and design for systems with input hystereses nonlinearities." In: *Journal of the Franklin Institute* 340.5 (2003), pp. 371–390.

[62] Hongtao Hao, Tongli Lu, Jianwu Zhang, and Bin Zhou. "A new control strategy of the filling phase for wet dual clutch transmission." In: *Proceedings of the Institution of Mechanical Engineers, Part C: Journal of Mechanical Engineering Science* (2015), p. 0954406215590187.

[63] Claude Henry. "An existence theorem for a class of differential equations with multivalued right-hand side." In: *Journal of Mathematical Analysis and Applications* 41.1 (1973), pp. 179–186.

[64] João P. Hespanha. *Linear systems theory*. 2009.

[65] João P. Hespanha and A.Stephen Morse. "Switching between stabilizing controllers." In: *Automatica* 38.11 (2002), pp. 1905–1917.

[66] Joachim Horn, Joachim Bamberger, Peter Michau, and Stephan Pindl. "Flatness-based clutch control for automated manual transmissions." In: *Control Engineering Practice* 11.12 (2003), pp. 1353–1359.

[67] Tingshu Hu, Zongli Lin, and Ben M. Chen. "An analysis and design method for linear systems subject to actuator saturation and disturbance." In: *Automatica* 38.2 (2002), pp. 351–359.

[68] Lars Imsland, Tor A. Johansen, Thor I. Fossen, Håvard Fjær Grip, Jens C. Kalkkuhl, and Avshalom Suissa. "Vehicle velocity estimation using nonlinear observers." In: *Automatica* 42.12 (2006), pp. 2091–2103.

[69] Bayu Jayawardhana, Ruiyue Ouyang, and Vincent Andrieu. "Stability of systems with the Duhem hysteresis operator: The dissipativity approach." In: *Automatica* 48.10 (2012), pp. 2657–2662.

[70] Hassan K Khalil and Laurent Praly. "High-gain observers in nonlinear feedback control." In: *International Journal of Robust and Nonlinear Control* 24.6 (2014), pp. 993–1015.

[71] Markus Kunze and Manuel DP Monteiro Marques. "An introduction to Moreau's sweeping process." In: *Impacts in mechanical systems*. Springer, 2000, pp. 1–60.

[72] Huibert Kwakernaak and Raphael Sivan. *Linear optimal control systems*. Vol. 1. Wiley-Interscience New York, 1972.

[73] Daniel Liberzon, João P. Hespanha, and A.Stephen Morse. "Stability of switched systems: a Lie-algebraic condition." In: *Systems & Control Letters* 3.3 (1999), pp. 117–122.

[74] Hai Lin and Panos J. Antsaklis. "Stability and stabilizability of switched linear systems: a survey of recent results." In: *IEEE Transactions on Automatic control* 54.2 (2009), pp. 308–322.

[75] Chia-Shang Liu and Huei Peng. "A State and Parameter Identification Scheme for Linearly Parameterized Systems." In: *Journal of Dynamic Systems, Measurement, and Control* 120.4 (1998), p. 524.

[76] Lennart Ljung. *System Identification: Theory for the User, PTR Prentice Hall Information and System Sciences Series*. 1999.

[77] Hartmut Logemann and Eugene P Ryan. "Systems with hysteresis in the feedback loop: existence, regularity and asymptotic behaviour of solutions." In: *ESAIM: Control, Optimisation and Calculus of Variations* 9 (2003), pp. 169–196.

[78] Hartmut Logemann, Eugene P Ryan, and Ilya Shvartsman. "Integral control of infinite-dimensional systems in the presence of hysteresis: an input-output approach." In: *ESAIM: Control, Optimisation and Calculus of Variations* 13.3 (2007), pp. 458–483.

[79] David G. Luenberger. "Observers for multivariable systems." In: *IEEE Transactions on Automatic Control* 11.2 (1966), pp. 190–197.

[80] David G. Luenberger. "Observing the state of a linear system." In: *IEEE transactions on military electronics* 8.2 (1964), pp. 74–80.

[81] Anatoliy Isakovich Lur'e and Vladimir N. Postnikov. "On the theory of stability of control systems." In: *Applied mathematics and mechanics* 8.3 (1944), pp. 246–248.

[82] Manfredi Maggiore, Mario Sassano, and Luca Zaccarian. "Reduction Theorems for Hybrid Dynamical Systems." In: *IEEE Transactions on Automatic Control* (2018).

[83] Jose Luis Massera. "On Liapounoff's conditions of stability." In: *Annals of Mathematics* (1949), pp. 705–721.

[84] David Q. Mayne, R.W. Grainger, and Graham C. Goodwin. "Nonlinear filters for linear signal models." In: *IEE Proceedings-Control Theory and Applications* 144.4 (1997), pp. 281–286.

[85] Bruce Moore. "Principal component analysis in linear systems: Controllability, observability, and model reduction." In: *IEEE transactions on automatic control* 26.1 (1981), pp. 17–32.

[86] Jean Jacques Moreau. "Evolution problem associated with a moving convex set in a Hilbert space." In: *Journal of Differential Equations* 26.3 (1977), pp. 347–374.

[87] A. Stephen Morse. "Supervisory control of families of linear set-point controllers. 2. Robustness." In: *IEEE Transactions on Automatic Control* 42.11 (Nov. 1997), pp. 1500–1515.

[88] Matthias Mueller, Walter Scandella, and Steffen Mutschler. *Power-split transmission for a traction drive and method for controlling the transmission*. US Patent 9,243,701. Jan. 2016.

[89] Anna Nagurney and Ding Zhang. *Projected dynamical systems and variational inequalities with applications*. Vol. 2. Springer Science & Business Media, 2012.

[90] Kanghyun Nam, Hiroshi Fujimoto, and Yoichi Hori. "Lateral stability control of in-wheel-motor-driven electric vehicles based on sideslip angle estimation using lateral tire force sensors." In: *IEEE Transactions on Vehicular Technology* 61.5 (2012), pp. 1972–1985.

[91] Kenji Natori, Roberto Oboe, and Kouhei Ohnishi. "Stability Analysis and Practical Design Procedure of Time Delayed Control Systems With Communication Disturbance Observer." In: 4.3 (2008), pp. 185–197.

[92] Mattias Nordin and Per-Olof Gutman. "Controlling mechanical systems with backlash–a survey." In: *Automatica* 38.10 (2002), pp. 1633–1649.

[93] Navid Noroozi, Dragan Nešić, and Andrew R. Teel. "Gronwall inequality for hybrid systems." In: *Automatica* 50.10 (2014), pp. 2718–2722.

[94] "Notions and Sufficient Conditions for Pointwise Asymptotic Stability in Hybrid Systems." In: *IFAC-PapersOnLine* 49.18 (2016), pp. 140–145.

[95] Ruiyue Ouyang and Bayu Jayawardhana. "Absolute stability analysis of linear systems with Duhem hysteresis operator." In: *Automatica* 50.7 (2014), pp. 1860–1866.

[96] Giulio Panzani, Matteo Corno, Mara Tanelli, Sergio M Savaresi, Andrea Fortina, and Sebastiano Campo. "Control-oriented vehicle attitude estimation with online sensors bias compensation." In: *ASME 2009 Dynamic Systems and Control Conference*. American Society of Mechanical Engineers. 2009, pp. 819–826.

[97] Giulio Panzani, Matteo Corno, Mara Tanelli, Annalisa Zappavigna, Sergio M. Savaresi, Andrea Fortina, and Sebastiano Campo. "Designing on-demand four-wheel-drive vehicles via active control of the central transfer case." In: *IEEE Transactions on Intelligent Transportation Systems* 11.4 (2010), pp. 931–941.

[98] Gridsada Phanomchoeng, Rajesh Rajamani, and Damrongrit Piyabongkarn. "Nonlinear observer for bounded Jacobian systems, with applications to automotive slip angle estimation." In: *IEEE Transactions on Automatic Control* 56.5 (2011), pp. 1163–1170.

[99] Damrongrit Piyabongkarn, Rajesh Rajamani, John A Grogg, and Jae Y Lew. "Development and experimental evaluation of a slip angle estimator for vehicle stability control." In: *IEEE Transactions on control systems technology* 17.1 (2009), pp. 78–88.

[100] Alexis A. Prasov and Hassan K. Khalil. "A nonlinear high-gain observer for systems with measurement noise in a feedback control framework." In: *IEEE Transactions on Automatic Control* 58.3 (2013), pp. 569–580.

[101] Alexis A. Prasov and Hassan K. Khalil. "Tracking performance of a high-gain observer in the presence of measurement noise." In: *International Journal of Adaptive Control and Signal Processing* 30.8-10 (2016), pp. 1228–1243.

[102] Rajesh Rajamani. *Vehicle dynamics and control*. Springer Science & Business Media, 2011.

[103] Ricardo G. Sanfelice and Laurent Praly. "On the performance of high-gain observers with gain adaptation under measurement noise." In: *Automatica* 47.10 (2011), pp. 2165–2176.

[104] Ricardo G Sanfelice, Rafal Goebel, and Andrew R Teel. "Invariance principles for hybrid systems with connections to detectability and asymptotic stability." In: *IEEE Transactions on Automatic Control* 52.12 (2007), pp. 2282–2297.

[105] Sergio M. Savaresi and Mara Tanelli. *Active braking control systems design for vehicles*. Springer Science & Business Media, 2010.

[106] Andrea Serrani. "Rejection of harmonic disturbances at the controller input via hybrid adaptive external models." In: *Automatica* 42.11 (2006), pp. 1977–1985.

[107] Hyungbo Shim, Jin Heon Seo, and Andrew R. Teel. "Nonlinear observer design via passivation of error dynamics." In: *Automatica* 39.5 (2003), pp. 885–892.

[108] Robert N Shorten, Oliver Mason, Fiacre O'Cairbre, and Paul Curran. "A unifying framework for the SISO circle criterion and other quadratic stability criteria." In: *International Journal of Control* 77.1 (2004), pp. 1–8.

[109] Xingyong Song and Zongxuan Sun. "Pressure-based clutch control for automotive transmissions using a sliding-mode controller." In: *Mechatronics, IEEE/ASME Transactions on* 17.3 (2012), pp. 534–546.

[110] Eduardo D Sontag. "Comments on integral variants of ISS." In: *Systems & Control Letters* 34.1-2 (1998), pp. 93–100.

[111] Zehang Sun, George Bebis, and Ronald Miller. "On-road vehicle detection using optical sensors: A review." In: *Intelligent Transportation Systems, 2004. Proceedings. the 7th International IEEE Conference on*. IEEE. 2004, pp. 585–590.

[112] Gang Tao and Petar V Kokotovic. "Adaptive control of systems with unknown output backlash." In: *IEEE Transactions on Automatic Control* 40.2 (1995), pp. 326–330.

[113] Sophie Tarbouriech, Christophe Prieur, and Isabelle Queinnec. "Stability analysis for linear systems with input backlash through sufficient LMI conditions." In: *Automatica* 46.11 (2010), pp. 1911–1915.

[114] Sophie Tarbouriech, Isabelle Queinnec, and Christophe Prieur. "Stability analysis and stabilization of systems with input backlash." In: *IEEE Transactions on Automatic Control* 59.2 (2014), pp. 488–494.

[115] Andrew R. Teel and Laurent Praly. "Global stabilizability and observability imply semi-global stabilizability by output feedback." In: *Systems & Control Letters* 22.5 (1994), pp. 313–325.

[116] Andrew R. Teel and Laurent Praly. "Tools for semiglobal stabilization by partial state and output feedback." In: *SIAM Journal on Control and Optimization* 33.5 (1995), pp. 1443–1488.

[117] Andrew R Teel, Fulvio Forni, and Luca Zaccarian. "Lyapunov-based sufficient conditions for exponential stability in hybrid systems." In: *IEEE Transactions on Automatic Control* 58.6 (2013), pp. 1591–1596.

[118] Andrea Tilli and Marcello Montanari. "A low-noise estimator of angular speed and acceleration from shaft encoder measurement." In: *Automatika-Zagreb* 42.3/4 (2001), pp. 169–176.

[119] Hongtei Eric Tseng. "Dynamic estimation of road bank angle." In: *Vehicle system dynamics* 36.4-5 (2001), pp. 307–328.

[120] Ali Y. Ungoren, Huei Peng, and H.E. Tseng. "A study on lateral speed estimation methods." In: *International Journal of Vehicle Autonomous Systems* 2.1 (2004), pp. 126–144.

[121] Ardalan Vahidi, Anna Stefanopoulou, and Huei Peng. “Recursive least squares with forgetting for online estimation of vehicle mass and road grade: theory and experiments.” In: *Vehicle System Dynamics* 43.1 (2005), pp. 31–55.

[122] Luma K. Vasiljevic and Hassan K. Khalil. “Error bounds in differentiation of noisy signals by high-gain observers.” In: *Systems & Control Letters* 57.10 (2008), pp. 856–862.

[123] Augusto Visintin. *Differential models of hysteresis*. Vol. 111. Springer Science & Business Media, 1994.

[124] Vladimir Andreevich Yakubovich. “The method of matrix inequalities in the theory of stability of nonlinear controlled systems. III - Absolute stability of systems with hysteresis nonlinearities.” In: *Automation and Remote Control* 26 (1965), pp. 753–763.

[125] Luca Zaccarian and Andrew R Teel. “The $\mathcal{L}_2$ (ℓ_2) bumpless transfer problem for linear plants: Its definition and solution.” In: *Automatica* 41.7 (2005), pp. 1273–1280.

[126] Garo Zarikian and Andrea Serrani. “Harmonic Disturbance Rejection in Tracking Control of Euler-Lagrange Systems: An External Model Approach.” In: *IEEE Transactions on Control Systems Technology* 15.1 (Jan. 2007), pp. 118–129.

[127] Jing Zhou, Chengjin Zhang, and Changyun Wen. “Robust adaptive output control of uncertain nonlinear plants with unknown backlash nonlinearity.” In: *IEEE Transactions on Automatic Control* 52.3 (2007), pp. 503–509.

Abstract — In this thesis we study linear time-invariant systems feedback interconnected with three specific nonlinear blocks; a play/stop operator, a switching-reset mechanism, and an adaptive dead-zone. This setup resembles the Lure problem studied in the absolute stability framework, but the types of nonlinearities considered here do not satisfy (in general) a sector condition. These nonlinear blocks give rise to a whole range of interesting phenomena, such as compact sets of equilibria, hybrid omega-limit sets, and state constraints. Throughout the thesis, we use the hybrid systems formalism to describe these phenomena and to analyze these loops. We obtain sharp stability conditions that can be formulated as linear matrix inequalities, thus verifiable with numerically efficient solvers. Finally, we apply the theoretical findings to two automotive applications.

Keywords: Hybrid systems, reset control, Lure systems, play/stop operator, adaptive systems, pointwise asymptotic stability, linear matrix inequalities.

Résumé — Dans cette thèse, nous étudions la rétroaction de systèmes linéaires invariants dans le temps reliés entre eux par trois blocs non linéaires spécifiques : un opérateur de lecture/arrêt, un mécanisme de réinitialisation de commutation et une zone morte adaptative. Cette configuration ressemble au problème de Lure étudié dans le cadre de stabilité absolue, mais les types de non-linéarités considérés ici ne satisfont pas (en général) une condition sectorielle. Ces blocs non linéaires donnent lieu à toute une série de phénomènes intéressants, tels que des ensembles compacts d'équilibres, des ensembles hybrides oméga-limites et des contraintes d'état. Tout au long de la thèse, nous utilisons le formalisme des systèmes hybrides pour décrire ces phénomènes et analyser ces boucles. Nous obtenons des conditions de stabilité très précises qui peuvent être formulées sous forme d'inégalités matricielles linéaires, donc vérifiables avec des solveurs numériques efficaces. Enfin, nous appliquons les résultats théoriques à deux applications automobiles.

Mots clés : Systèmes hybrides, contrôle de remise à zéro, systèmes Lure, opérateur de jeu/arrêt, systèmes adaptatifs, stabilité asymptotique ponctuelle, inégalités de matrice linéaire.

University of Trento, via Calepina 14, 38122 Trento, Italy
LAAS, 7 avenue du Colonel Roche, 31031 Toulouse, France